Proceedings of

THE PALEOSEISMOLOGY WORKSHOP

March 15, 1999, Tsukuba, Japan

as a part of

Twin Institute Program between

Geological Survey of Japan and United States Geological Survey

Edited by Kenji Satake[1] and David Schwartz[2]

1. Geological Survey of Japan, 1-1-3 Higashi, Tsukuba 305-8567 Japan

2. U. S. Geological Survey, 345 Middlefield Road, MS 977, Menlo Park, CA 94025 U.S.A.

GSJ Interim Report No.EQ/99/2
(地質調査所速報 No.EQ/99/2)

USGS Open-File Report 99-400

Preface

Both Geological Survey of Japan (GSJ) and United States Geological Survey (USGS) have been leading the paleoseismological research in each country. After the 1995 Kobe earthquake, GSJ has expanded its researchers and funding for the paleoseismology program, particularly for trenching surveys of active faults. USGS recently started BAYPEX program, in which active faults in the Bay Area will be studied in detail. Both institutions have been collaborating on paleoseismological research across the Pacific. For example, geological evidence in Washington and Oregon postulated a giant earthquake along the Cascadia Subduction Zone about 300 years ago. From tsunami damage recorded in Japanese historical documents, the date of the earthquake is known as January 26, 1700.

GSJ and USGS recently started the Twin Institute Program on earthquake research supported by Agency of Industrial Science and Technology, Ministry of International Trade and Industry of Japan. As a part of this activity, International Workshop on Paleoseismology was held at Geological Survey of Japan, Tsukuba, on March 15, 1999. Ten oral presentations and sixteen poster presentations with brief oral introductions were made at the workshop. The workshop was preceded by a five-day field-trip to visit the 1891 Nobi earthquake fault system including the trench site at Umehara and Itoshigawa-Shizuoka tectonic line. Stimulus discussions on various problem were made in the field.

This proceedings volume of the workshop is compiled in order to document the workshop, record the presentations. It is hoped that the data and ideas presented here would be useful for future collaboration. We need to identify common problems and create a joint research program under the Twin Institute Program. The workshop was merely a first step for future collaboration of both geological surveys.

Kenji Satake, Geological Survey of Japan
Dave Schwartz, United States Geological Survey

Program of Workshop on Paleoseismology
(15 th March, 1999 at GSJ, Tsukuba)

9:20- 9 :30 Opening
9:30-10:00 Yuuichi Sugiyama(GSJ)
" Recent Progress in Earthquake Potential Evaluation of Main Active Faults in the Kinki Triangle"
10:00-10:30 Yasuo Awata(GSJ)
" Behavioral Segments and Their Cascades for Earthquake Occurrence in the 85-km-long Arima-Takatsuki-Rokko Fault Zone, Central Japan"
10:30-11:00 Koji Okumura(Hirosima Univ.)
" Paleoseismology of the fastest-moving onshore fault in Japan "

(coffee break : 11:00-11:10)

11:10-11:40 Steve Personius(USGS, Denver)
" Paleoearthquake Recurrence in the Rio Grande Rift near Albuquerque, New Mexico "
11:40-12:10 Thomas Fumal(USGS, Menlo Park)
" The paleoseismic record of the San Andreas fault in southern California: Implications for fault segmentation models "

(lunch time : 12:10-13:30)

13:30-14:00 Brian Atwater(USGS, Seattle)
"Earthquake Recurrence and Probabilities at Cascadia"
14:00-14:30 Alan Nelson(USGS, Denver)
"Multiple large earthquakes in the past 1500 years on a fault in Metropolitan Manila, The Philippines "
14:30-15:00 David Yamaguchi(Xylometric Co.)
"The 1700 Cascedia Earthquake: Tree-ring Data Processing, A Progress Report and Opportunities for Continuing Japan-US Collaboration"
15:00-15:10 Short Comments for the Posters

(coffee break : 15:10-15:30)

15:30-16:15 Yoshihiro Kinugasa(GSJ)
"On and Off Fault Paleoseismology"
16:15-17:00 David Schwartz(USGS Menlo Park)
"Paleoseismology: Challenges for the 21st Century"

(Posters)

1. Paleoseismology and Activity Study of the Hinagu Fault System, Southwest Japan
   K. Shimokawa, Y. Kinugasa, T. Tanaka
2. Characteristics of a Behavioral Fault Segment in the Western Coast of Northeast Japan Deduced From the Height Change of Former Shoreline
   T. Azuma, Y. Awata
3. Recent Progress in Earthquake Potential Evaluation of Main Active Faults in the Kinki Triangle
   Y. Sugiyama
4. Behavioral Segments and Their Cascades for Earthquake Occurrence in the 85-km-long Arima-Takatsuki-Rokko Fault Zone, Central Japan
   Y. Awata, A. Sangawa, Y. Sugiyama
5. Susunayskaya Lowland Fault in South Sakhalin Revealed by A Trenching Study: A preliminary report
   Y. Kariya, R. Bulgakov, K. Shimokawa
6. Geologic Evidence for Five Large Earthquakes on the North Anatolian Fault at Ilgaz, During the Last two Millennia
   T. Sugai, O. Emre, T. Y. Duman, T. Yoshioka, I. Kushu
7. Structure and paleoseismology of the Kongo fault system in Nara Prefecture
   K. Satake, T. Sugai, A. Sangawa, M. Yanagida, H. Yokota, T. Iwasaki, M. Omata, A. Ishikawa
8. High-resolution Multi-proxy Analyses and Dating of Lake Deposits Affected by Recent Faulting Event: a Case Study of Lake Suwa on the Itoigawa-Shizuoka Tectonic Line (ISTL), Central Japan
   K. Okumura, K. Saito, H. Fukuzawa, K. Mizuno, O. Fujiwara
9. Sedimentary systems and earthquake events? confined by active faults: a case of the western Biwako fault system in the Hira-Adogawa region, Shiga prefecture, central Japan.
   F. Nanayama, H. Mizuno, T. Komatsubara
10. Sedimentary characteristics of tsunami deposits from the 1993 Hokkaido Nansei-oki tsunami, northern Japan.
    F. Nanayama, K. Satake, K. Shimokawa
11. Most recent event constraints and interpretations from initial paleoseismic study along the Hurricane fault, southwestern USA
    H. Stenner
12. AMS 14C Dating of a 7300-year Earthquake History from an Oregon Coastal Lake
    A. R. Nelson
13. Deformation of Quaternary Deposits and Ground Surface Caused by Bedrock Fault Movements -Trenching Studies and Model Experiments-
    K. Ueta, K. Tani, N. Onizuka, T. Kato, K. Maruyama
14. Recent surface-faulting events along the southern part of the Itoigawa-Shizuoka Tectonic Line
    S. Toda, D. Miura, S. Abe, K. Miyakoshi, D. Inoue
15. Faulting Processes of the 1955 Futatsui Earthquake (M=5.5), Akita Prefecture, inferred from pre- and co- seismic elevation changes
    T. Komatsubara, Y. Awata
16. Subaqueous sand blow deposits induced by the 1995 Southern Hyogo Prefecture earthquake, Japan
    A. Kitamura, E. Tominaga, H. Sakai

Table of contents

Progress in evaluating earthquake potential of major active faults in the Kinki Triangle

Yuichi Sugiyama

Geological Survey of Japan

sugiyama@gsj.go.jp

National Survey of Active Faults in Japan

After the 1995 Kobe earthquake, the Science and Technology Agency (STA) and the Geological Survey of Japan (GSJ) began systematic study of major active faults throughout Japan. It was hoped that the study would yield long-term earthquake forecasts, and that these forecasts would help to reduce losses from future earthquakes.

The study targets ninety-eight faults or fault systems (Fig. 1). These faults were selected because they meet one or more of the following criteria: (1) average slip rate greater than 0.1 m per thousand years; (2) length at least 20 km; and (3) location in a densely populated area.

Under this program, STA has granted over one billion yen ($8 million) annually to prefectural governments and big cities. These local entities use the funds for study of active faults within areas they administer.

GSJ has spent about 0.3 billion yen (about $2.5 million) annually for active fault studies since the Kobe earthquake. We at GSJ use these funds to evaluate regional seismic hazards, fault interaction, and individual faults believed especially hazardous.

By the year 1999, some 80 percent of the 98 targeted faults will have been studied by GSJ or by local governments that receive STA funds.

Overview of GSJ Study of Active Faults in the Kinki Triangle

GSJ chose the Kinki Triangle as its first target for regional study of seismic hazards. The triangle, bounded to the south by the Median Tectonic Line, contains large cities as Kobe, Osaka, Kyoto, and Nagoya. It is home to some 25 million people and a lot of active faults as well. Twenty-two of the 98 nationally targeted faults are within the Kinki Triangle.

GSJ has now obtained data on the time of the most recent rupture along over 13 of these 22 faults. We have also clarified which of these faults are probably responsible for four earthquakes revealed by old documents between the 1300's and 1600's.

Progress has been slower, however, in obtaining reliable estimates of recurrence intervals. Such estimates are now available for less than half of the studied faults. We hope to improve this situation in the next few years.

Examples of Findings from the Northern Part of the Kinki Triangle

Our work in the Kinki Triangle included attempts to learn which faults ruptured during two earthquakes known from documents: the 1325 Shochu and 1662 Kanbun events. The main candidates for the 1325 Shochu are the south part of the Yanagase fault; a conjugate structure called the south Tsuruga fault; and the Daguchi fault, which adjoins the south Tsuruga fault (Fig. 2).

Documents provide some guidance about location of the 1325 earthquake. They state that the earthquake damaged a shrine in Tsuruga City. In addition, they show that the earthquake caused landslides on an island in northern Lake Biwa and at a small town in mountains north of Lake Biwa.

Our trench survey on the south Tsuruga fault in 1997 shows that the last rupture on this fault occurred between late 1100's and the 1300's. We estiamted the average recurrence interval at 2500 to 4000 years on the basis of 0.5-0.6 m/ky average vertical slip rate and 1.5-2.0 m vertical displacement associated with the last event (Sugiyama *et al.,* 1998). Accordingly, the south Tsuruga fault may have a low probability of producing a big earthquake in the next 100 years.

As for the south Yanagase fault, two trenches 4 km apart gave very different results. While one showed the fault last rupturing 600-700 years ago, the other provided no evidence of rupture more recent than 7000 years ago (Yoshioka *et al.,* 1998b). So the south Yanagase fault is believed to divide into two behavioral segments at a slight bend between the two trench sites, although theirb recurrence intervals are still unknown.

A 1998 trench across the Daguchi fault showed that it ruptured after the 1325 earthquake and before or during the 1662 earthquake.

Contagious and Multiple Ruptures in the Northern Kinki Triangle

From these results we infer that the 1325 and 1662 earthquakes were part of a serial, contagious rupture of active faults in the Kinki Triangle. It is difficult, however, to use paleoseismic evidence to distinguish among individual events in such a series.

Much of the difficulty is due to uncertainties in dating. As is usually the case in paleoseismology, serial earthquakes as much as centuries apart can give overlapping ages.

A further problem is the temptation to shoehorn paleoearthquakes into historical earthquake catalogs. This practice is risky not only because the geologic dating is uncertain but also because the catalogs may be incomplete, particularly for times of civil unrest in Japan. The 1325 event occurred during such an era.

Multiple Ruptures During the 1586 Tensho Earthquake

The Tensho earthquake of 1586, which caused severe damage in both the Hida district and Nobi Plain (Fig. 3), probably resulted from some combination of rupture on the Miboro, Atera, and Yoro-Kuwana fault systems.

The earthquake has been ascribed by Tsuneishi (1980) and Usami (1996) to rupture on the Miboro fault system (Fig. 4) because the shaking caused severe damage along this fault. Our trenching in 1990 showed that the fault last ruptured after 1100.

The latest rupture on the Atera fault system was correlated to the Tensho earthquake by Central Research Institute of Electric Power Industry (Toda *et al.*, 1995).

GSJ array boring of the Yoro-Kuwana fault system showed that this fault system also ruptured after 1300 (Sugai *et al.*, 1998). Because the nearby Nobi area was severely damaged by the 1586 Tensho earthquake, the earthquake probably caused this rupture on the Yoro-Kuwana fault system. The array boring also showed that the penultimate rupture on this fault system postdates 600; this rupture may represent a documented earthquake in 745.

The average recurrence interval of the Yoro-Kuwana fault in the Holocene is estimated at 1000 to 2000 years on the basis of array boring and seismic reflection data (Sugai *et al.*, 1998). But if the penultimate rupture occurred in 745, the interval between the two most recent ruptures becomes only about 800 years. Vertical displacement during both ruptures was nearly the same, about 6 m. I therefore speculate that the fault produces characteristic earthquakes at irregular intervals.

According to historical documents, the Tensho earthquake may comprise two events about a day apart. Perhaps rupture of Miboro and Atera faults caused

premature rupture of the Yoro-Kuwana fault system. Such induced rupture may contribute to irregularity of recurrence intervals.

Long Elapsed Times, Unmeasured Recurrence Intervals, and Plans for Osaka

Some active faults in the Kinki Triangle have now gone thousands of years without rupturing (Fig. 5). For the north segment of the fault system along the west side of Lake Biwa, this elapsed time exceeds 2500 years (Komatsubara *et al.,* 1998). For the south Hanaore fault near Kyoto, the elapsed time is 1300-2500 years (Yoshioka *et al.,* 1998a).

Reliable estimates of recurrence intervals are available for less than half the active faults in the Kinki Triangle.

GSJ has plans to focus on earthquake hazards at Osaka. The paleoseismic targets there include the Uemachi fault system, which runs through the city, and the Osaka Bay fault.

References

Araki, R., K. Ishimaru, and O. Fujiwara, 1996, Holocene cumulative displacements of the Osaka bay fault off Kobe, *Abstracts of the 1996 Japan Earth and Planet. Sci. Joint Meeting*, 672.

Daicho, A. and T. Matsuda, 1982, Kanbun 2-nen no Oumi no zisin, in Hagiwara T. *(ed.)*, *Kozisin (Paleo-earthquakes)*, Univ. Tokyo Press,

Earthquake Research Committee, 1998, *Seismic Activity in Japan –Regional perspectives on the characteristics of destructive earthquakes-*, Headquartes for Earthquake Research Promotion, Prime Minister's Office, 222p.

Iida, K., 1987, *Tensho dai-zisin shi*. Nagoya Univ. Press, 552p.

Komatsubara, T., K. Mizuno, A. Sangawa, and F. Nanayama, 1998, Trenching study of the Aibano fault, a northern segment of the Biwako-seigan active fault system, *Geol. Surv. Japan Interim Rep., no. EQ/98/1*, 125-136.

Matsuda, T., A. Okada, and A. Daicho, 1978, The great earthquake of 1662 and the associated crustal deformation around Lake Biwa -a preliminary report, in Horie, S. *(ed.)*, *Paleolimnology of Lake Biwa and the Japanese Pleistocene, 6*, 54-65.

Mizuno, K., E. Tsukuda, and Y. Miyachi, 1998, Boring surveys of a concealed active fault in the Wakayama Plain, *Geol. Surv. Japan Interim Rep., no. EQ/98/1*, 179-186.

Mizuno, K., T. Yoshioka, M. Okamura, and H. Matsuoka, 1996, Active fault study of the Minato-Honjo fault off the southwestern part of Awaji Island by sonic prospecting and coring, *Open-file Rep., Geol. Surv. Japan, no. 235*, 59pp.

Nanayama, F., N. Kitada, K. Takemura, and Y. Sugiyama, 1998, Paleoseismological study of the Suminoe flexure in Osaka Prefecture by array boring and S-wave seismic reflection survey, *Geol. Surv. Japan Interim Rep., no. EQ/98/1*, 137-149.

Okumura, K., A. Sangawa, T. Sugai, M. Takada, and H. Soma, 1997, Integrated geological investigation of the Nara-Tenri fault zone, *Open-file Rep., Geol. Surv. Japan, no. 303*, 51-62.

Sangawa, A., 1997, *Yureru daichi*. Dohosha, Tokyo, 272p.

Satake, K., A. Sangawa, and T. Sugai, 1998, Trenching study of the Kongo fault system. *Geol. Surv. Japan Interim Rep., no. EQ/98/1*, 151-159.

Shimokawa, K., Y. Kariya, Y. Miyachi, and A. Sangawa, 1997, Activity study of the Ikoma fault system, *Open-file Rep., Geol. Surv. Japan, no. 303*, 37-49.

Sugai, T., Y. Awata, and K. Shimokawa, 1998, Paleoseismological study of the Kuwana fault and the Yokkaichi fault in Mie Prefecture, central Japan, *Geol. Surv. Japan Interim Rep., no. EQ/98/1*, 75-90.

Sugiyama, Y., Y. Awata, and E. Tsukuda, 1991, Holocene activity of the Miboro fault system, central Japan, and its implications for the Tensho earthquake of 1586 - verification by excavation survey-, *Zisin, 44*, 283-295.

Sugiyama, Y., T. Yoshioka, A. Sangawa, and K. Satake, 1998, Paleoseismological study of the Tsuruga fault, *Geol. Surv. Japan Interim Rep., no. EQ/98/1*, 101-112.

Toda, S., D. Inoue, A. Kubouchi, N. Takase, and M. Nikaido, 1995, Paleoseismicity of the Atera fault system and 1586 Tensho earthquake: trenching study at Ogo, Aonohara and Dendahara, central Japan, *Zisin, 48*, 401-421.

Tsukuda, E., K. Mizuno, Y. Miyachi, and A. Sangawa, 1998, Trench excavation survey of the Negoro fault, the Median Tectonic Line active fault system, Kii Peninsula, Japan. *Geol. Surv. Japan Interim Rep., no. EQ/98/1*, 161-177.

Tsuneishi, Y., 1980, The Hakusan earthquake of 1586 and the Shirakawa fault. *Abstracts of the Seismological Society of Japan, no. 2*, 110.

Usami, T., 1996, *Materials for comprehensive list of destructive earthquakes in Japan, 416-1995*, Univ. Tokyo Press, 493p.

Yoshioka, T., Y. Kariya, F. Nanayama, A. Okada, and K. Takemura, 1998a, Latest faulting of the Hanaore fault, central Japan, revealed by trenching studies, and the 1662 Kambun earthquake, *Zisin, 51*, 83-97.

Yoshioka, T., Y. Sugiyama, T. Hosoya, K. Henmi, S. Watanabe and H. Tanaka, 1998b, Last faulting of the Yanagase fault based on trenchig studies in Yogo Town, central Japan, *Zisin, 51*, 281-289.

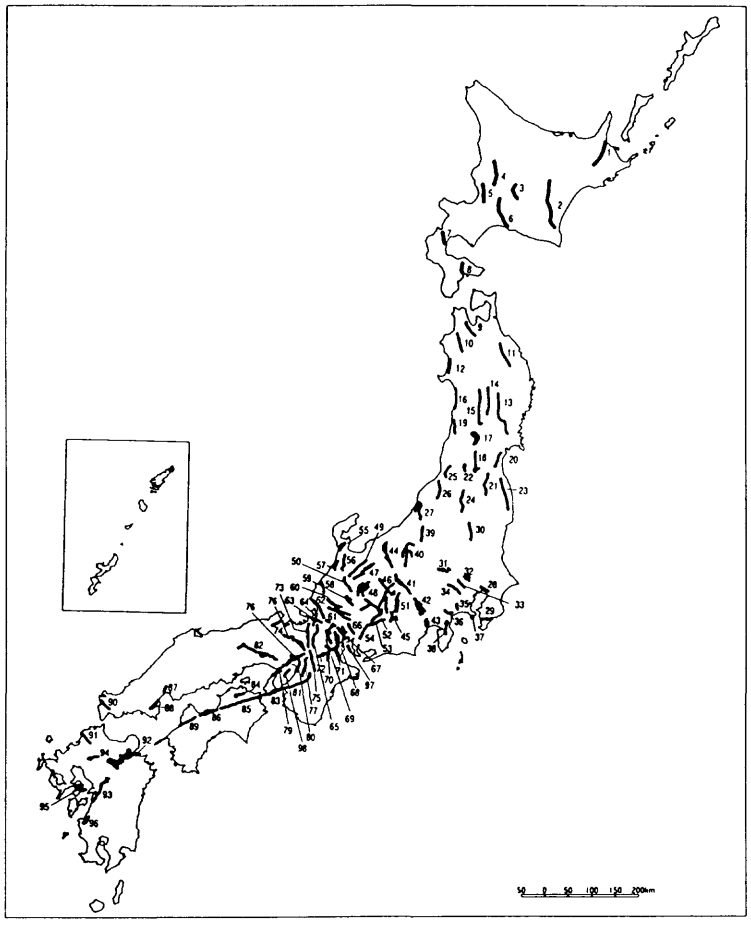

Figure 1. Location of the 98 active faults for the national survey (Earthquake Research Committee, 1998).

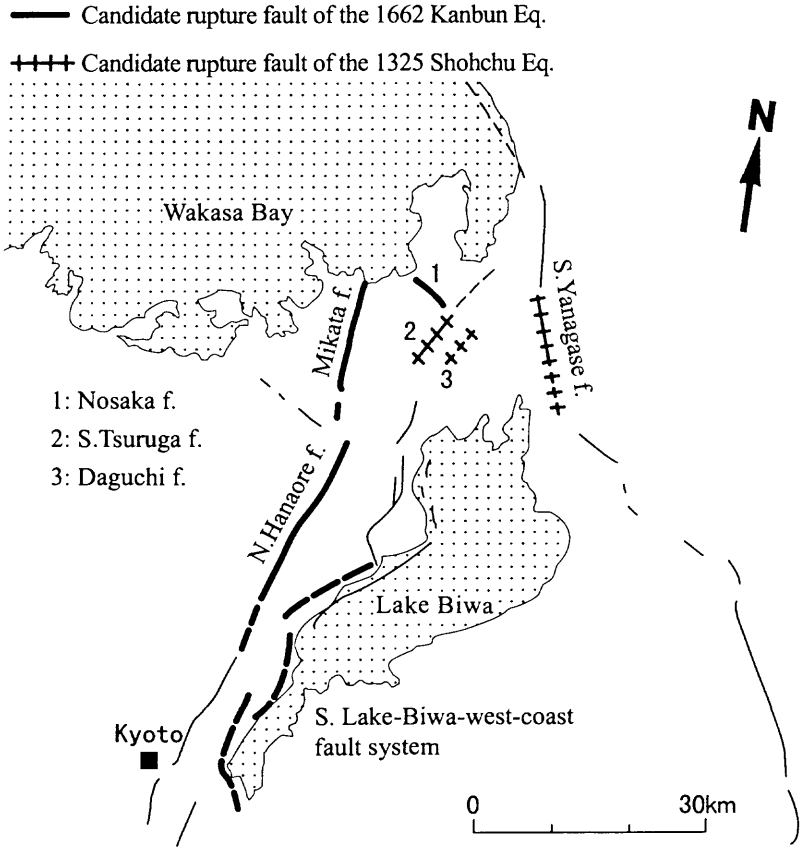

Figure 2. Faults that may have ruptured during the 1325 Shohchu and 1662 Kanbun earthquakes.

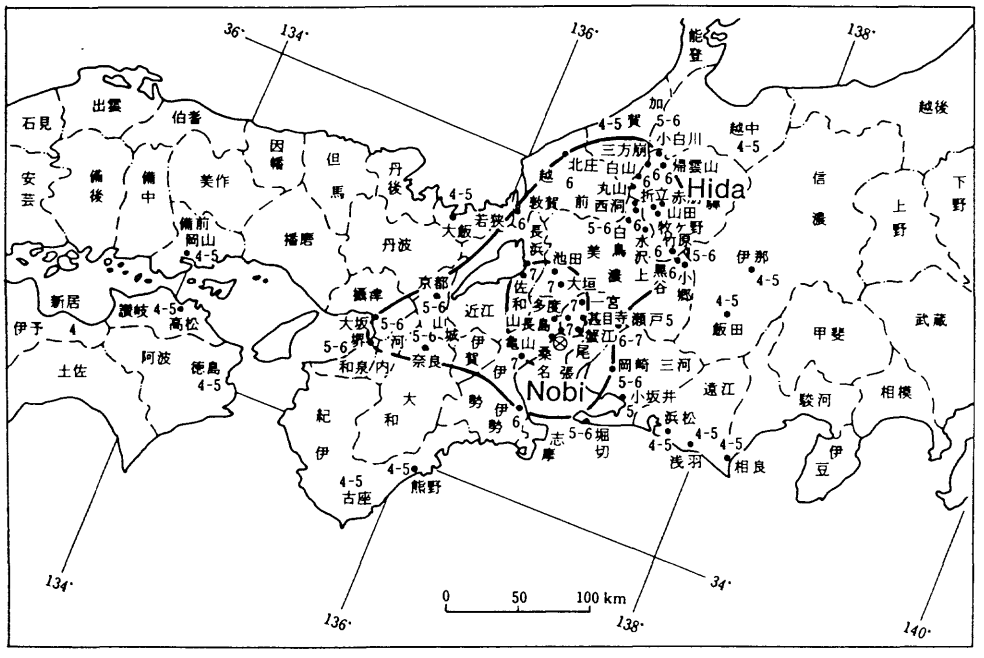

Figure 3. Estimated areas of seismic intesity 6 and 7 for the 1586 Tensho earthquake (Iida, 1987). Intensity 6 on the JMA scale is close to intensity 9 or 10 on the Modified Mercalli scale.

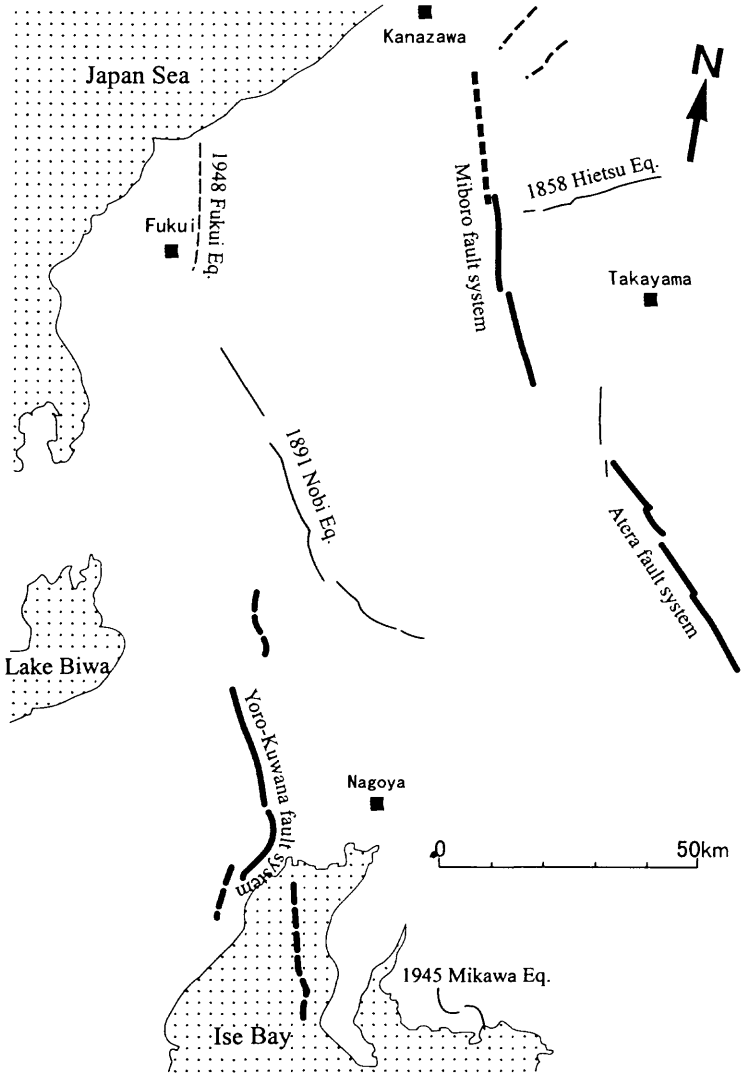

Figure 4. Three fault systems that may have ruptured during the 1586 Tensho earthquake.

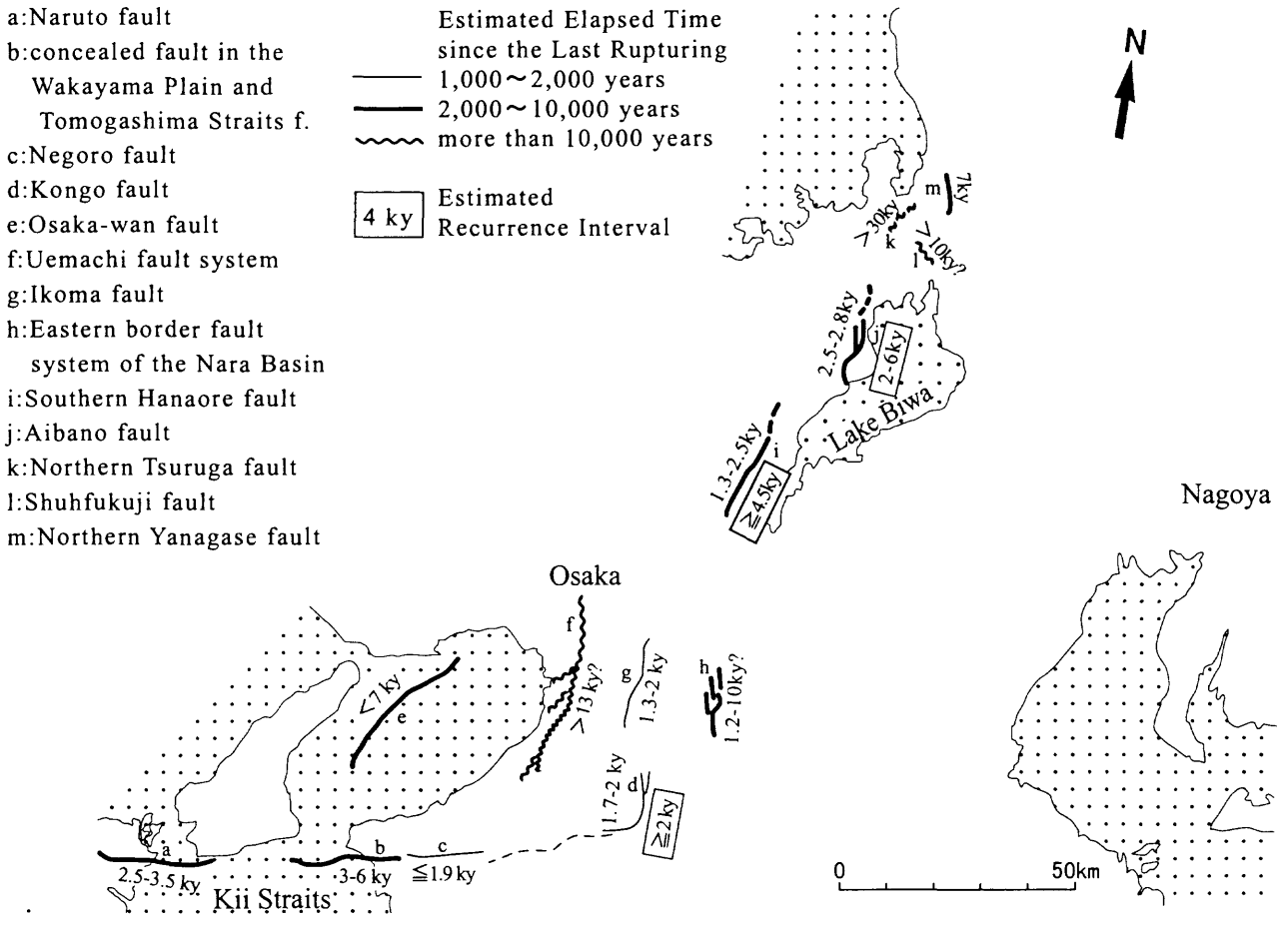

Figure 5. Active faults in the Kinki Triangle that are not known to have ruptured in the past 1000 years or longer.

Behavioral segments and their cascades for the earthquake occurrence in the Japanese surface ruptures

Yasuo Awata

Geological Survey of Japan

awata@gsj.go.jp

1. Introduction

Estimation of the probable earthquake magnitude using the paleoseismic data is based on two principle models of fault behavior; characteristic faulting model for the behavioral segments and cascade model for the earthquake segments.

Along a behavioral segment (McCalpin, 1996) or at a site on the segment, the displacement has occurred repeatedly with almost same recurrence interval and same amount of displacement (e.g. Schwartz and Coppersmith, 1984; 1986). I term this behavior of segments " the characteristic faulting model ". The displacement per event is the only evidence taken from each site on a segment to estimate the size of paleo-faulting event. If we accept the existence of persistent segments and the scaling laws among the fault parameters; length, width and slip per event, the displacement per event is a primary set of data to estimate the size of the behavioral segment.

A single behavioral segment can rupture in an earthquake. On the other hand, adjacent two or more segments can simultaneously rupture in a single earthquake. This behavior for the earthquake occurrence is termed "the cascade model" (W.G.C.E.P., 1995). In this model, it is assumed that each time a segment ruptures, whether alone or with others, it slips about the same amount. However, the length of the earthquake segment also has a relation with the displacement per event (*e.g.* Matsuda *et al.*, 1980; Bonilla *et al.*, 1984; Wells and Coppersmith, 1994).

In this paper, I analyze the relationships among the behavioral segment length, earthquake segment length and maximum displacement of the surface ruptures on land in Japan. The relations are the keys to quantify the size of probable earthquake using the geologic and paleoseismic data.

2. Segmentation of surface faults

Sixteen earthquakes have generated surface faultings on land in Japan since the 1891 Nobi earthquake. Some of the surface ruptures associated with each earthquake are subdivided into more than one behavioral segment based on its timing of paleo-faultings, slip rate, displacement per event and sense of faulting. Table 1 lists the parameters of 15 earthquake segments and its behavioral segments. The surface ruptures associated with the 1923 Kanto earthquake is excepted from Table 1, because the main faulting occurred offshore the Kanto district, central Japan. Four examples of the segmentation of earthquake segments, which are mainly based on the timings of the paleo-faultings, are described as follows;

1891 Nobi earthquake segment: The 1891 Nobi earthquake (*M* 8.0) associated an 80-km-long left-lateral surface rupture system. The system is subdivided in to three behavioral segments based on its timing of characteristic faulting, long-term activity, distribution of displacement and fault geometry. The Neodani behavioral segment in the central portion of the system is traced for 31 km and has been ruptured every 2,700 years during the Holocene (Awata *et al.*, 1998). On the other hand, the Umehara behavioral segment in the southeast of the system has ruptured only one time since 11,500 years B.P. (Awata and Nelson, 1999; in preparation communication). The northwestern Nukumi behavioral segment is less active and has a smaller displacement per event than the Neodani segment.

1896 Rikuu earthquake segment: Associated with the 1896 Rikuu earthquake (*M* 7.2), two behavioral segments of reverse fault were ruptured. On the western foot of the Ou Mountains, 36-km-long Senya behavioral segment appeared. The penultimate event on the Senya segment occurred about 3,500 years B.P. ago (Research Group for the Senya Fault , 1986). On the eastern foot of the mountains, the Kawafune behavioral segment ruptured for 9-14 km. The 1896 rupture is the only one faulting event on the Kawafune fault since 5,600 years B.P. (Oyama et al., 1991).

1930 Kita-Izu earthquake segment: The 1930 Kitaizu earthquake (*M* 7.3) shows a complicated fault strands. The Tanna behavioral segment of 15-km-long has an average recurrence interval of 700-1,000 years during the Holocene (Tanna Fault Trenching Research Group, 1983). However, the Himenoyu segment of 19-km-long, which is located on the south of the Tanna segment, has an interval of 3,000-4,600 years (Tsukuda and Yamazaki, 1984; Mizuno, 1988).

1945 Mikawa earthquake segment: The 1945 Mikawa earthquake (*M* 6.8) ruptured two behavioral segments. The Yokosuka behavioral segment has generated

only one faulting event since 54,000 years B.P. (Sone *et al.*, 1990). However, the penultimate event of the Fukozu behavioral segment occurred 20,000-30,000 years B.P. (Ueta *et al.*, 1998).

3. Scaling laws for the behavioral segment and earthquake segment

Fig. 1 shows the relations between the maximum displacements and the lengths of earthquake segments and behavioral segments for the Japanese surface ruptures listed in Table 1. Each relation shows a good correlation. The relation between the maximum displacements and the behavioral segments can be approximated as,

$$L_{\text{b-seg}}=4.9\times D_{\max} \tag{1}$$

where $L_{\text{b-seg}}$ represents a behavioral segment length (in kilometer) and $D_{\max}$ represents a maximum displacement per event (in meter). Scaling law for the behavioral segments is expressed as

$$L_{\text{e-seg}}=9.0\times D_{\max} \tag{2}$$

where $L_{\text{e-seg}}$ represents a earthquake segment length (in kilometer).

4. Discussion

The Japanese inland surface ruptures are well explained using the characteristic faulting and cascade models, and scaling law of the behavioral and earthquake segments. These models and empirical relations are applicable to make a segmentation of the active faults, and to estimate the probable earthquake magnitude in a fault system or a region in Japan. In this application, the most commonly used paleoseismic data is the displacement per event. However, it is hard to measure the maximum displacement through the paleoseismic investigations, because it occurs infrequently in a segment.

In case of the 1995 Hyogo-ken Nanbu (Kobe) earthquake, the maximum displacement of 2.5 m occurred at a central location in the behavioral segment. The most frequently observed displacements were 1.6±0.2m for the reliable data, which were measured along the two thirds portion of the whole segment (Fig. 2; Awata *et al.*, 1996). The average displacement of all the measurements including underevaluated displacements is about one-half of the maximum displacement, and a little smaller than the mode displacement. In the Gomura behavioral segment of the 1927 Kita-Tango earthquake, the maximum displacement was 3.8 m at one site, and frequently measured displacements were 2.0 m (Okada and Matsuda, 1997).

Accordingly, relationship between the maximum displacement and the mode displacement may be

$$D_{max} = \sim(3/2 - 2) \times D_{mode}$$

where D_{mode} is the mode displacement of a segment, in meter. The paleoseismic measurements of displacement are more likely to be the mode displacement of the segment than to be the maximum displacement. Hence, the regressions among the behavioral segment length, earthquake segment length and displacement per event are transformed into

$$L_{b\text{-}seg} = \sim(3/4 - 1) \times 10 \times D_{mode} \quad (3)$$

$$L_{e\text{-}seg} = \sim(3/2 - 2) \times 10 \times D_{mode} \quad (4)$$

Both lengths of the behavioral and earthquake segments are functions of the maximum displacement. Therefore, the ratio (cascade ratio) of an earthquake segment length to the length of the longest behavioral segment in the earthquake segment, 1.8 to 1, is applicable to estimate the cascades for probable earthquakes. The number of behavioral segments in an earthquake segment (cascade number) varies from 1 to 3 and the average is 1.5. This cascade number may also be used for the evaluation of cascades.

Wells and Coppersmith (1994) analyzed the worldwide data of the surface ruptures and calculated the regression of earthquake segment length (surface rupture length) versus maximum displacement; that is

$$\log D_{max} = -1.38 + 1.02 \times \log L_{e\text{-}seg} \quad (5)$$

from which it followed that

$$L_{e\text{-}seg} = 24.0 \times D_{max}^{0.98}. \quad (6)$$

The regressive length of the earthquake segment on a maximum displacement for the worldwide surface rupture is two to three times as large as that for Japanese inland surface ruptures. The scaling laws of the size of faulting parameters, cascade ratio and cascade number may be functions of tectonic setting, faulting-type and slip rate.

Reference

Awata, Y., Y. Kariya, M. Nikaido, and N. Takase, 1998, Recurrence interval and displacement per event of the Neodani fault, which ruptured in 1891, central Japan, *Abstracts 1998 Japan Earth Planet. Sei. Joint Meeting, S-41.* (J)

Awata, Y., K. Mizuno, Y. Sugiyama, R. Imura, K. Shimokawa, K. Okumura, E. Tsukuda, and K. Kimura, 1996 Surface fault ruptures associated with the Hyogo-ken Nanbu earthquake of 1995, central Japan. *Zisin, 49*, 113-124. (J+E)

Bonilla, M. G., R. K. Mark, and J. J. Lienkaeper, 1984 Statistic relations among earthquake magnitude, surface rupture rength, and surface fault displacement, *Bull. Seismol. Soc. Am, 74*, 2379-2411.

McCalpin, J. P., 1996 Application of paleoseismic data to seismic hazard assessment and neotectonic research, *Paleoseismology*, Academic Press, 439-493.

Matsuda, T., 1975 Magnitude and recurrence interval of earthquake from a fault, *Zisin, 28*, 269-283. (J+E)

Matsuda, T., 1990, Seismic zoning map of Japanese Islands, with maximum magnitudes derived from active fault data, *Bull. Earthq. Res. Inst.Univ.Tokyo. 65*, 289-319. (J+E)

Matsuda, T., H. Yamazaki, T. Nakata, and T. Imaizumi, 1980, The Surface faults associated with the Rikuu earthquake of 1896, *Bull. Earthq. Res. Inst. Univ.Tokyo. 55*, 795-855. (J+E)

Okada, A. and T. Matsuda, 1997, Surface faults assosiated with the Kita-Tango Earthquake of 1927 in the northwestern part of kinki district, central Japan, *Active Fault Res., 19*, 95-135. (J+E)

Oyama, T., K. Sone, and K. Ueta, 1991, A fault survey under alluvial deposite- (3) trench log survey of the Kawafune fault, *Abiko Res. Lab. Rep., Central Res. Inst. Elec. Power Indus., U91032*, 1-35. (J+E)

Research Group for the Senya Fault (1986) Holocene activity and near-surface features of the Senya Fault, Akita Prefecture, Japan - Excavation study at Komari, Senhata-cho -, *Bull. Earthq. Res. Inst. Univ.Tokyo, 61*, 339-402. (J+E)

Schwartz, D. P. and K.I. Coppersmith, 1984, Fault behavior and characteristic earthquakes- Examples from Wasatch and San Andreas fault zones, *Geophys. Res. 89*, 5681-5698.

Schwartz, D. P. and K.I. Coppersmith, 1986, Seismic hazards; new trend in analysis using geologic data, *Active Tectonics*, Natl. Acad. Press, Washington, DC., 215-230.

Sone, K. and K. Ueta, 1990, A fault activity study under alluvial deposits - Excavation study at the Fukozu Fault -, *Abiko Res. Lab. Rep., Central Res. Inst. Elec. Power Indus., U90029*, 1- 32. (J+E)

Table 1 Earthquake segments and their behavioral segments of the Japanese inland surface ruptures

EARTHQUAKE SEGMENT						BEHAVIORAL SEGMENT								
Date	Earthquake name	Magnitude M	Length (km)	Dmax (m)	Casacade ratio	Segment name	Length (km)	net	Dmax ver. (m)	hori.	Dmode (m)	Fault type	Recurrence interval (ky)	Slip rate (m/ky)
1891	Nobi	8	80	7.4	2.6	Nukumi	16	3.5	1.8	3		LL		B
						Neodani	31	7.4	0	7.4		LL	2.7	≧2
						Umehara	26	5.3	1.7	5		LL	≧12	B
1896	Rikuu	7.2	50	7.2	1.4	Senya	36	7.2	3.6			R	3.5	1.6
						Kawafune	14	2.8	2			R	≧5.7	B
1918	Omachi	6.1	1.1	0.2	1	Terakaido	1.1	0.2				R		
1925	Tajima	6.8	1.6	1	1	Tai	1.6	1	1			V		
1927	Kita-Tango	7.3	26.5 +	3.8	1.5?	Gomura	18 +	3.8	1	3.7	2.0	LL	≧6.1	B-C
						Yamada	8.5	1.2	0.9	1		R	≧4.5	B
1930	Kita-Izu	7.3	35	3.8	1.8	Tanna	15	3.8	1.5	3.5		LL	0.7-1.0	2
						Himenoyu	19	3		3		LL-RL	3.0-4.6	B-C
1938	Kucharo	6.8	12	2.6	1	Kucharo	10	2.6		2.6		LL		
1943	Totori	7.2	13	1.7	1	Shikano-Yoshioka	13	1.7	0.8	1.5		RL	4-8	C
1945	Mikawa	6.8	26	2.4	2	Fukozu	13	2.7	2			R	20-30	C
						Yokosuka	13	2.9	2	1.3		R-LL	≧54	C
1959	Teshikaga	6.1	2	0.1	1	Teshikaga	2	0.1	0.1			V		
1965	Matsushiro	SW	4	0.3	1	Matsushiro	4	0.3	0.2	0.3		LL		
1974	Izu-hanto Oki	6.9	6 +	0.5	1?	Irozaki	6 +	0.5	0.2	0.4		RL		B
1978	Izu-Oshima Kinkai	7.1	4.5 +	1.2	1.1 ?	Inatori-Omineyama	4 +	1.2	0.2	1.2		RL		
						Nekinota	0.5	0.2	0.1	0.2		RL		B
1995	Hyogo-ken Nanbu	7.2	16.6	2.5	1.1	Hokudan	15	2.5	1.4	2	1.6	RL	2-2.5	B
						Nadagawa	1.6	0.2	0.2	0.1	0.2	R		
1998	Iwata-ken N. H.	6.1	0.9	0.4	1	Shinozaki	0.9	0.4	0.3	0.3	0.4	R		B

Slip rate; B: 0.9-0.1 m/ky, C: <0.1 m/ky

Tanna Fault Trenching Research Group, 1983, Trenching study for Tanna Fault, Izu, at Myoga, Shizuoka Prefecture, Japan, *Bull. Earthq. Res. Inst. Univ.Tokyo. 58*, 797-830.

Ueta, K., D. Inoue, and K. Miyakoshi, 1998, Trenching study of the Fukozu fault at Isshiki, Gamagori City, Aichi Pref, *Program and Abst. Seismol. Soc. Japan 1998, Fall Meeting*.C47. (J)

Wells, D. L. and K. J. Coppersmith, 1994, Empirical relationships among magnitude, rupture length, rupture area, and surface displacement, *Bull. Seismol. Soc. Am, 84*. 974-1002.

Working Group on California Earthquake Probabilities (1995) Seismic Hazards in southern California: probable earthquakes, 1994 to 2024, *Bull. Seismol. Soc. Am, 85*, 379-439.

Tsukuda, E. and H. Yamazaki, 1984, Excavation survy of active fault for earthquake prediction in Japan - with special reference to the Ukihashi central and the Atera fault, *Geol. Surv. Japan Rep., 263*, 349-361.

Mizuno, K. (1988) Trenching study of the Himenoyu fault at Himenoyu site in 1983, *Active Fault Res., 5*, 29-34. (J)

(J): in Japanese; (J+E): in Japanese with English abstract.

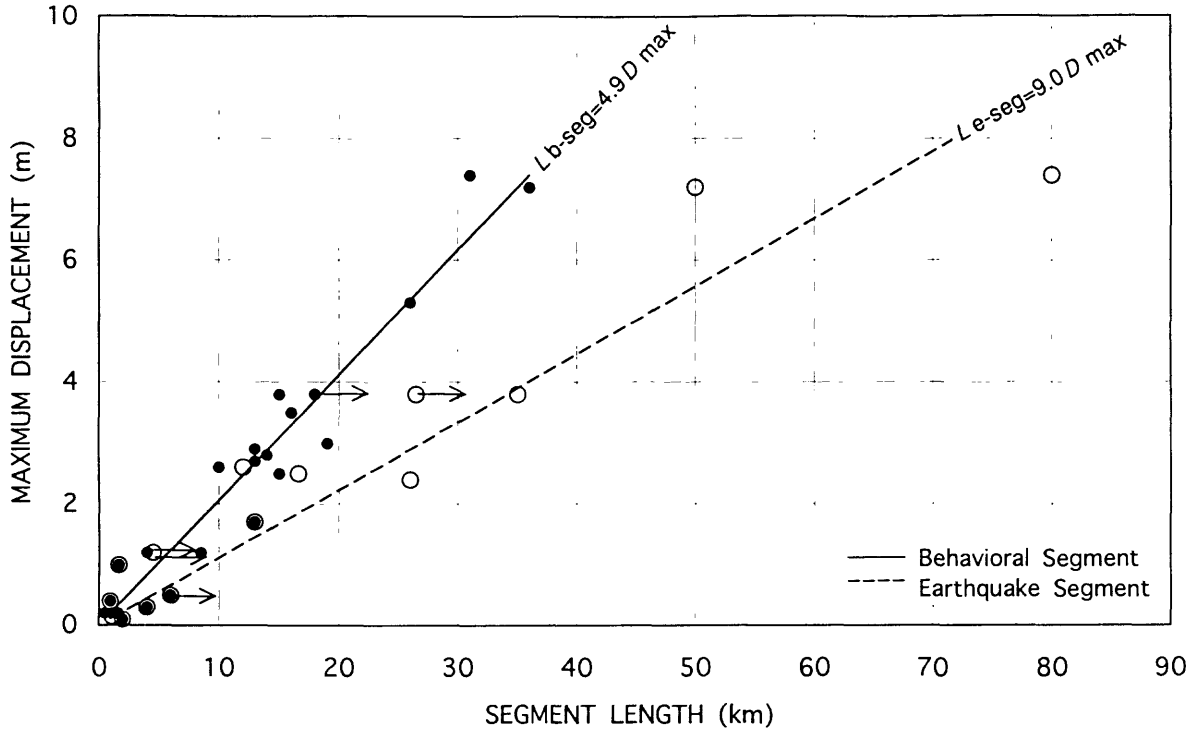

Fig. 1 Relations between maximum displacement, and earthquake and behavioral segment length for Japanese surface ruptures.

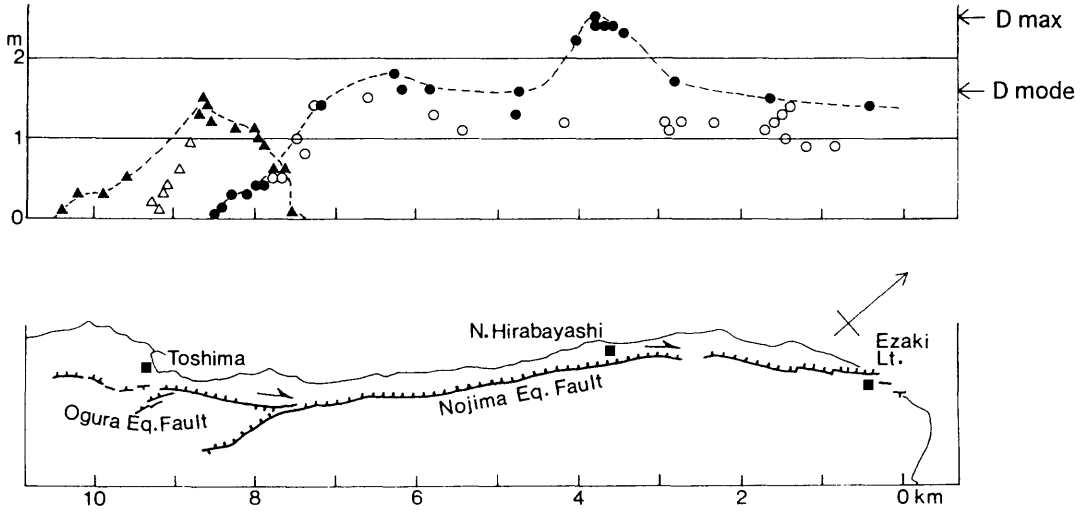

Fig. 2 Distribution of displacement along a segment associated with the 1995 Hyogo-ken Nanbu earthquake [from Awata et al., 1996] . Solid symbols denote the reliable measurements for the whole zone of the fault strand. Open symbols denote the measurement with insufficient reference. Northeast portion of the segment is traced on the sea bottom for more than 2 km, probably for 5 km.

Paleoseismology of the Itoigawa-Shizuoka tectonic line active fault system in central Japan

Koji Okumura

Hiroshima University

kojiok@ipc.hiroshima-u.ac.jp

The middle part of the Itoigawa-Shizuoka Tectonic Line active fault system (Middle ISTL) is a cluster of active faults that extends NW-SE for 50 km from Matsumoto to Kobuchizawa in central Japan (Figs. 1 and 2). The Middle ISTL is characterized by high average slip-rate reaching 8 to 10 mm/yr during the Late Pleistocene and Holocene (Ikeda and Yonekura, 1986; Fujimori, 1991). This is one of the highest slip-rate active faults reported from onshore in Japan. Empirical relation between slip-rate and recurrence time indicates that the Middle ISTL may rupture more than once a thousand year. The previously known recurrence time estimates of 3500 to 5000 years (Research Group for Ito-Shizu Tectonic Line Active Faults, 1988; Togo *et al.*, 1988) were significantly longer than the expected recurrence time. The last faulting event on the Middle ISTL most likely occurred in 841or 762 AD according to historic record and paleoseismological works (Usami, 1996; Matsuda, 1998). Since the elapsed time is 1158 or 1236 years, the estimation of recurrence time is critical to evaluate the potential of next earthquake.

In order to know the history of recent faulting events, Okumura *et al.* (1993) excavated the Gofukuji fault, the northernmost segment of the Middle ISTL at Namiyanagi, south of Matsumoto. Investigation of 6 trenches, 3 test pits and topography around the trenches brought following results. The ages of three most recent faulting events are 445-1386 AD, 150-334 AD, and 839-189 BC. The recurrence time is between 111 and 1236 years. Assuming the correlation of the last event with the 841AD event, the recurrence time is estimated to be 339 to 1173 years. Average recurrence interval in this case ranges 515 to 840 years. The elapsed time of 711 to 1152 years is probably longer than the recurrence time. The average slip rate of the fault since c.a. 6000 BC is 9.4 ~ 4.5 mm/yr left-lateral. The left-lateral coseismic slip during the last event is estimated as 7.5 ~ 1.5m. The results from the other two trenches on the Gofukuji fault (Namiyanagi: Okumura and Tsukuda, 1995; Nakayama:

Okumura *et al.*, 1998a) agreed very well with that of the Namiyanagi trench (Fig. 3: Okumura *et al.*, 1993).

Beside the Middle ISTL, the fault system north of Matsumoto (Northern ISTL) consists of east dipping reverse faults along the east foot of the Hida range to form a narrow N-S tectonic depression (Figs. 1 and 2). In 1995 and 1996, Okumura *et al.* (1998) opened three exploratory trenches in the northern ISTL. The Hakuba trench on the Kamishiro fault brought four earthquake events since 6738 BP (in calendar year) with the average recurrence interval for the three recent events to be between 1000 and 1800 years. The last event here postdates 1538 BP. The Omachi trench exposed the last event after 6th to 7th century AD and before 12th century at the latest. Only one event after 3rd to 4th century AD was identified in the Ikeda trench. The timing of the last event from each trench is between 500 and 1500 BP, whose interval coincides with the timing of the last event in the middle section as well as the 841 AD or 762 AD earthquake reported in historical documents. The dating of the upper age limit of the last event is not precise enough to correlate the event with any of known earthquakes. The recurrence interval of the northern section, however, is significantly longer than that of the Gofukuji fault, but is much shorter than that in the middle section except for the Gofukuji fault. The regional difference in the recurrence time is concordant with the difference in the slip rate (Fig. 4).

The results from over 10 trenches considerably revealed the rupture history of the ISTL. The rupture history of the North and Middle ISTL is one of the best examples of paleoseismological works in Japan, and the results lead to the first official evaluation of long-term seismic risks in Japan announced by the federal government in 1996 as well as the first attempt on probagilistic seismic hazard assessment in Japan (Kumamoto, 1998). However, the precision and reliability of time-constraints are not enough. Trenching study in the areas of utter human modification should have certain limitation. In order to push this limitation further, Saito *et al.* (1998) and Okumura *et al.* (1998b) tried to extract fine data from the lake deposits of Suwa Lake on the Middle ISTL. The idea and the interim results are as follows after Okumura *et al.* (1998b).

Disturbance of water-laid deposits and anomalous sedimentation such as liquefaction, mixed-layer, slump structure, and turbidite are usually taken as evidence of severe shaking from to a nearby fault. Those shaking records, however, cannot be regarded as evidence of faulting events on a particular structure in case there are a number of earthquake sources that may generate ground motion strong enough to disturb the deposits. In this situation, if we are to study an tectonic lake bounded by

syndepositional faults, there are chances to distinguish proximal faulting events from distal ones using the abrupt deepening as a signature of faulting by the lake. If the tectonic lake has a stable level of outlet altitude and maintains very shallow (just a few meters) depth over a several recurrence period, the lake deposits would be very sensitive to faulting events. Suwa lake in Central Japan is an ideal field to test this idea. The lake is located in a pull-apart basin formed by left-lateral strike-slip faulting of the ISTL. A pair of NW-SE strike normal faults bounds the rectangular lake-basin from surrounding mountains. The basin-fill sediments conceals another pair of the NW-SE graben-forming faults inside the basin. The basin is divided into three tectonic blocks, and the middle block in the graben has been subsided at 2.5 mm/yr on average over 100,000 years. However, very shallow depth of water and stable level of outlet have been maintained at least during these 10,000 years.

We drilled 3 pairs of boreholes in respective three tectonic blocks as deep as around 30m to penetrate Holocene sediments. In each pair of boreholes, 2 to 3 m long cores by thin-wall tube sampler overlapping by 50 cm are hauled switching from one to another borehole. This method ruled out the possibility of loss and contamination of the both ends of cores. Lithological analyses using soft X-ray photographs indicate normal accumulation of diatomaceous clay is interrupted by scattering clastic particle accompanying siderite concentration and bioturbation in more than 10 levels in each core. The clastic particle may indicate turbidite-like sedimentation caused by shaking. High-resolution chemical and physical analysis were carried out 5 cm interval on bulk density, magnetic susceptibility, quartz content, diagenetic mineral assemblage, total sulfur, organic carbon, and L*-a*-b* space color spectrum. Among them, a* value distinctively shows abrupt decrease and gradual increase repeatedly. The decrease well coincides with increase of total sulfur and decrease of organic carbon. These parameters indicate sudden change from oxidizing to deoxidizing condition and slow recovery that corresponds with sudden deepening and slow shallowing of the lake depth in order of a few meters.

The average recurrence time of deepening event is about 1000 years in this single core and is much shorter than that previously estimated 3000 to 5000 year faulting recurrence time on shore in trenches (Fig. 4). Comparison of deepening history among the three cores is under way and it may indicate differential rupture history of the fault strands in the basin. This information will be crucial constraints on the paleoseismology of the ISTL.

Reference

Fujimori, T., 1991, Active faults in the Suwa basin, and its evolution as a pull-apart basin on the Itoigawa-Shizuoka tectonic line, Central Japan, *Geogr. Rev. Japan, 64A*, 665-696.

Ikeda, Y. and N. Yonekura, 1986, Determination of late Quaternary rates of net slip on two major fault zones in central Japan, *Bull. Dept. Geogr. Univ. Tokyo, 18*, 49-63.

Kumamoto, T., 1998, Long-term conditional seismic hazard of Quaternary active faults in Japan, *Zisin*, 50, 53-71.

Matsuda, T., 1998, Present state of long-term prediction of earthquakes based on active fault data in Japan, *Zisin*, 50, 23-33.

Okumura,K., and E. Tsukuda, 1995, 1988 Trenching study of the Gofukuji fault of the Itoigawa-Shizuoka tectonic line active fault system at Namiyanagi, Matsumoto, central Japan, *Active Fault Research, 13,* 54-59

Okumura, K., K. Shimokawa, H. Yamazaki, and E. Tsukuda, 1994, Recent surface faulting events along the middle section of the Itoigawa-Shizuoka tectonic line - Trenching survey of the Gofukuji fault near Matsumoto, central Japan-, *Zisin, 46*, 425-438.

Okumura,K., R. Imura, T. Imaizumi, M. Togo, H. Sawa, K. Mizuno, Y. Kariya, and E. Saito, 1998, Recent surface faulting events along the northern part of the Itoigawa-Shizuoka tectonic line -Trenching survey of the Kamishiro fault and east Matsumoto basin faults, central Japan-, *Zisin, 50*, 35-51.

Okumura, K., K. Mizuno, H. Fukuzawa, K. Saito, and O. Fujiwara, 1998a, Paleoseismology of the middle part of Itoigawa-Shizuoka tectonic line active fault system, *Abstracts of the 1998 Japan Earth and Planetary Science Joint Meeting*, 317.

Okumura, K., H. Fukuzawa, K. Saito, K. Mizuno, and O. Fujiwara,1998b, High-resolution multi-proxy analyses and dating of lake deposits affected by recent faulting events: a case study of the Suwa Lake on the Itoigawa-Shizuoka tectonic line (ISTL), central Japan, *EOS, Transactions , American Geophysical Union, 79*, F614.

Reserach Group for Active Faults in Japan, 1991, *Active faults in Japan*, revised edition. University of Tokyo Press, 437 pp.

Research Group for Ito-Shizu Tectonic Line Active Faults, 1988, Late Quaternary activities in the central part of Itoshizu tectonic line--excavation study at

Wakamiya and Osawa faults, Nagano prefecture, central Japan--. *Bull. Earthq. Res. Inst., Univ. Tokyo, 63*, 349-408.

Saito, K., H. Fukuzawa, K. Okumura, K. Mizuno, and O. Fujiwara (1998) Anomalous layers in lake sediments from Lake Suwa and slip on the faults at the Suwa Basin since 16,500 cal. yr BP, *Abstracts of the 1998 Japan Earth and Planetary Science Joint Meeting*, 197.

Shimokawa, K., K. Mizuno, R. Imura, K. Okumura, Y. Sugiyama, and H. Yamazaki, 1995, Strip map of the Itoigawa-Shizuoka tectonic line active fault system. *Tectonic Map Series, 11,* Geological Survey of Japan.

Togo, M. and Research Group for the Excavation of Okaya Fault, 1988, Rupture history of Okaya fault in the Itoigawa-Shizuoka tectonic line active fault system. *Programme and Abstracts, Seismol. Soc. Japan, 1988, no. 1*, 223.

Usami, T., 1996, *Materials for comprehensive list of destructive earthquakes in Japan* [revised and enlarged edition], University of Tokyo Press, 493 pp.

Utsu, T., 1996, *A catalog of damage earthquakes in the world,* an online WWW catalogue at the Earthquake Research Institute, University of Tokyo [http://www.eri.u-tokyo.ac.jp/UTSU/index.html].

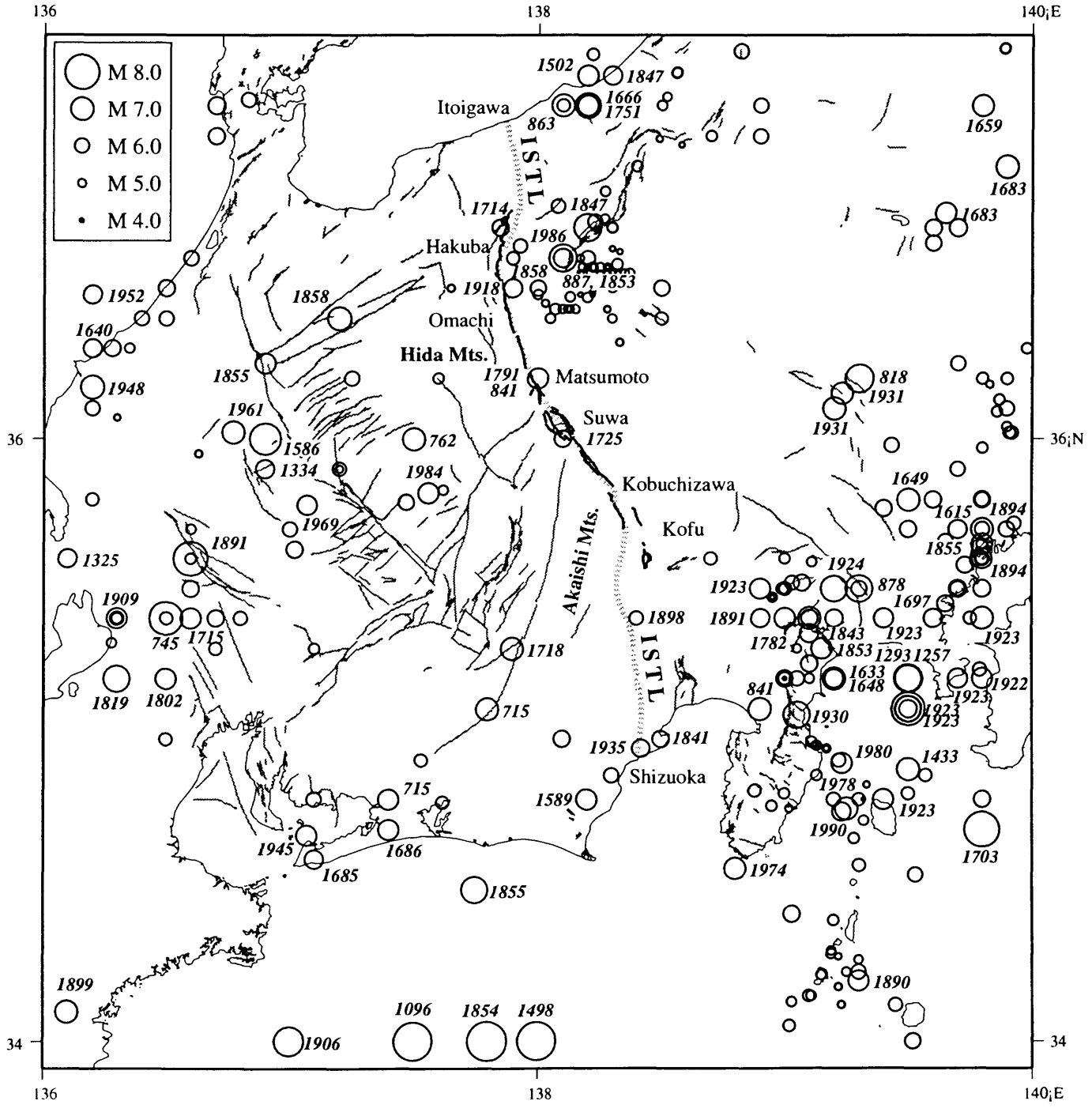

Figure 1. Active faults and large historic earthquakes in central Japan. After Reserach Group for Active Faults in Japan (1991) and Utsu (1996). The dashed line marked ISTL is a geologic structure formed during Miocene. The solid lines on the ISTL indicates the trace of the ISTL active fault system.

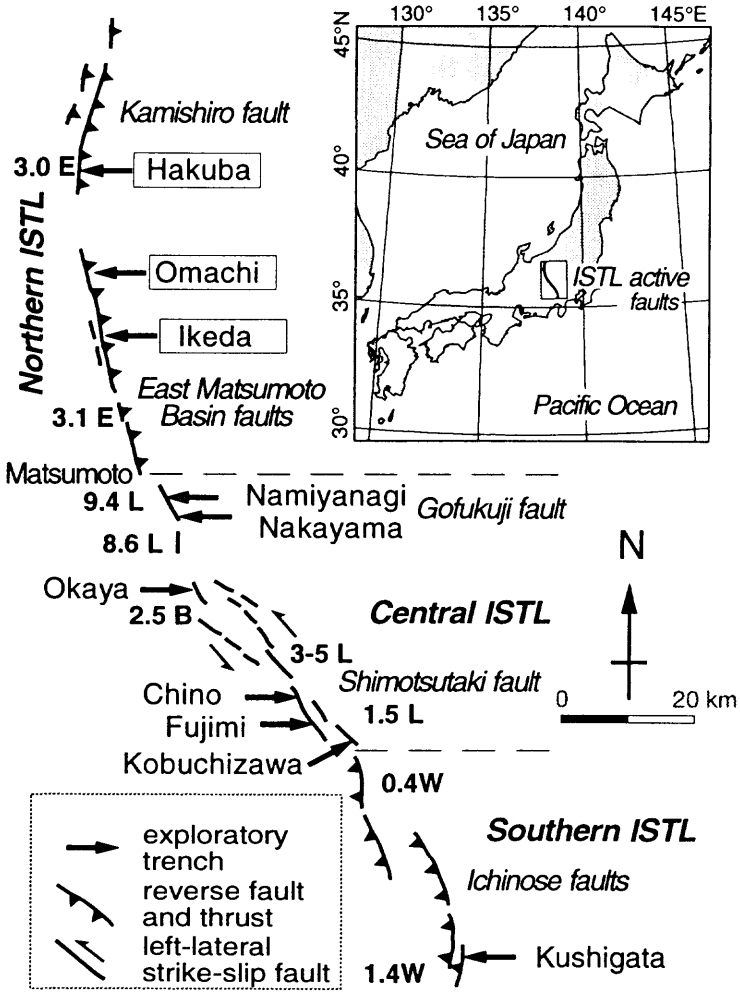

Figure 2. Outline of the Itoigawa-Shizuoka tectonic line [ISTL] active fault system and sites of exploratory trenches. Numerals indicate average slip rate of the faults in m/10^3 yr E: east-side up, W: west-side up, L: left-lateral, and B: subsidence of Suwa pull-apart basin. After Shimokawa *et al.* (1995).

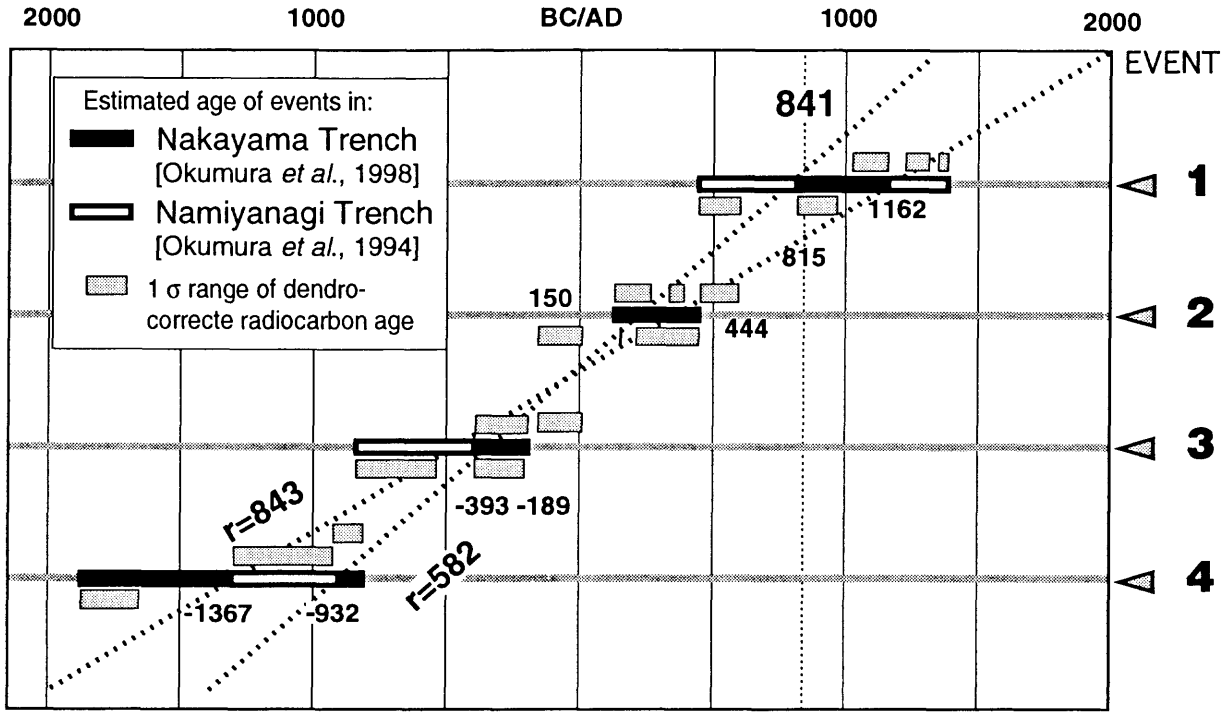

Figure 3. Timing of earthquakes on the Gofukuji fault near Matsumoto.

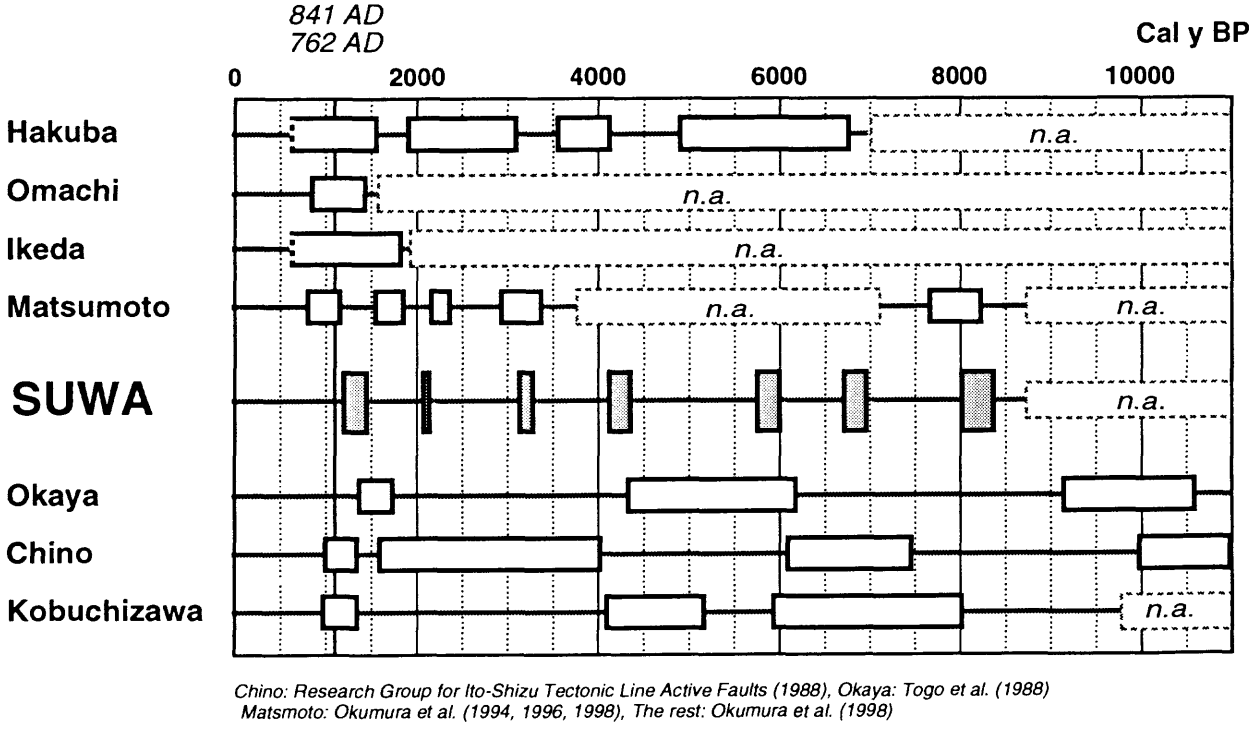

Figure 4. Timing of earthquakes along the middle and northern ISTL after Saito *et al.* (1998) and Okumura *et al.* (1998b).

Paleoearthquake recurrence in the Rio Grande rift near Albuquerque, New Mexico, USA

Stephen F. Personius

U.S. Geological Survey, Denver, USA

personius@usgs.gov

The purpose of this research is to obtain geologic information useful for seismic-hazard evaluations in the Albuquerque Basin, a prominent structure of the Rio Grande rift in central New Mexico, USA. The Rio Grande rift is part of the Basin and Range physiographic province, a broad region of primarily extensional faulting in the western United States. In northern New Mexico and southern Colorado, the rift consists of linked basins or half grabens formed by normal faulting that began in the late Oligocene, culminated in the middle to late Miocene, and continues intermittently to the present (Chapin and Cather, 1994). The rift takes its name from the Rio Grande, a large river system that flows from southern Colorado through the rift to the Gulf of Mexico.

Seismic-hazard studies of regions of low to moderate seismicity commonly rely on geologic (paleoseismic) studies to provide long-term information on slip rate and paleoearthquake recurrence. Paleoseismic studies of Quaternary faults are especially important in areas such as the Rio Grande rift, where recurrence intervals between large earthquakes commonly exceed the length of the historical seismic record. The historical record of seismicity of the Albuquerque Basin (1849-present) is typical of much of the Intermountain West in showing little association between patterns of diffuse seismicity and mapped Quaternary faults; no earthquakes larger than M_L 5.5 have been recorded in the last 150 years in this region (Northrop, 1976, 1982; House and Hartse, 1995).

Despite the lack of damaging historical earthquakes, the presence of more than 25 Quaternary faults in the Albuquerque region (Fig. 1) attest to the occurrence of large, surface-rupturing earthquakes. Faults near Albuquerque can be grouped as (1) rift-margin normal faults that form the steep western flanks of the Sandia, Manzanita, and Manzano Mountains, (2) a larger group of intrabasin normal faults that offset the floor of the Albuquerque Basin, and (3) a few poorly exposed transverse structures that may

allow accommodation between zones of differing fault polarity (Hawley, 1996; Machette, 1998). The most prominent transverse structure, the Tijeras-Cañoncito fault system, may be part of an accommodation zone that divides the Albuquerque Basin into an east-tilted domain to the north and a west-tilted domain to the south (Russell and Snelson, 1994).

At least five faults in the Albuquerque area have been active in the late Pleistocene or Holocene (Fig. 1). However, most faults shown on Figure 1 have not been studied in any detail, so several other faults in the area probably have been active in the late Quaternary. In addition, the conspicuous lack of Quaternary faults in the central portion of Figure 1 may be an artifact of preservation—this area is heavily urbanized and is partly underlain by Holocene alluvium of the Rio Grande and Tijeras Arroyo. Trench investigations have been conducted on four faults near Albuquerque (Fig. 1) and only three of these studies, East Paradise, County Dump, and Hubbell Spring fault zones (summarized below), yield data on paleoearthquake recurrence and slip per event.

Exposures of the intrabasin East Paradise fault zone were examined by the author in a house excavation in western Albuquerque in 1996. These exposures revealed a sequence of middle Pleistocene alluvial and eolian deposits vertically displaced 2.75 m across a down-to-the-west fault zone. The prefaulting deposits were overlain by two deposits of scarp colluvium and eolian sand that probably were deposited in response to two surface-faulting events. Both fault-related deposits are faulted and fractured, indicating that at least one additional surface-faulting event has occurred at this site. Unfortunately, stratigraphic evidence for the third event was removed during construction. Thermoluminescence (TL) dating of the two preserved fault-related deposits yield ages of 208 ± 25 ka and 75 ± 7 ka for the two older faulting events. The youngest event is undated, but the lack of recognizable fault scarps along most of the fault trace suggests this event probably did not occur in the Holocene (Fig. 2A). Pre-fault stratigraphic reconstructions suggest vertical displacements of about 1 m, 0.5 m, and 1.25 m, respectively, for the last three surface-faulting events on the East Paradise fault zone.

A series of trenches on the intrabasin County Dump fault excavated in 1996 by J.P. McCalpin revealed one of the longest paleoseismic records of normal faulting in the western United States (McCalpin, 1997; Machette *et al.*, 1998; McCalpin *et al.*, in press). These excavations exposed as many as 13 buried soils and associated sandy colluvial deposits, cumulatively displaced about 20 m across the County Dump fault.

If each soil represents burial after a surface-faulting event, then vertical surface displacements have averaged about 1.4 m during the middle and late Pleistocene. Approximate ages based on accumulation rates of calcium carbonate in the buried soils suggest average recurrence intervals of about 40 ± 48 ka; if two anomalous intervals (4 ka and 200 ka) are excluded, recurrence estimates are about 30 ± 11 ka (McCalpin, 1997; Machette *et al.*, 1998; McCalpin *et al.*, in press).

A third set of paleoseismic data was obtained from a trench across an 8-m-high scarp on the Hubbell Spring fault excavated by the author in 1997. The Hubbell Spring fault lies several kilometers westward of the steep flank of the Manzano Mountains, but probably represents the active margin of the Rio Grande rift in this part of the Albuquerque Basin. The trench exposed a complex fault zone and three mixed deposits of scarp colluvium and eolian sand that probably were deposited in response to individual surface-faulting events. Preliminary TL ages on these deposits suggest that the last three surface-faulting events on the Hubbell Spring fault occurred about 70 ka, 20 ka, and 10 ka (Fig. 2B). Vertical displacements during these events are difficult to determine, but probably were 1.5-1.6 m per event.

From the limited paleoseismic data discussed above, Quaternary faults in the Albuquerque area have low rates of slip and long recurrence intervals. Rift margin faults, such as the Hubbell Spring fault, are more active than the intrabasin faults such as the East Paradise and County Dump faults, but limited trench data indicate wide variations in slip rate and paleoearthquake recurrence intervals for most faults near Albuquerque (Table 1). However, average vertical displacements of 1-2 m and probable fault rupture lengths of 10-40 km indicate rare prehistoric earthquakes as large as moment magnitude 6.8-7.0 (Wells and Coppersmith, 1994). The inconsistency between historic and prehistoric seismicity is typical of the Basin and Range province in the western United States. The large number of faults in this area call for more paleoseismic data to better quantify seismic hazards in the Albuquerque metropolitan area.

References

Chapin, C. E., and S. M. Cather, 1994, Tectonic setting of the axial basins of the northern and central Rio Grande rift, *in* Keller, G. R., and S. M. Cather, (eds.), Basins of the Rio Grande rift: Structure, stratigraphy, and tectonic setting: *Geological Society of America Special Paper, 291*, 5-25.

Hawley, J. W., 1996, Hydrogeologic framework of potential recharge areas in the Albuquerque basin, central New Mexico, *in* Hawley, J.W., and T. M. Whitworth, (compilers), Hydrogeology of potential recharge areas and hydrogeochemical modeling of proposed aquifer recharge methods in basin- and valley-fill aquifer systems, Albuquerque basin, New Mexico, *New Mexico Bureau of Mines and Mineral Resources, Open-File Report, 402-D,* 1-71.

House, L., and H. Hartse, 1995, Seismicity and faults in northern New Mexico, *New Mexico Geological Society, Guidebook, 46*, 135-137.

Machette, M. N., 1998, Contrasts between short- and long-term records of seismicity in the Rio Grande rift—Important implications for seismic-hazard assessments in areas of slow extension; *in* Lund, W. R., (ed.), Proceedings volume Basin and Range province seismic hazards summit, *Utah Geological Survey Miscellaneous Publication 98-2*, 84-95.

Machette, M. N., S. F. Personius, K. I. Kelson, K. M. Haller, and R. L. Dart, 1998, Map and data for Quaternary faults in New Mexico, *U.S. Geological Survey Open-File Report, 98-521*, 443 pp.

McCalpin, J. P., 1997, Paleoseismicity of Quaternary faults near Albuquerque, New Mexico, *Final Technical Report to U.S. Geological Survey, under Contract 1434-HQ-96-GR-02751*, 18 pp.

McCalpin, J. P., S. S. Olig, J. B. J. Harrison, and G. W. Berger, Paleoseismicity and soil formation in the past 500 ka on the County dump fault, Albuquerque, New Mexico, *New Mexico Bureau of Mines and Mineral Resources Circular*, in press.

Northrop, S. A., 1976, New Mexico's earthquake history, 1849-1975, *in* Woodward, L. A., and S. A. Northrop, (eds.), Tectonics and mineral resources of southwestern North America, *New Mexico Geological Society Special Publication, 6*, 77-87.

Northrop, S. A., 1982, Earthquakes of Albuquerque Country, *New Mexico Geological Society, Guidebook, 33*, 171-178.

Russell, L. R. and S. Snelson, 1994, Structure and tectonics of the Albuquerque Basin segment of the Rio Grande rift: Insights from reflection seismic data; *in* Keller, G. R., and S. M. Cather, (eds.), Basins of the Rio Grande rift, Structure, stratigraphy, and tectonic setting, *Geological Society of America Special Paper 291*, 83-112.

Wells, D. L. and K. J. Coppersmith, 1994, New empirical relationships among magnitude, rupture length, rupture width, rupture area, and surface displacement: Bulletin of the Seismological Society of America, *Bull. Seism. Soc. Am., 84*, 974-1002.

Table 1. Estimated ranges of slip rates and recurrence intervals of surface-rupturing earthquakes on Quaternary faults near Albuquerque, New Mexico.

Fault type	Recurrence Intervals (ka)	Slip Rates (mm/yr)
Basin margin faults	10-50	0.02-0.2
Intrabasin faults	10-200	0.004-0.05

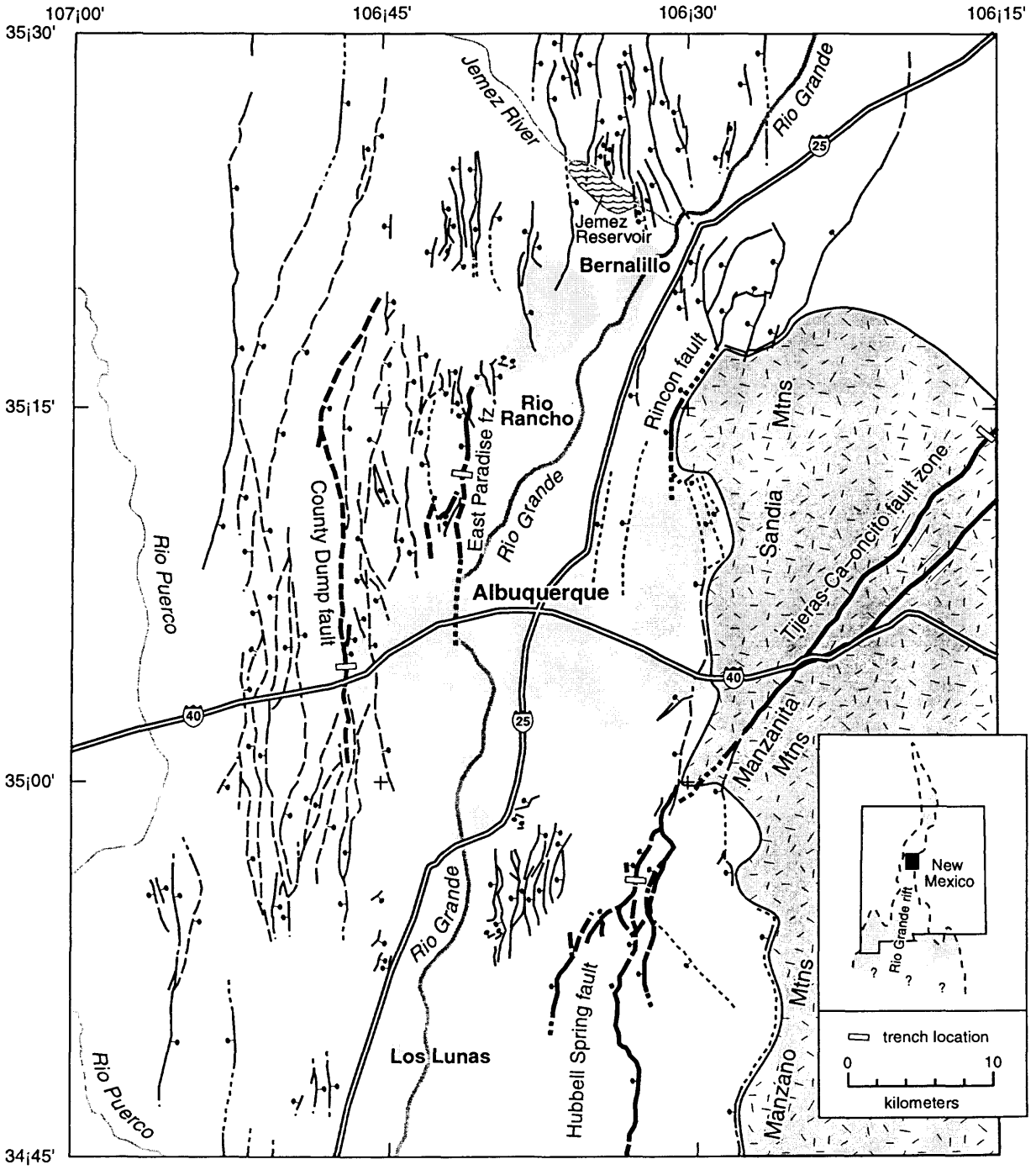

Figure 1. Map showing faults with known and suspected displacements in Quaternary deposits near Albuquerque, New Mexico; fault data modified from Machette et al. (1998). Faults with known displacements in the late Pleistocene (10-130 ka) or Holocene (<10 ka) are shown with heavier line weight; hollow bars mark locations of detailed trench studies. Shading and stipple depict pre-Tertiary rocks in the Manzano, Manzanita, and Sandia Mountains; lighter shading depicts urbanized areas.

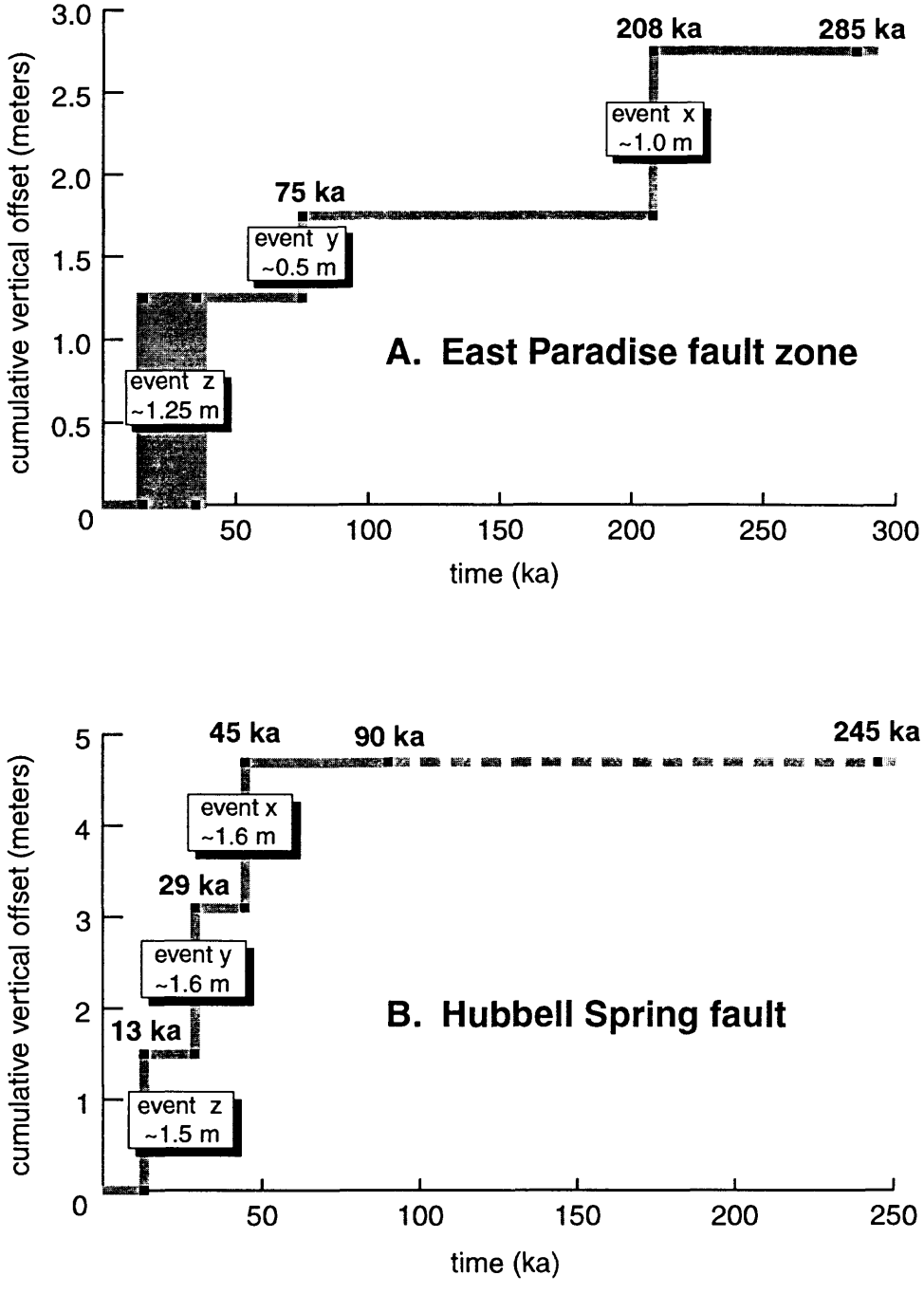

Figure 2. Time/displacement diagrams for two faults near Albuquerque, New Mexico (S. F. Personius, unpublished data, 1999): (A) East Paradise fault zone, and (B) Hubbell Spring fault. Most dates are based on thermoluminescence (TL) ages on sandy colluvial deposits that closely post-date surface-faulting events; 2 sigma errors are 10-15%. The two oldest ages from Hubbell Spring fault (90 ka and 245 ka) are U-series ages on calcic soil rinds on clasts in alluvial gravels that predate the oldest event. The older of these two ages is more consistent with extensive soil development in these deposits, so the 90 ka age is probably too young. Displacement errors are difficult to quantify, but probably are at least ± 0.25 m.

Implications of paleoseismicity for rupture behavior of the south-central San Andreas Fault

Thomas E. Fumal [1] and Gordon G. Seitz [2]

[1] U.S. Geological Survey, Menlo Park, USA
[2] University of Oregon

tfumal@isdmnl.wr.usgs.gov

The most recent large earthquake on the south-central portion of the San Andreas fault was the 1857 Fort Tejon earthquake (M=7.9) (Fig. 1). The southern termination of this rupture, just to the southeast of Wrightwood, has been used by the Working Group on California Earthquake Probabilities (1988, 1995) to define the boundary between the Mojave and San Bernardino segments of the fault. However, a growing body of paleoseismic data indicates that the 1857 termination point is the exception rather than the rule. In fact, the paleoseismic evidence does not support the existence of a persistent barrier to rupture anywhere along the fault within about 25 km of Wrightwood.

Three paleoseismic sites with long records of large earthquakes are located along this portion of the fault: Pallett Creek (Sieh,1978, 1984; Sieh *et al.,* 1989, Salyards *et al.*, 1992), Wrightwood (Weldon, 1991; Fumal *et al.,* 1993), and Pitman Canyon (Seitz *et al.*, 1997; Seitz and Weldon, 1994a, 1994b). The depositional setting at each of these locations has favored rapid accumulation of debris flow and/or fluvial sediments and the formation of many thin peat layers, resulting in stratigraphy that is excellent for recording and dating paleoearthquakes (Fig. 2). Multiple lines of evidence have been used to recognize earthquake horizons at these sites, including upward termination of ruptures, formation of scarps and scarp-derived colluvium, ground fissures, liquefaction features, and folding (Fig. 3a, 3b).

A key to the high-resolution dating of paleoearthquakes at these sites is the abundance of peat horizons. At Wrightwood, for example, nearly every contact between successive clastic deposits is a thin peat layer (Fig. 2). These peats are excellent materials for radiocarbon dating because the organic fraction consists primarily of plant matter that has accumulated in place, usually over a few decades. More than 50 samples of peat from Wrightwood have been dated using three different

radiocarbon laboratories. The results of these measurements give an excellent, stratigraphically consistent chronology of peat accumulation at this site (Fig. 4).

The pretreatment procedure used is a critical factor in obtaining accurate dates for peat. Prior to 1997, all of the samples from each of the sites were pretreated using an acid wash only (AO: Beta,QL) or an acid wash/weak, short duration alkali wash/acid wash (AWA:USGS). Recently, we submitted additional samples from Wrightwood and from Pitman Canyon to Beta Analytic Inc. Results for these samples were inconsistent with dates previously obtained for the same peat layers (Fig. 5). More importantly, the dates were stratigraphically inconsistent: dates for samples in the upper part of the section were much older than dates for samples in the lower part. We discovered that these samples had been pretreated using acid wash/strong alkali wash/acid wash (AAA), and we attribute the inconsistent dates to this pretreatment procedure.

The organic matter in the peats consists of three fractions (Fig. 6). Fulvic acid and humic acid form *in situ* by the chemical and biological decomposition of the original plant matter. The third fraction, humin or the fine residual fraction, includes wood, charcoal and cellulose, all of which can have a detrital origin. In an environment free from contamination all three fractions have the same age and the pretreatment method is not critical. But normally, the organic fractions are contaminated to some extent by both younger and older material, and the goal of pretreatment is to concentrate that fraction which is closest to the true age of the layer. Fulvic acid is the most mobile fraction and the most subject to younger contamination. This fraction is routinely removed by a weak acid wash (Fig. 6). Humic acids in solution can circulate through the groundwater, but only if the pH is greater than 2. It does not appear that humic acids are mobile to any significant extent at Wrightwood or the AO/AWA dates would not show the stratigraphic consistency observed. Removal of this fraction by AAA pretreatment (Fig. 6) concentrates detrital wood, charcoal, and cellulose. Thus, samples from a part of the section containing reworked organic matter can give dates that are too old (Fig. 5). Nearly all of the peats at Wrightwood contain roots that have penetrated from the overlying peat. These roots are close in age to the peat which they contaminate and have only a small (5-10 years) effect on the age of samples that are pretreated with AO or AWA. However, when the humic acids are removed with the more aggressive AAA pretreatment, the younger root cellulose makes up a more significant portion of the sample. Thus, samples from those parts of the section that have little or no detrital carbon can give dates which are too

young (Fig. 5). We plan further investigations into the most appropriate pretreatment for the peat samples at these sites. It may well be that isolation of the humic acid (alkali soluble) fraction alone may give the most accurate dates.

Laboratory radiocarbon dates for each site were dendrochronologically calibrated (Stuiver and Reimer, 1993). Peat layer dates were then refined using new applications of Bayesian statistical techniques; for Wrightwood and Pallett Creek the method of Biasi and Weldon was used (Biasi and Weldon, 1994a, b) while for Pitman Canyon, the OxCal program was used (Bronk Ramsey,1995, see also OxCal website). These techniques make use of dates of historic earthquakes, stratigraphic ordering, and peat accumulation rate to reduce layer-date distribution variance (Fig. 7) and allow better constrained age estimates. Prehistoric earthquake dates are obtained by calculating the probability distribution of the time interval between the bounding layer-date distributions.

Peat has been accumulating almost continuously at each site for at least the past several thousand years as water tables have remained high until about the turn of this century. Clastic sedimentation is essentially instantaneous and a small amount of time is unrecorded due the lag between sedimentation and colonization by plants. Peat accumulation rates average about 0.5mm/yr at each of the sites, but alternate between episodes of faster or slower rates (Fig. 8). These episodes, or peat accumulation stages, correlate very well between Wrightwood and Pallett Creek but the transitions occur earlier at Pitman Canyon. We believe that the peat accumulation rates are climatically controlled, being higher during relatively wet times and slower during drier times. Changes in rate occur earlier at Pitman Canyon either because it is below a critical elevation or perhaps because it faces SW rather than NE as the other sites do. The similarity in the peat accumulation rate curves at the three sites gives us increased confidence that the radiocarbon dates are reliable.

Refined earthquake-date distributions for the past 1000 years are shown for each site in Fig. 9. Overlap of these distributions suggests likely correlation of events between sites, but dating resolution is insufficient to prove such correlations for prehistoric earthquakes. If the distributions at adjacent sites do not overlap, we can be reasonably certain that the rupture stopped somewhere between the two sites. Rupture length is known only for the 1857 AD earthquake. Comparison of these results suggests that even with the exceptional stratigraphy and high-resolution dating at these sites, the paleoseismic record at a particular site may be incomplete. For example, Event T at Pallett Creek is likely the same earthquake as EV 6 at Pitman Canyon (Fig.

9). If so, this earthquake is not recognized at Wrightwood. This was apparently a dry period at Wrightwood: peat accumulation rate was low and essentially no clastic sediment was deposited. Hence, it is not surprising that an earthquake rupture during this period might not be preserved as a discrete event. Similarly, WE5 at Wrightwood apparently does not correspond to any event at Pallett Creek or Pitman Canyon. If our interpretation of the evidence for this event horizon and our dating of this event are correct, then either this earthquake rupture was short (<50km) or it is unrecognized at one or both of the other sites. It may be the same as EV4 or EV5 at Pitman Canyon if the event dating is incorrect at either or both sites.

Keeping in mind these uncertainties in event correlation, completeness of the paleoseismic record, and event dating, a possible pattern of earthquake ruptures on the south-central San Andreas fault may be emerging from the paleoseismic data. It appears that large earthquakes rupturing through all three sites, such as 1812 AD, alternate with earthquakes that rupture into the region from the northwest or southeast, such as 1857 AD or event WE3/EV2. This latter earthquake may be the same as the most recent event reported at Indio on the Coachella Valley segment (Sieh, 1986).

The paleoseismic records from these three closely spaced sites allow re-evaluation of the fault segmentation model proposed by the Working Group on California Earthquake Probabilities. The 1857 earthquake rupture stopped somewhere between Wrightwood and Pitman Canyon (Weldon and Sieh, 1985). This led the Working Group to place the Mojave/San Bernardino segment boundary between these two locations. But wherever this rupture stopped, it cannot be a persistent barrier to fault rupture as it appears likely that no more than one other earthquake in the past 1000 years also terminated between Wrightwood and Pitman Canyon (WE5). It does not appear that a strong boundary exists between Wrightwood and Pallett Creek either, as large earthquakes frequently appear to rupture through this portion of the fault. The paleoseismic evidence suggests that there is no persistent segment boundary anywhere between Pallett Creek and Pitman Canyon.

References

Biasi, G., and Weldon II, 1994a, Quantitative refinement of C-14 distributions, *Quaternary Research,* 41, 1-18.

Biasi, G., and R. J. Weldon II, 1994b, Quantitative approaches to event dating and constraint, *Proceedings of the Workshop on Paleoseismology; U.S. Geological Survey Open-File Report 94-568,* 18.

Bronk Ramsey, C., 1995, Radiocarbon calibration and analysis of stratigraphy: the OxCal program, *Proceedings of the 15th International Radiocarbon Conference, Radiocarbon,* 37, 425.

Fumal, T. E., S. K. Pezzopane, R. J. Weldon II, and D. P. Schwartz, 1993, A 100-year recurrence interval for the San Andreas Fault at Wrightwood, California: *Science, 259*, 199-203.

Salyards, S. L., K. E. Sieh, and J. L. Kirschvink, 1992, Paleomagnetic measurement of nonbrittle coseismic deformation across the San Andreas Fault at Pallett Creek, *J. Geophy. Res., 97*, 12457-12470.

Seitz, G., R. J. Weldon II, and G. Biasi, 1997, The Pitman Canyon paleoseismic record: a re-evaluation of southern San Andreas Fault segmentation, *Journal of Geodynamics, 24*, 129-138.

Seitz, G. , and R. J. Weldon II, 1994a, The paleoseismology of the southern San Andreas Fault at Pitman Canyon, San Bernardino, California, *Geological Society of America Cordilleran Guidebook, Geological investigations of an active margin* McGill, S.F. and T. M. Ross, (eds.), 152-156.

Seitz, G. , and R. J. Weldon II, 1994b, The Pitman Canyon paleoseismic record will test San Andreas Fault segmentation, *Proceedings of the workshop on paleoseismology, U.S. Geological Survey Open-File Report 94-568,* 166 pp.

Sieh, K.E., 1978, Prehistoric large earthquakes produced by slip on the San Andreas Fault at Pallett Creek, California: *J. Geophy. Res., 83*, 3907-3939.

Sieh, K.E., 1984, Lateral offsets and revised dates of large earthquakes at Pallett Creek, California: *J. Geophy. Res., 89*, 7641-7670.

Sieh, K.E., 1986, Slip rate across the San Andreas fault and prehistoric earthquakes at Indio, California, *EOS Transactions, American Geophysical Union, 67*, 1200.

Sieh, K.E., M. Stuiver, and D. Brillinger, 1989, A more precise chronology of earthquakes produced by the San Andreas Fault in southern California, *J. Geophy. Res.,* 94, 603- 623.

Stuiver, M., and P. Reimer, 1993, Extended C14 data base and revised CALIB 3.0 C14 age calibration program, *Radiocarbon, 35*, 215-230.

Weldon, R.J. II, 1991, Active tectonic studies in the United States, 1987-1990, *Reviews of Geophysics. Supplement. American Geophysical Union, U.S. National Report to International Unions of Geodesy and Geophysics* 1987-1990, 890-906.

Weldon, R.J. II, and K. E. Sieh, 1985, Holocene rate of slip and tentative recurrence interval for large earthquakes on the San Andreas fault, Cajon Pass, southern California, *Geol. Soc. Am. Bull., 96*, 793-812.

WGCEP, 1988, Probabilities of large earthquakes occurring in California on the San Andreas Fault, *U.S. Geological Survey Open-File Report 88-398.*

WGCEP, 1995, Seismic hazards in Southern California: probable earthquakes, 1994-2024, *Bull. Seism Soc. Am., 85*, 379-439.

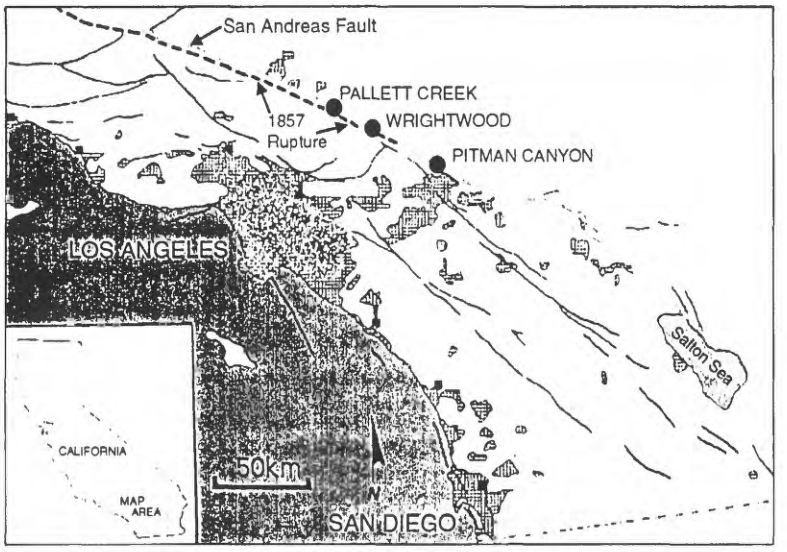

Figure 1. Map of southern California showing major faults (lines) and urban areas (patterned). Locations of paleoseismic sites along the south central San Andreas fault are shown as solid circles. Southern part of the 1857 rupture indicated by dashed line.

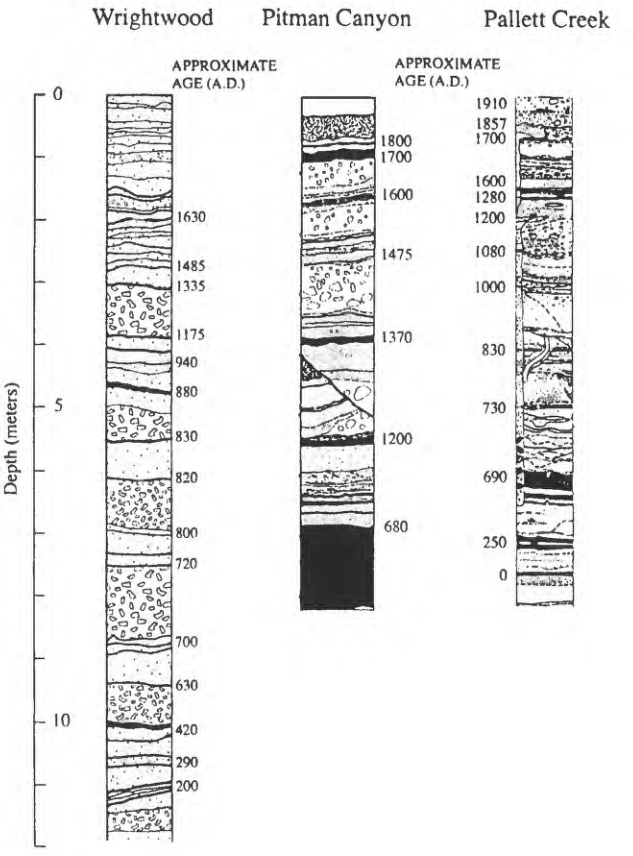

Figure 2. Composite stratigraphic sections at the paleoseismic sites. Peat layers are black, other layers are fluvial and/or debris flow deposits. Clastic sedimentation at Pallet Creek is entirely fluvial in origin. Debris flows dominate at Wrightwood and Pitman Canyon. Approximate ages of selected peat layers are indicated. Note that at Wrightwood, nearly every depositional contact is a peat layer.

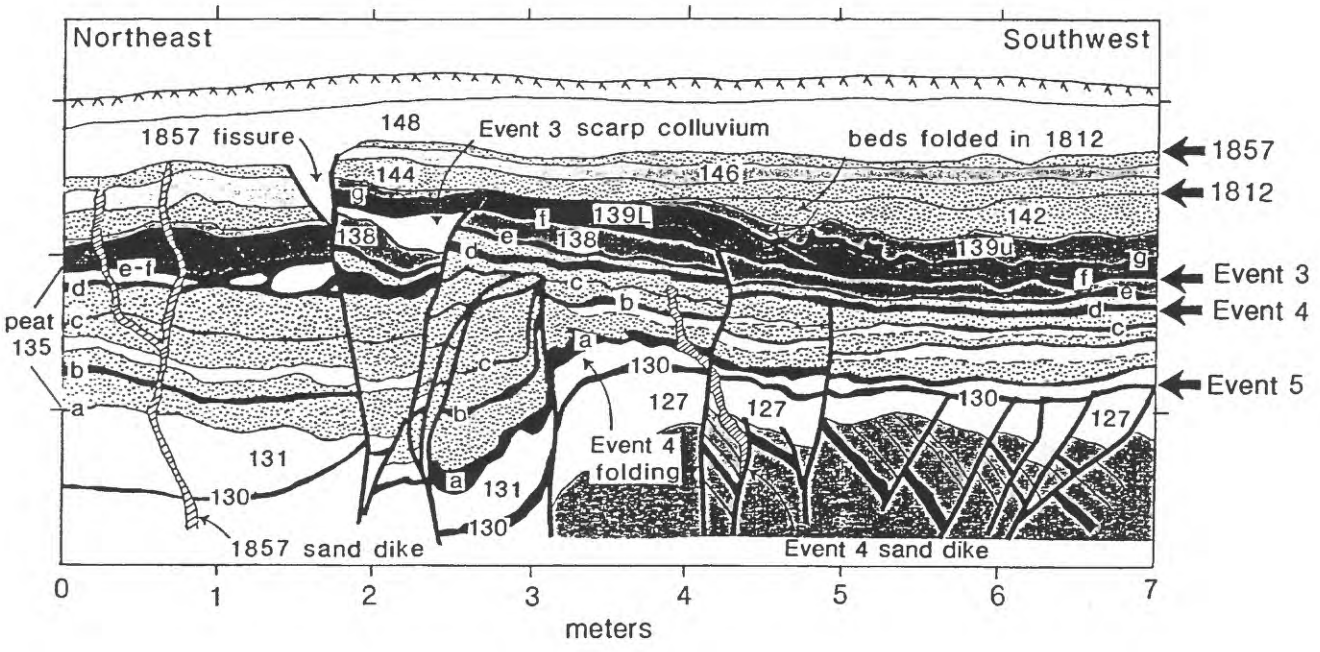

Figure 3a. Composite log of main fault zone at Wrightwood showing deformation associated with past five earthquakes. Fault strands shown by heavy lines. Peat layers are black, stippled units are granitic fluvial deposits. All other units are debris flow deposits. Earthquake horizons are shown by broad arrows.

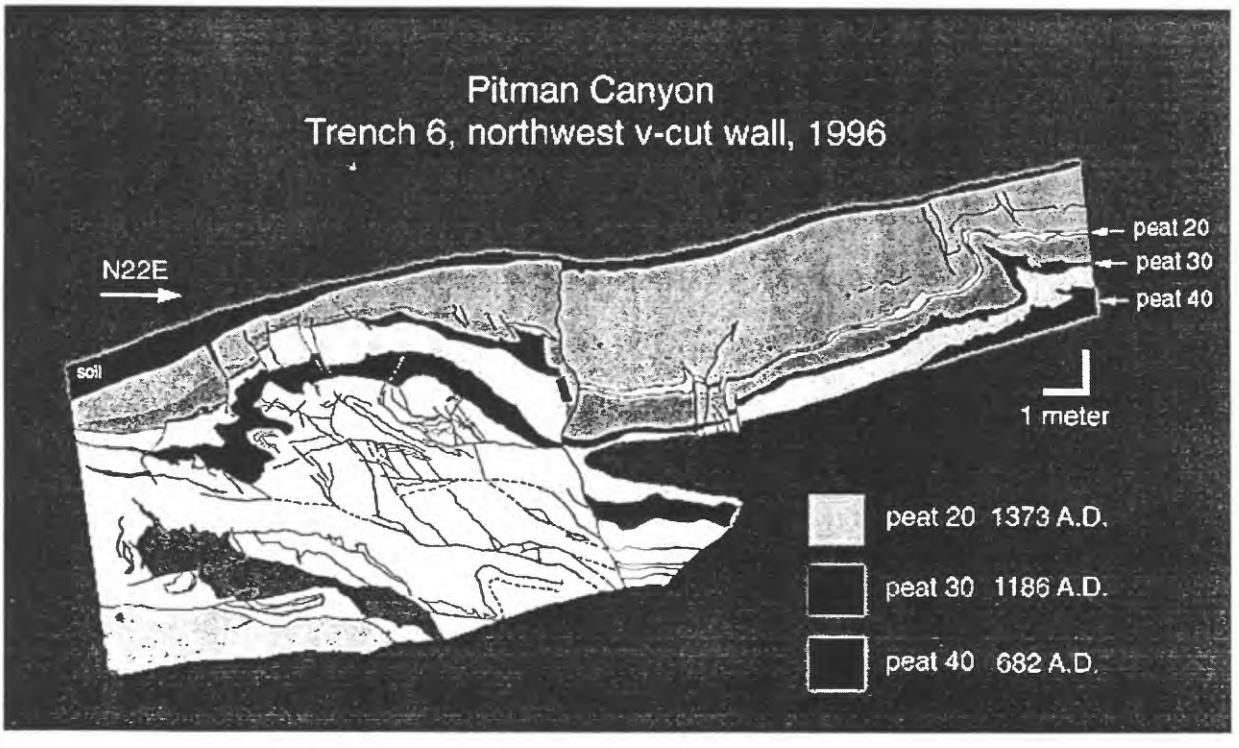

Figure 3b. Simplified log of northwest wall of trench 6 at Pitman Canyon. Note that movement of major vertical fault near center of exposure produces an uphill-facing scarp. Subsequent debris flow deposits are significantly thicker on the uphill side of the fault. This relationship is repeated many times down-section. Analysis of fold at uphill end of excavation indicates that it formed by movement during three separate events.

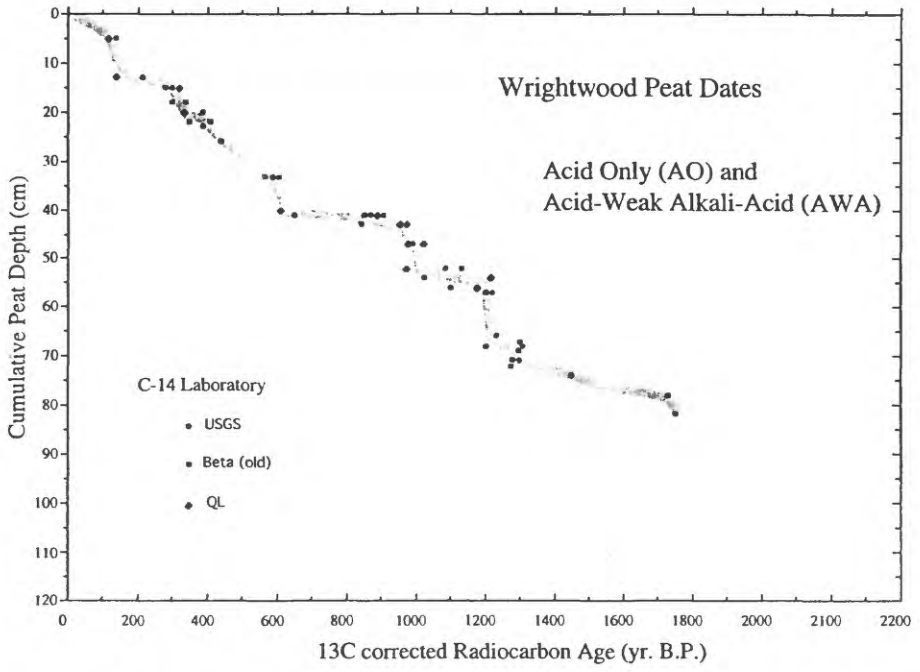

Figure 4. Radiocarbon dates at Wrightwood. USGS samples were treated with an acid wash/ short duration weak alkali wash/ acid wash (AWA) pretreatment. Samples from other laboratories were treated with acid wash only (AO).

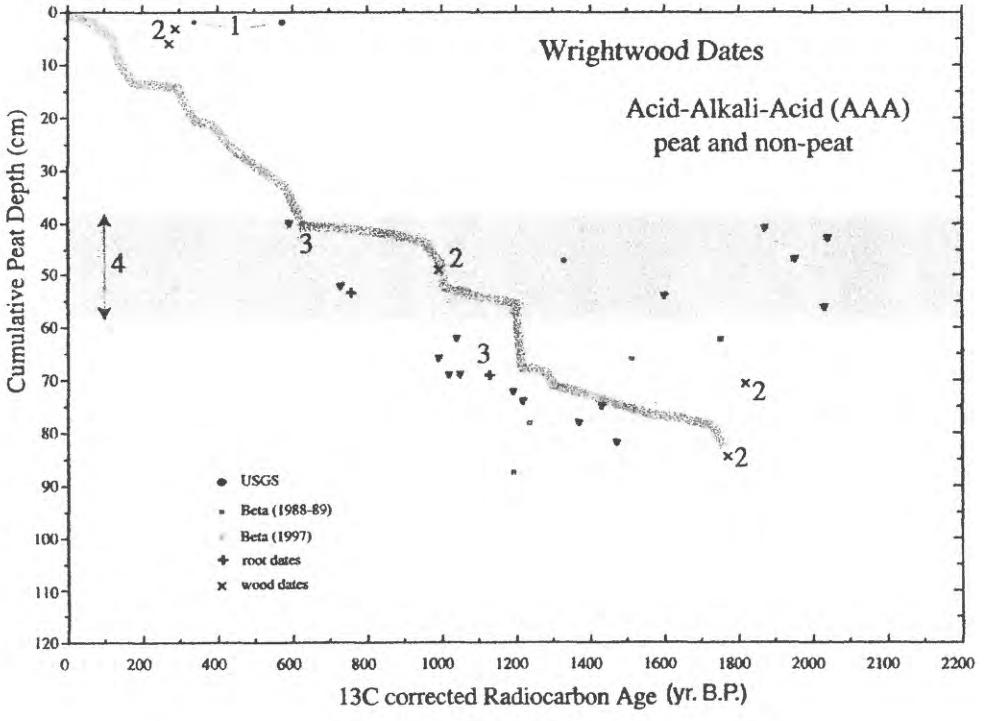

1 - peat 140 only exists in fault graben; almost certainly contains detrital material exposed from older peats
2 - small sticks or pine cones in clastic units: dates must be the actual age
3 - roots invading peat from overlying peat layer
4 - part of section rich in charcoal and wood, probably due to a fire in the headwaters

Figure 5. Radiocarbon dates for samples from Wrightwood with acid wash/ strong alkali wash/ acid wash pretreatment (AAA). Mean trend of dates for samples with AO and AWA pretreatments shown as heavy grey line.

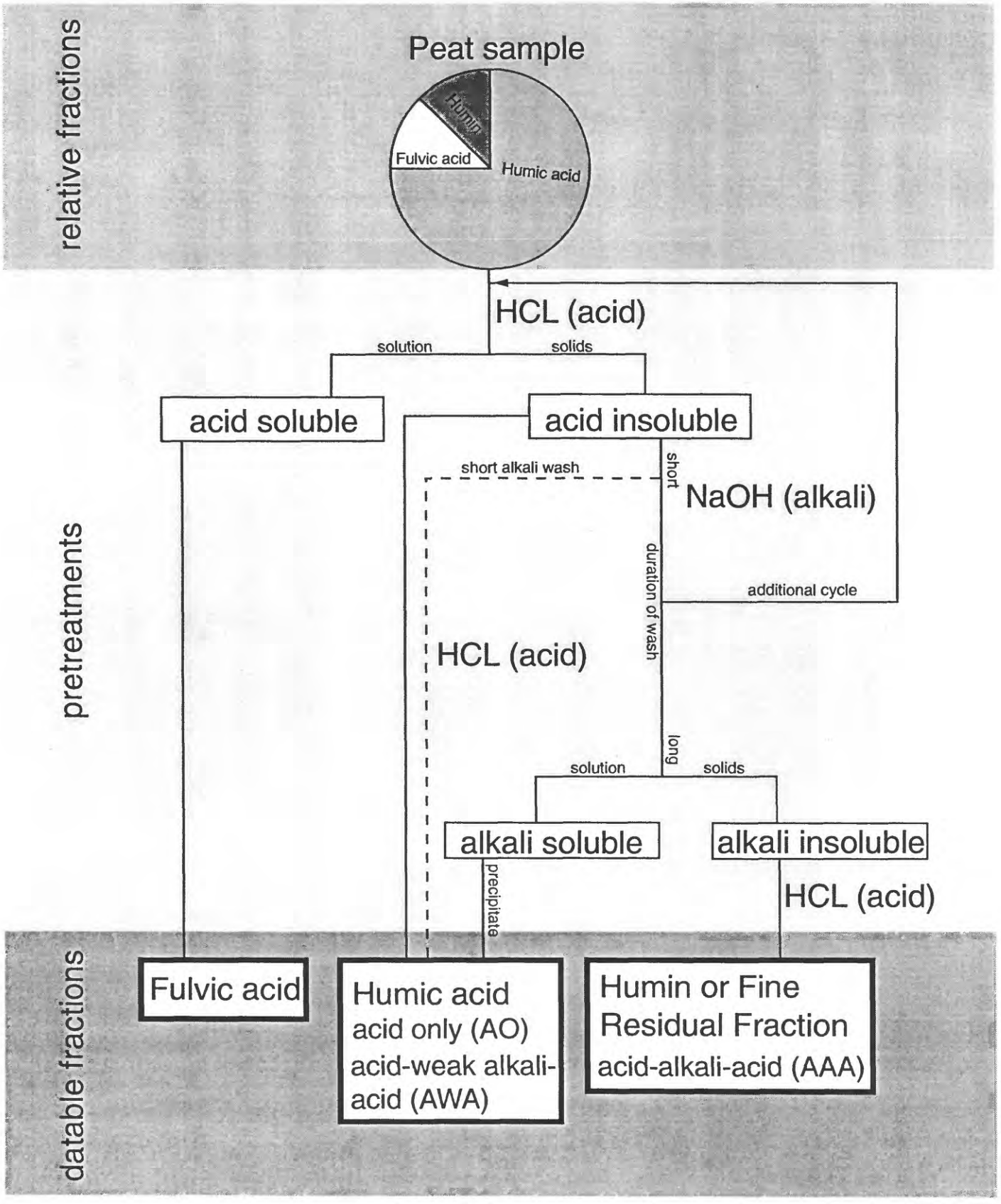

Figure 6. Flow chart of organic fractions and pre-treatment procedures for radiocarbon dating of peaty materials.

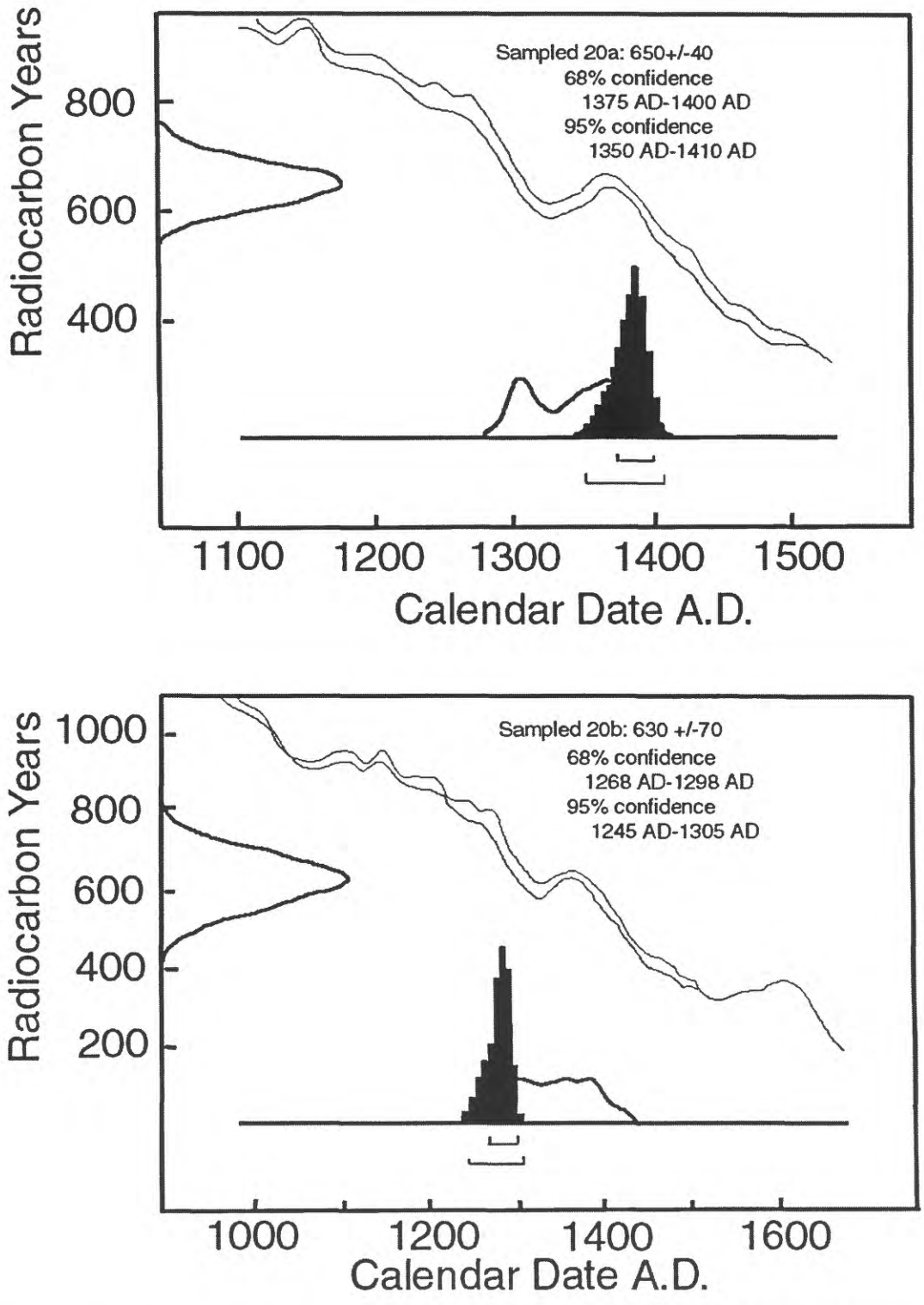

Figure 7. Dendrochronological calibration for samples from two different layers. Note that that the initial calibrated layer date distributions (line) have considerable overlap. Using stratigraphic ordering and/or sedimentation rate constraints allows re-calculation of the distributions (solid).

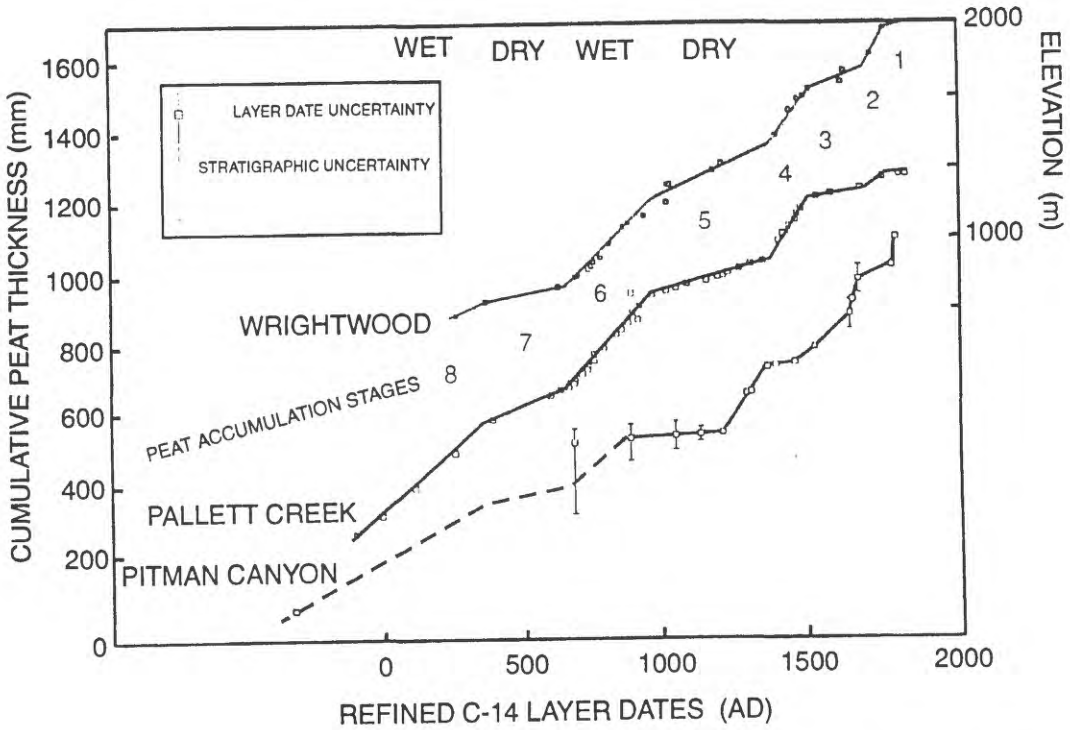

Figure 8. Peat accumulation rates for Wrightwood, Pallett Creek, and Pitman Canyon with possible climatic stages. Note that timing of rate changes correlate very well at Wrightwood and Pallett Creek but occur earlier at Pitman Canyon.

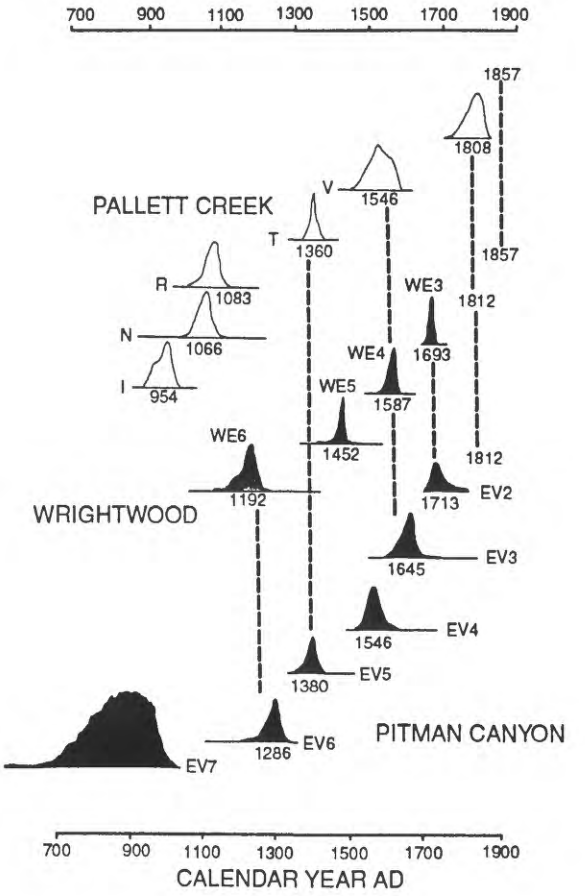

Figure 9. Paleoseismic records for Wrightwood. Pallett Creek and Pitman Canyon for the past 1000 years. Event date distributions calculated from layer date distributions constrained by historic earthquake dates, stratigraphic ordering, and sedimentation rate. Mean dates are shown under the event distributions. Events in AD 1812 and 1857 are historic. Dashed lines indicate likely, but unprovable, event correlations.

Earthquake recurrence on the Washington part of the Cascadia subduction zone

Brian F. Atwater

U.S. Geological Survey, Seattle, USA

atwater@u.washington.edu

Subduction-zone earthquakes of magnitude 8 or larger pose a poorly quantified threat to the northwestern United States and southwestern Canada (Clague, 1997). Their history in southwestern Washington state has been inferred from a 3500-year record sudden subsidence (Atwater and Hemphill-Haley, 1997).

This record contains seven events each interpreted as a great earthquake on the Cascadia subduction zone. Although seven is a large number of events for a paleoseismic record, these events may be too few to provide much guidance about the conditional probability of the next great earthquake on the southern Washington part of the Cascadia subduction zone.

Geologic evidence for the seven events and mostly unpublished estimates of their ages are summarized on an accompanying page of illustrations (Fig. 1).

References

Atwater, B. F., and E. Hemphill-Haley, 1997, Recurrence Intervals for Great Earthquakes of the Past 3,500 Years at Northeastern Willapa Bay, Washington. *U.S. Geological Survey Professional Paper, 1576*, 108 pp.

Clague, J. J., 1997, Evidence for large earthquakes at the Cascadia subduction zone. *Reviews of Geophysics, 35*, 439-460.

Bronk Ramsey, C., 1995, Radiocarbon calibration and analysis of stratigraphy: the OxCal program, *Radiocarbon, 37*, 425-430.

Stuiver, M., P. J. Reimer, E. Bard, J. W. Beck, G. S. Burr, K. A. Hughen, B. Kromer, F. G. McCormac, J. v. d. Plicht, and M. Spurk, 1998, INTCAL98 Radiocarbon age calibration 24,000 - 0 cal BP, *Radiocarbon, 40*, 1041-1083.

The study area is along a central part of the Cascadia subduction zone (upper right). Cascadia is about as long as Honshu.

Geologic evidence for Cascadia earthquakes most commonly consists of buried soils at estuaries. Differences among successive soils provide field evidence for correlating the soils among estuaries in the study area (middle left).

Some of the inferred earthquakes are more convincing than others. They differ in the strength of known evidence that land subsided and that this subsidence accompanied a tsunami, shaking, or both (middle right).

The inferred history contains seven events in the past 3500 years. Some are dated much more exactly than others (bottom).

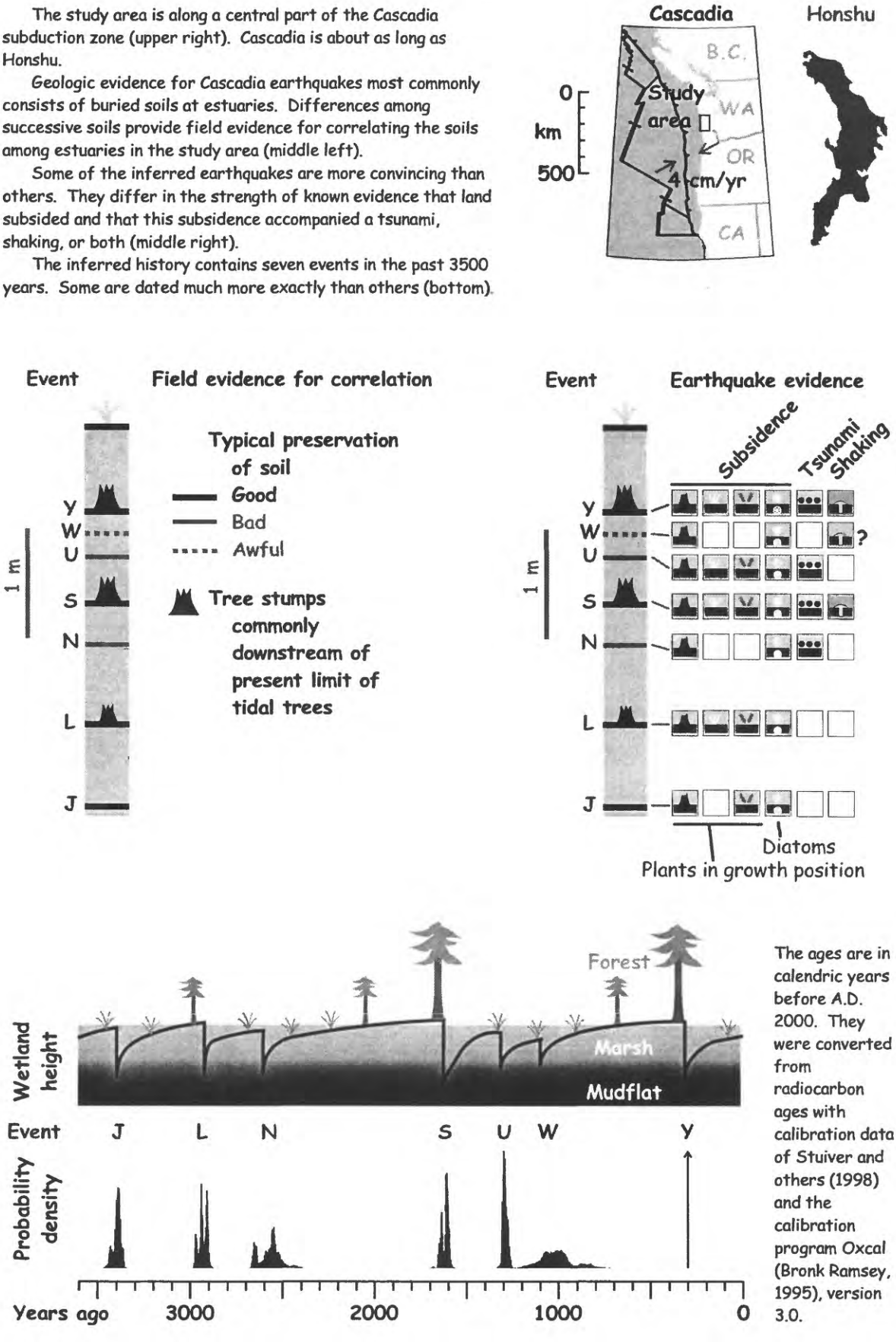

The ages are in calendric years before A.D. 2000. They were converted from radiocarbon ages with calibration data of Stuiver and others (1998) and the calibration program Oxcal (Bronk Ramsey, 1995), version 3.0.

Figure 1. Index map, generalized columnar sections, and inferred history of coseismic subsidence in southern coastal Washington.

Multiple large earthquakes in the past 1500 years on a fault in metropolitan Manila, The Philippines

Alan R. Nelson [1], Stephen F. Personius [1], Rolly E. Rimando [2],
Raymundo S. Punongbayan [2], Norman Tuñgol [2],
Hannah Mirabueno [2] and Ariel Rasdas [2]

[1] U.S. Geological Survey, Denver, USA
[2] Philippine Institute of Volcanology and Seismology
University of the Philippines, The Philippines

anelson@gldvxa.cr.usgs.gov

Recent assessment of the earthquake hazard posed by crustal faults in cities such as Los Angeles and Seattle and the economic and human loss resulting from recent damaging earthquakes in Northridge, California and Kobe, Japan highlight the need for evaluating potentially active crustal faults in urban areas. Manila—with a metropolitan population of about 10 million—is subject to earthquakes on nearby crustal faults as well as earthquakes on more distant plate-boundary faults. The city has been heavily damaged by earthquakes at least six times in the past 400 years, but specific sources for the earthquakes are uncertain. The Marikina Valley fault system, on the northeastern edge of the Manila metropolitan area (Fig. 1), is a likely source of one or more of these earthquakes. Determining the rate of recurrence of large earthquakes on these crustal faults is critical for estimating the strength and probability of future earthquake ground motions in the metropolitan area.

Here we report the first earthquake recurrence estimate based on radiocarbon ages on a hazardous fault in The Philippines—the westernmost fault in the Marikina Valley system, which lies only 10 km east of central Manila. Trenches and stream-bank exposures at the Maislap site on a northern splay of the west Marikina Valley fault (Fig. 1) show fault strands displacing silty hillslope colluvium, gravelly stream-channel alluvium, and cobbly debris-flow deposits (Fig. 2). Stratigraphic relations among upward terminations of fault strands and soil B horizons developed on three sequences of stream and colluvial sediment in the trenches suggest 2-3 surface-faulting events (Fig. 3). Although most of the 19 ^{14}C ages on detrital charcoal from these deposits are older than their host sediment, the closest maximum ages constrain the entire stratigraphic sequence to the past 1300-1700 years. Three reddish, clay-rich soil B horizons suggest

intervals of at least hundreds of years between surface-faulting events. Minimal soil development and modern ^{14}C ages from colluvium overlying a faulted debris-flow deposit in a nearby stream exposure point to a historic age for a probable third or fourth (most recent) faulting event (Fig. 2).

Neither radiocarbon dating nor the degree of soil development on stratigraphic units at the Maislap site provide entirely consistent numerical ages for most units. Most ^{14}C samples (Fig. 2) consist of detrital charcoal and, therefore, their ages are only maximum ages for the host sediment. We did not measure or directly calibrate the rate of soil development on stratigraphic units using ^{14}C or any other numerical dating method. Furthermore, many soil horizons are hard to interpret because they have been partially eroded or incorporated into younger overlying soils. Nevertheless, we estimated the times of surface-faulting events at the site by considering the maximum (17 samples) and minimum (two samples) age constraints provided by ^{14}C ages and the position of remnants of clay-rich soil horizons within the stratigraphic sequence.

Based on our interpretation of the exposures at the Maislap site, at least two and perhaps four surface-rupturing earthquakes have occurred on the northeastern splay of the west Marikina Valley fault since AD 600 (Fig. 2). This is a short interval of time relative to the total errors in the ^{14}C dating of faulting events, and most ^{14}C ages are on detrital (transported) charcoal that provide only maximum constraints on the times of faulting. For these reasons, we cannot determine the time of each faulting event or calculate precise earthquake recurrence intervals. Four surface-rupturing earthquakes over a period of <1300 years (the interval AD 600 to AD 1863) suggests average recurrence intervals of <500 years. But if only two earthquakes occurred (If A? and B are same event, and C and D are the same event; Figs. 2 and 3), recurrence could be more than 1000 years.

We suggest a conservative range of 300-1000 years be used in assessing the hazard from surface-rupturing earthquakes on the northern part of the west Marikina Valley fault. Such a range reflects the uncertainty of our dating and the fact that recurrence data are available from only a single site on a splay of the fault. Both historic and detailed prehistoric records of large earthquakes illustrate that recurrence on individual faults is commonly clustered. However, the time intervals needed to form the three soils with argillic B horizons in trench 1 argue for earthquakes that were not tightly clustered in time. For this reason and because we think events C and D are separate events, we favour shorter recurrence intervals of roughly 400-600 years over longer intervals of 1000 years.

Acknowledgements

S. T. Algermissen (USGS) obtained funding for the project from the U.S. Agency for International Development—The Philippines. R.S. Punongbayan obtained further funding from the Philippine Department of Public Works and the insurance industry in Manila. We thank David Nelson and José Garzon of U.S. AID in Manila for being strong advocates of our work. Takashi Nakata (Hiroshima University, Japan) identified the Maislap trench site and encouraged us to trench it. We especially thank Rodolfo Alito and his family for permission to dig up their rice paddies and for hiring and supervising laborers at the site.

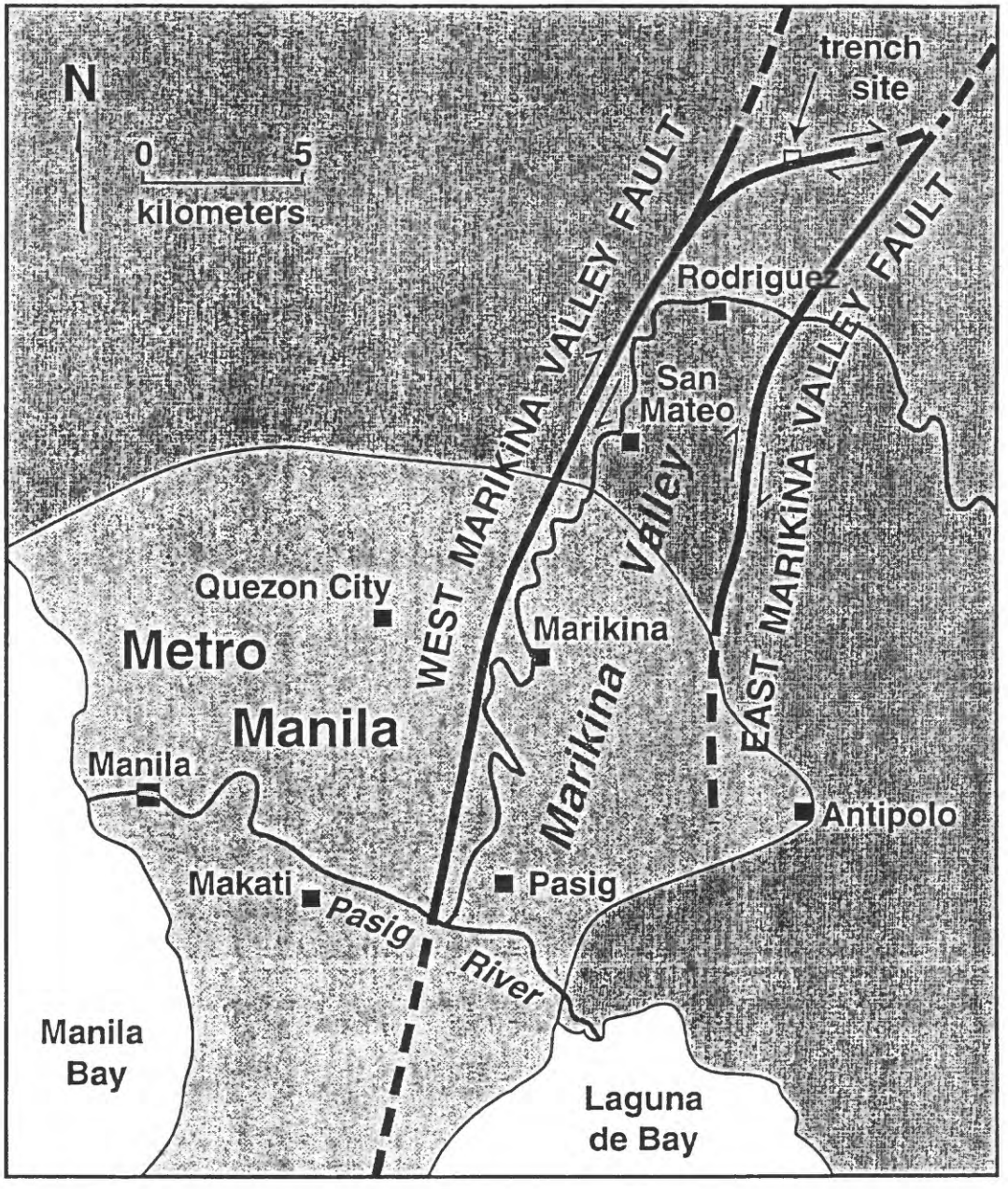

Figure 1. Map showing the locations of the east and west Marikina Valley faults, which strike through the metropolitan Manila area (Metro Manila, light shading) of central Luzon. The Maislap trench site is on a northeast-trending splay of the west Marikina Valley fault in the northern part of the Marikina Valley.

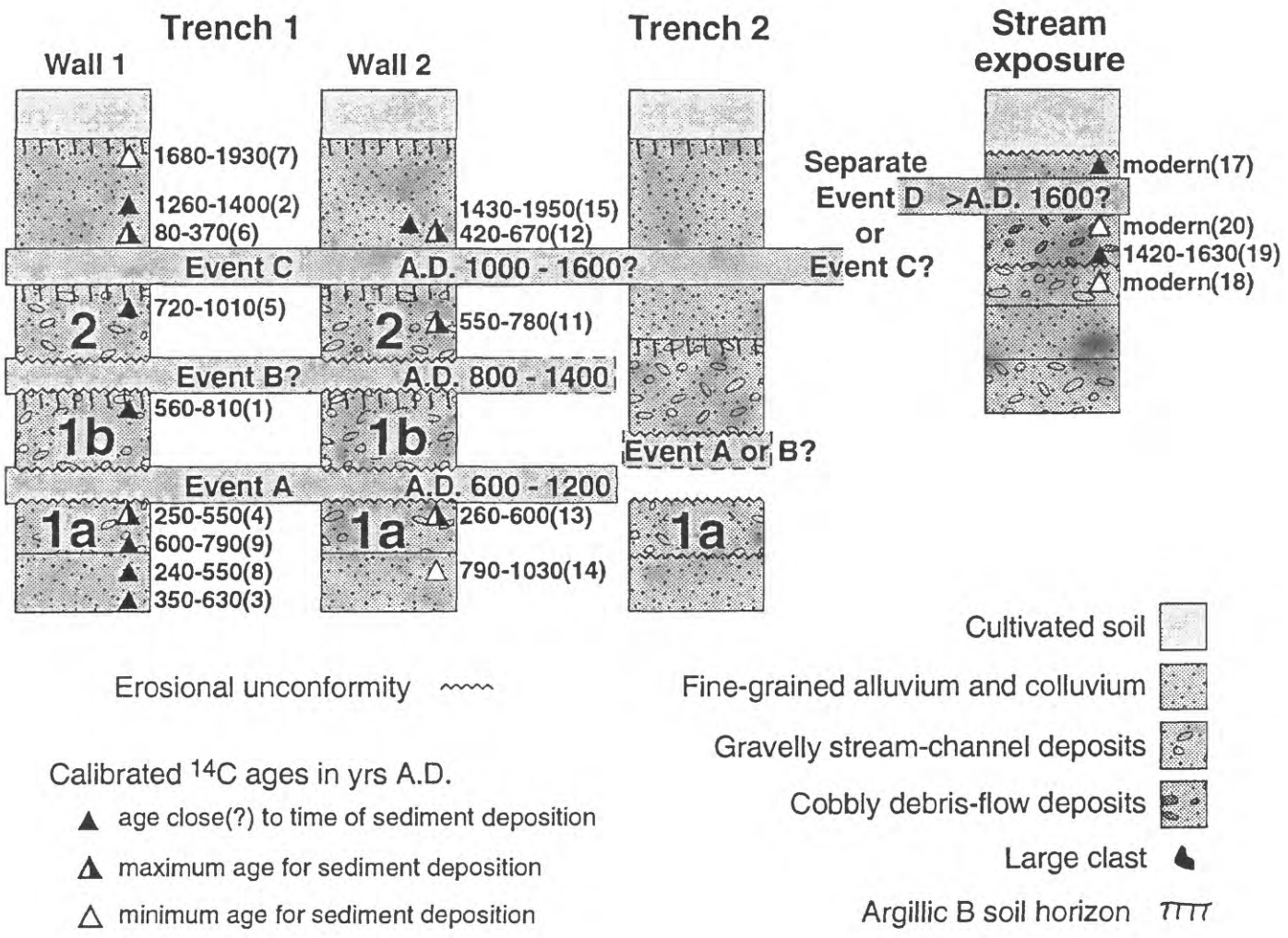

Figure 2. Diagram showing relations among stratigraphic units and timing of surface-faulting earthquakes at the Maislap site. Triangles show ^{14}C-dated charcoal samples; ^{14}C ages are calibrated and expressed as time intervals in cal yr AD (approximate calendar years A.D.) at two standard deviations and rounded to the nearest 10 years. Large numbers correspond with sequences of stream-channel and colluvial deposits (sequences 1a, 1b, and 2) displaced during faulting events A?, B, and C, respectively. Erosional unconformities bounding deposits are inferred from truncated bedding and soil horizons. Question marks indicate uncertainty in the existence of event A, the stratigraphic position of events B and C in trench 2, and the age range of event C.

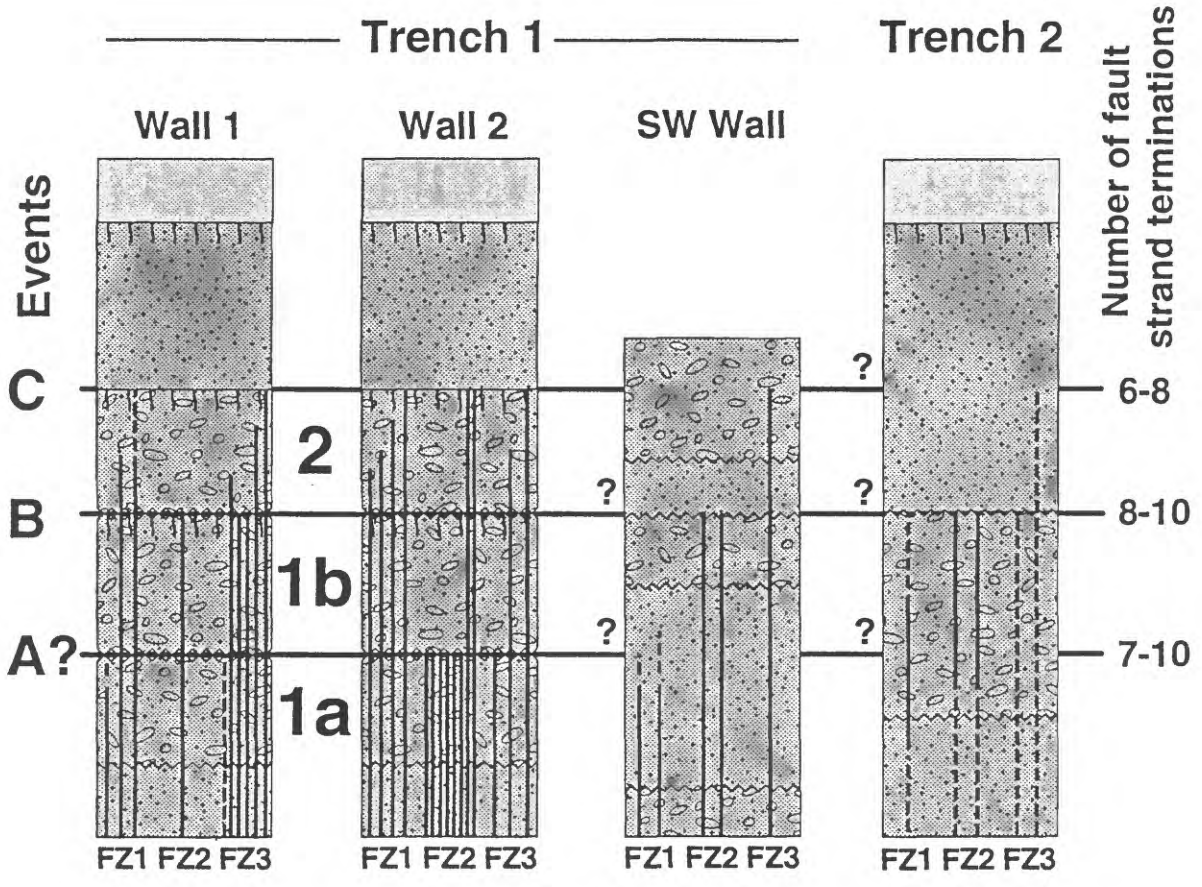

Figure 3. Vertical extent of fault strands (solid vertical lines) in fault zones (FZ1, FZ2, FZ3) relative to the stratigraphic position of surface faulting events A?, B, and C in trenches 1 and 2. Patterns, symbols, and labels for faulting events, stratigraphic sequences, and fault zones as in Figure 2. Indistinct or inferred parts of strands are dashed. The range in the number of terminations for each faulting event (right edge of figure) is the number of distinct strands and the total number of strands. Question marks indicate uncertainty in the correlation of faulting events to strands in the southwest wall of trench 1 and in trench 2. Although as many strands were mapped terminating near the position of event A? as for any other event (7-10), all but one of the distinct strands terminating at this position were in one fault zone (FZ2, Wall 2). For this reason, we cannot demonstrate that event A? is a separate faulting event.

The 1700 Cascadia earthquake: Tree-ring data processing, a progress report, and opportunities for continuing Japan-US collaboration

David Yamaguchi

Xylometric Co., USA

TrRingzRUs@aol.com

Introduction

I thank our Japanese hosts for their generous invitation to come here and speak today. I'm always happy to come to Japan. It's very fun because I can "pass" for a Japanese person on the street even though I am really a foreigner. This creates many amusing situations, as I'm sure you can imagine.

The 1700 Cascadia earthquake, which occurred on the Cascadia subduction zone offshore of the Pacific Northwest coast of North America, has been a major focus of paleoseismic research in the US and in Japan over the past decade. Accordingly, today I had planned to review four topics--(1) the research setting for tree-ring dating the 1700 earthquake; (2) details of data processing; (3) a progress report; and (4) opportunities for continuing Japan-US collaboration. However, after submitting my title, I decided to omit the data processing. (It seemed too "boring" to discuss here today, even though it has not yet been reported in detail and is an important component of the work.) Instead, I will cover only topics (1), (3), and (4).

(1) The research setting

As most of you know, the 1700 Cascadia earthquake has been dated to 9 p.m. local time on January 26, 1700. This remarkable result evolved from a series of steps:

(a) Conventional radiocarbon dating first identified the time of occurrence as "about 300 years BP" (*e.g.*, Nelson, 1992).

(b) High-precision radiocarbon dating focused the possible interval to 1680 to 1720, at least for southern coastal Washington (Atwater *et al.*, 1991).

(c) High-precision dating, applied to the entire Cascadia coast from British Columbia to northern California, raised the possibility of a moment-magnitude 9 event (Nelson *et al.*, 1995).

(d) Japanese historical records of a large tsunami from afar supported the inference of a magnitude 9 event, as well as assigned the calendar date and time (Satake *et al.*, 1996).

(e) Last, tree-ring dating of killed trees along 90 km of southern Washington coast proved that the tsunami came from Cascadia. The dated trees have outermost ring dates of 1699--the last growing season before the earthquake (Yamaguchi *et al.*, 1997).

The evidence in (d) for a magnitude 9 event can be summarized by paraphrasing the Japanese pop song, "*Ai hitotsu, yume hitotsu*" ["One love, one dream" by Kye Eunsook] as "*Tsunami hitotsu, jisshin hitotsu.*" ["One wave, one quake"]. In other words, only one big tsunami was recorded in Japan instead of several smaller ones spaced closely in time. Thus, there must have been only one big source-earthquake.

(3) Progress

The main progress I would like to report on is the presence of a likely 1700-earthquake-killed redcedar tree, the species we have been working with, 100 km north of the limit of our current sampling distribution on the Washington coast. A tip from a local resident places the tree at LaPush on the northern Washington coast. The presence of this rooted tree, near the beach, is significant because it holds the promise of doubling the length of coast over which we can demonstrate synchronous coastal submergence. The length of affected coastline is important because it improves knowledge of the area of slip of the earthquake, and thereby, of earthquake magnitude.

(4) Opportunities

During the past five years, I believe the world has changed from one of Japanese earthquake scientists doing their thing, and Americans doing theirs, to one where increasing efforts are being made to work together. These changes in part reflect the Kobe earthquake and the publication of Satake and *et al.* (1996) paper. Now, we're all on the same team. The question thus becomes, how can we best utilize our joint efforts?

Speaking as a Seattle resident, I can say that the "Person in the street" there is generally aware of the Cascadia great-earthquake hazard. The topic has received much recent media coverage, even in the time since Brian Atwater has been here in Japan

(since September; *e.g.*, Pierce, 1988). Ordinary people I've met recently such as a tow truck driver, my dental hygienist, and my doctor are all aware of the hazard.

In contrast, the Seattle public is *not* aware of the associated tsunami hazard. Unlike Japan, tsunami are outside of the experience of most Americans. Basic knowledge of tsunami is therefore lacking. (Lately, some efforts have been made to improve this situation, however, *e.g.*, Atwater *et al.* in press).

In addition to having long historical records of earthquakes and tsunami, Japan also appears to have abundant tsunami educational materials. One example is artwork of people caught in tsunami from the 1896 Sanriku earthquake (Fig. 1). Another is the detailed description of historical accounts of runup of the tsunami from the 1700 Cascadia earthquake (Tsuji *et al.* 1998). Accordingly, much can be accomplished by translating existing Japanese materials into English, and by repackaging it for American readers.

Starting tomorrow, Brian and I are setting out on a two-week tsunami tour, a *tsunami monogatari*, to see what we can learn of the Japanese tsunami record in this time. One purpose is to see for ourselves the sites and documents of the 1700 run-up. We will travel from Kii-Tanabe (Wakayama-ken) to Miyako (Iwate-ken), retracing the path of Satake *et al.* (1996) and Tsuji *et al.* (1998). A second purpose is to compare runup from that event with that from the 1960 Chilean earthquake to improve knowledge of the magnitude of the 1700 earthquake. A third purpose is to gather materials that will help us explain tsunami hazards to the American public. We will not be able to do much more than an exploratory survey on our brief trip, so undoubtedly we will have to come back at some point.

To complete these and related efforts, we will need the cooperation of many Japanese researchers. During the next few years, they may receive e-mail requests for help from us for various things. We hope that you will join us in these efforts.

References

Atwater B. F., M. Cisternas, J. Bourgeois, 1999, Tsunami survival, lessons from the Chilean tsunami of 1960, *U.S. Geological Survey Circular*, in press.

Atwater B. F., M. Stuiver, D. K. Yamaguchi, 1991, Radiocarbon test of earthquake magnitude at the Cascadia subduction zone, *Nature,* 353, 156-158.

Nelson A. R., 1992, Discordant ^{14}C ages from buried tidal-marsh soils in the Cascadia subduction zone, southern Oregon coast, *Quaternary Research,* 38, 75-90.

Nelson A. R., *et al.*, 1995, Radiocarbon evidence for extensive plate-boundary rupture about 300 years ago at the Cascadia subduction zone, *Nature*, 378, 371-374.

Pierce J. K., 1998, The Big One, *Seattle Magazine*, *7* (October), 30-35, [www.seatlemag.com].

Satake K, K. Shimazaki, Y. Tsuji, K. Ueda, 1996, Time and size of a giant earthquake in Cascadia inferred from Japanese tsunami record of January 1700, *Nature*, *379*, 246-249.

Tsuji Y, K. Ueda, K. Satake, 1998, Japanese tsunami records fromthe January 1700 earthquake in the Cascadia subduction zone, *Zisin, 51*, 1-17.

Yamaguchi D.K., B. F. Atwater, D. E. Bunker, D. E. Benson, M. S. Reid, 1997, Tree-ring dating the 1700 Cascadia earthquake, *Nature, 389*, 922-923 (correction in 390, 352).

Yamashita, 1995, *Meiji sanriku dai tsunami* [*The Meiji-period great Sanriku tsunami,* in Japanese].

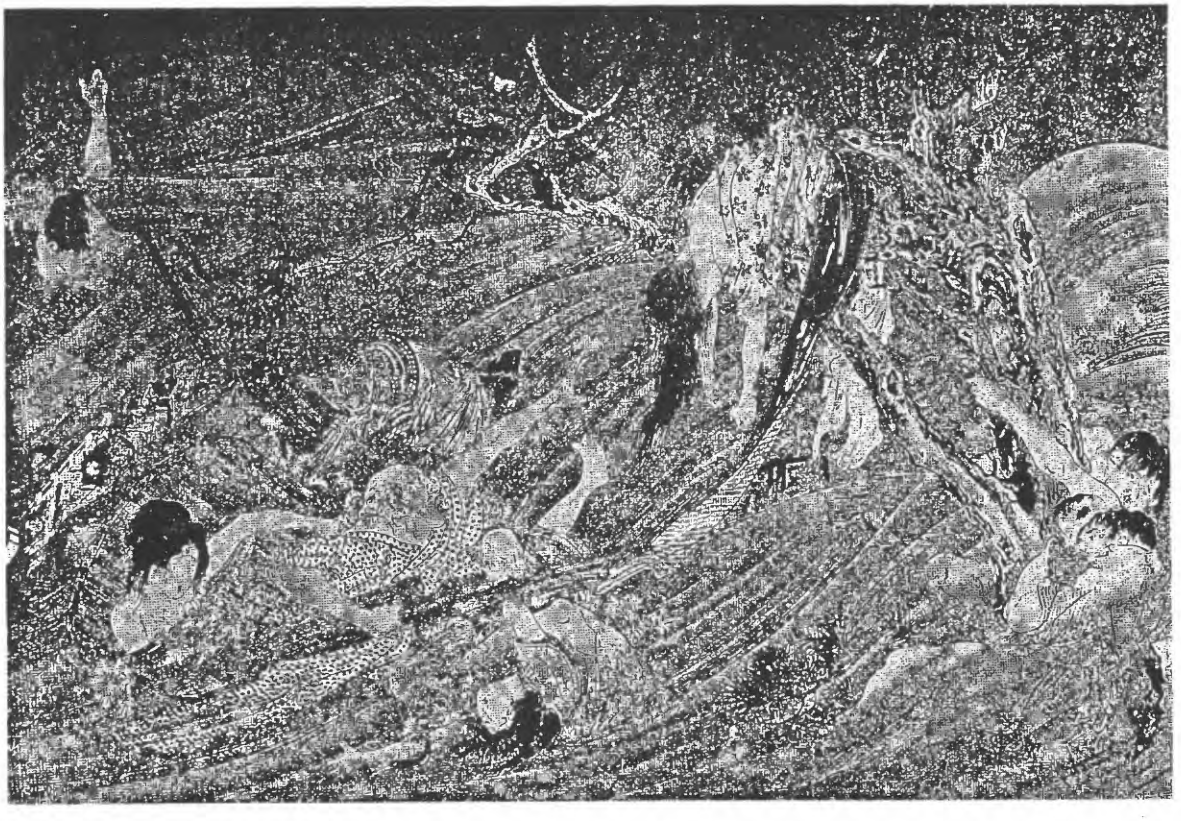

Figure 1. People in the 1896 Sanriku tsunami (from Yamashita 1995).

On/off fault paleoseismology

Yoshihiro Kinugasa *

Geological Survey of Japan
* Now at Tokyo Institute of Technology

king@depe.titech.ac.jp

Recurrence time of large or great earthquakes is much longer than the history of instrumental seismological observation; hence the paleoseismological method is essential to understand large earthquakes.

The accomplishments of paleoseismological studies in the last two decades are summarized as "On Fault Paleoseismology". During the past two decades extensive efforts to reveal paleoearthquakes have been made mostly by means of trench excavation on active faults, yielding many important concepts of paleoseismicity, such as the recurrence models of fault movement. Accuracy of dating past earthquakes has significantly improved by using the calibration curves with tree ring data, archaeological or tephrochronological evidence. The estimated dates of past earthquakes can be compared with records in historical documents. However, estimation of physical parameters of earthquakes is usually more difficult.

Off Fault Paleoseismology is a future challenge for seismological understanding of large earthquakes. Earthquakes leave various types of evidence off faults, which can be studied to approach more closely to the physics of paleoearthquakes. Several attempts to utilize these data have been already made including: distribution of marine terraces and their heights give a view of seismic deformation; inundation heights of paleo-tsunami recorded in the coastal deposits also provide information on size of a tsunamigenic earthquake; characteristics of paleo-liquefaction give macroseismic intensity; turbidities in marine or lake deposits also give macroseismic intensity. These are all off fault phenomena being preserved in the geologic deposits. Studies of these data could lead us more closely to the physical understanding of the past earthquakes.

Paleoseismology and Activity Study of the Hinagu Fault System, Southwest Japan

Koichi Shimokawa [1], Yoshihiro Kinugasa [1] and Takenobu Tanaka [2]

[1] Geological Survey of Japan
[2] I.N.A.Co.

shimo@gsj.go.jp

1. Introduction

The Hinagu fault system extends for about 75km from northeast to middle of Kumamoto Prefecture in Kyushu, southwest Japan. It consists of the Futagawa-Kitamukiyama fault (Watanabe and Ono, 1969; Watanabe, 1972) in the northern part and the Hinagu fault (Matsumoto and Kanmera, 1964) in the southern part. The former is 20km long and strikes N60°E, and the latter is 55km long and strikes N30°E. We conducted boring and trench excavating surveys at two sites, Takagi site in Mifune Town and Kakoi site in Miyahara Town, to reveal the paleoseismology and activity of the Hinagu fault system.

2. Results

2. 1. Takagi site in Mifune Town

The surveyed site locates the northern part of the Hinagu fault. In this area the Hinagu fault was revealed to have geographical evidence of active fault with dextral displacement (Chida, 1979). The boring survey across the fault reveals west-up displacement in the upper strata than the Aso-3 pyroclastic flow sediments (Watanabe, 1978) whose age is about 120ka (Matsumoto *et.al.*, 1991), on the contrary, east-up displacement in the lower strata. The trench excavating survey indicates two reverse faults striking N15°E and dipping 70-85°W. The west fault is overlain by the Holocene sediments; on the other hand, the east one cuts the same sediments forming vertical 15-30cm east-up displacement. Moreover, the latter cuts the lower peat layer of about 1,500 year BP and is overlain by the upper peat layer of about 1,350 year BP. The specific excavation tracing the boundary between the Holocene sediments and the basement rocks confirms the horizontal 2.2m right-lateral displacement.

2. 2. Kakoi site in Miyahara Town

This site is located at the middle of the Hinagu fault. The boring survey revealed two parallel faults 50m away from each other have east-up displacements, and trench excavation was conducted across each fault. In the east trench, the normal fault appeared, forming the boundary between peat layer of 15,500-15,900 year BP and interval sediments of Aso-4/Aso-3 (about 70-120 ka). This fault displaced the silt layer on the peat about 1m vertically, and is overlain by the sediments of 1,350-2,100 year BP. In the west trench, the high-angle reverse fault appeared, displacing the peaty silt layer of 8,100 year BP about 2m vertically.

3. Conclusion

From the result of the boring and trench excavating surveys across the Hinagu fault, the paleoseismology and activity of the Hinagu fault system are concluded as follows.

Based on the result of the surveys at Takagi site in the northern part of the Hinagu fault, the latest event occurred between 1,300 year BP and 1,500 year BP. Its vertical displacement is 0-0.3m and horizontal one is right-lateral 2.2m. Since the deposition of Aso-3 pyroclastic flow, this fault has not indicated significant vertical displacement, and its average vertical slip late is 0.04-0.2 m/ka.

On the other hand, based on the result at Kakoi in the southern part of the Hinagu fault, the latest event occurred before 2,000 year BP, and its vertical displacement is about 3m. This fault accumulated the vertical southwest-up displacement, and its average vertical slip rate is about 0.4 m/ka.

Consequently, the Hinagu fault can be divided into two segments, the northern Hinagu segment and the southern Hinagu segment, and adding the Futagawa segment, the Hinagu fault system is composed of the three segments.

References

Chida, N., 1979, Late Quaternary activity of Hinagu fault, west Central Kyushu (in Japanese), *Ann. Tohoku Geogr. Assoc., 31*, 172-179.

Matsumoto, A., K. Uto, K. Ono, and K. Watanabe, 1991, K-Ar age determination for Aso volcanic rocks (abstract in Japanese), *Bull. Vol. Soc.Japan, no.2*, 73-73.

Matsumoto, T. and K. Kanmera, 1964, *Geological map of Japan 1:50,000, Hinagu,* Geological Survey of Japan.

Watanabe, K., 1972, Geology of the western part of the Aso caldera (in Japanese), *Mem. Fac. Educ., Kumamoto Univ., no. 21, sec. 1*, 75-85.

Watanabe, K., 1978, Studies on the Aso pyroclastic flow deposits in the region to the west of Aso caldera, southwest Japan, I. Geology, *Mem. Fac. Edu. Kumamoto Univ., 27*, Nat. Sci., 97-120.

Watanabe, K. and K. Ono, 1969, Geology of the vicinity of Omine on the western flank of the Aso caldera (in Japanese), *J. Geol. Soc. Japan, 75*, 365-374.

Characteristics of a behavioral fault segment in the western coast of Northeast Japan deduced from the height change of former shoreline

Takashi Azuma and Yasuo Awata

Geological Survey of Japan

kero@gsj.go.jp

N-S trending thrust and fold systems are distributed in the Inner Arc Zone of Northeast Japan and they have deformed thick soft sediments (Miocene-Quaternary) and late Pleistocene marine terraces. In Noshiro Plain (Fig. 1), one of coastal plain along the Inner Arc Zone, late Pleistocene marine and fluvial terraces are widely distributed. Height of last interglacial (marine isotope stage 5e: 125 ka) marine terrace is uniform around 60 m in the northern and middle part of plain, while it declines southward from 50 m to 20 m in the southern part of the plain (Fig. 2A). Height of this terrace is over 100 m in further north area.

There are two west-dipping thrusts (Noshiro thrust and Moritake thrust) in Noshiro Plain. These thrusts run parallel with distance of about 7 km. Western margin of terrace is bounded with flexural scarp which are formed by Noshiro thrust. Vertical slip rate estimated from the height of flexural scarp is 0.3 - 0.4 m/ka. This rate agrees with uplift rate of this area based on former shoreline heights. Moritake thrust runs almost inner margin of the plain and the rate of its vertical slip is less than 0.1 m/ka.

Southern end of flexural scarp of Noshiro thrust corresponds to the point where the height of former shoreline would decrease southward gradually. Based on the both patterns of shoreline height change and distribution of vertical slip rate of Noshiro thrust (Fig. 2B), uplift of marine terrace is related to the activity of Noshiro thrust. Furthermore, these data show that segment of this thrust is c.30 km in length and long term vertical displacement of this thrust is uniform through it.

Historical records show that the area between two thrusts was uplifted by 1 m in 1694 Noshiro Earthquake ($M \sim 7$) which was produced by faulting of Noshiro thrust. Vertical slip rate of this thrust and uplift rate of marine terraces indicate that earthquakes like that had occurred with an interval of 2,000 - 2,500 years since at least last interglacial period.

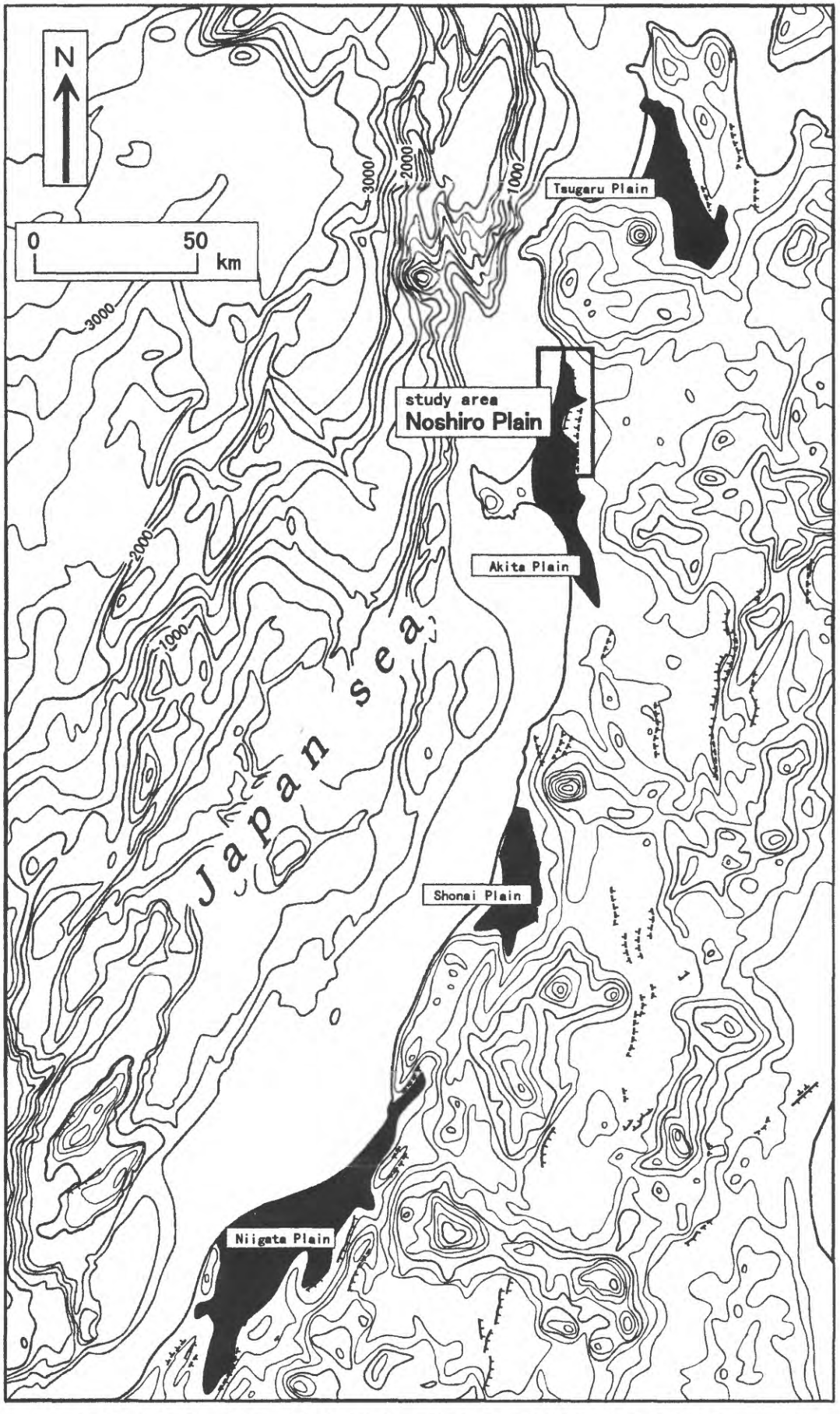

FIG.1 LOCATION OF STUDY AREA

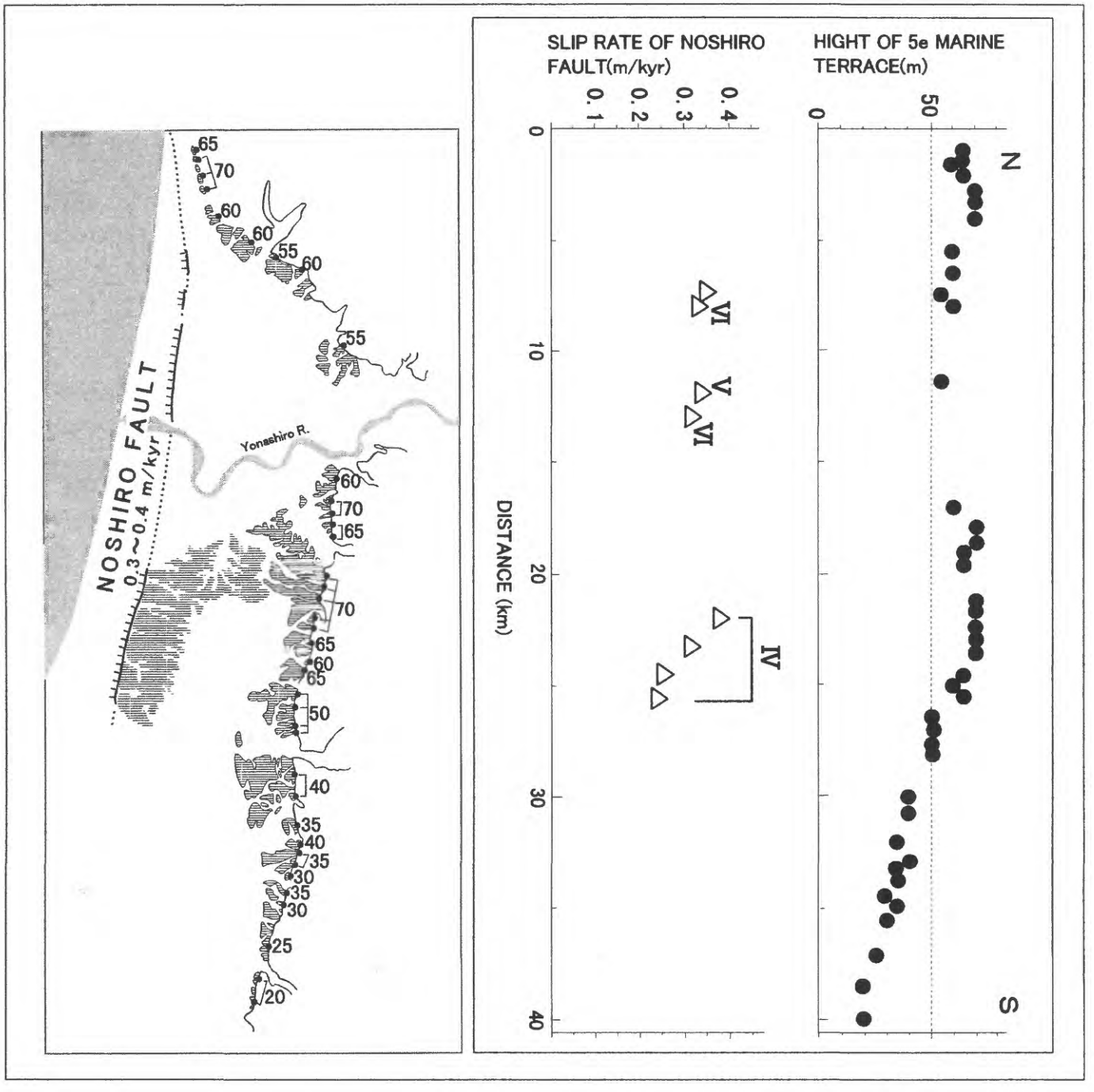

FIG.2 (A) DISTRIBUTION OF TERRACE Ⅳ AND HEIGHT OF ITS FORMER SHORELINE
(B) RELATIONSHIP BETWEEN HEIGHT CHANGE OF TERRACE Ⅳ AND SLIP RATE OF NOSHIRO FAULT

Susunayskaya lowland fault in south Sakhalin revealed by a trenching study: A preliminary report

Yoshihiko Kariya [1], Rustam F. Bulgakov [2] and Koichi Shimokawa [1]

[1] Geological Survey of Japan
[2] Institute of Marine Geology and Geophysics, RUSSIA

ykariya@gsj.go.jp

A landscape in south Sakhalin is characterized by topographic contrast between mountains and a basin: the west Yuzhno-Kamyshovyy Mts., the east Susunayskiy Mts., and the central Susunayskaya Lowland. Recently, on the basis of airphoto investigations, several researchers have pointed out that there would be active faults along the western side of the Susunayskaya Lowland from Sovetskoye to Aniva Gulf (about 47.5° to 46.5° N) or further. Nevertheless, no geological evidence has been obtained by a field survey yet. In order to confirm the presence of active faults and to evaluate their activities, we have conducted a trenching survey on a NNE-SSW-trending scarp in Taranay, 40 km SSW of Yuzhno-Sakhalinsk. As a result, we classified the topsoils and the Quaternary sediments into the sum of 11 units, and then we could find three west-dipping thrusts, F1 to F3, and specific deformation such as imbricated fabric of clasts subparallel to the faults. F1 and F2 cut the fluvial gravel layers that had been deposited during the Last Glacial (35-25 cal ka: radiocarbon basis). In contrast, these faults seemed to be capped by the topsoils (3-1 cal ka). No increasing displacement on the faults with age was identified. F1 and F2 converged smoothly near the bottom of the trench and the displacement of faulted beds by F2 was nearly equal to that by F1, suggesting the simultaneous activity. The timing of the last event of F1 and F2 is thought to be after 35 cal ka at the earliest and before 1 cal ka at the latest. The timing of F3 faulting, however, could not be determined since the geological relation between F3 and its surrounding beds was equivocal. Although the fluvial gravel layers truncated by the faults were tilted toward east over 40°, vertical slip of the faults ranged only from 0.25 to 0.45 m. Besides, these faults turned unclear and invisible in the lower part of the trench. These facts imply that the main fault with large displacement might exist under the trench bottom. The presence of active faults along the Susunayskaya Lowland has been confirmed but some important parameters are still uncertain.

Geologic evidence for five large earthquakes on the north Anatolian fault at Ilgaz, during the last 2000 years -- a result of GSJ – MTA international cooperative research --

Toshihiko Sugai [1]*, Omer Emre [2], Tamer Y. Duman [2], Toshikazu Yoshioka [1] and Ismail Kuscu [2]

[1] Geological Survey of Japan,
* now at Graduate School of Frontier Sciences, University of Tokyo
[2] Geological Research Department, MTA
(General Directorate of Mineral Research and Exploration), Turkey.

sugai@geogr.s.u-tokyo.ac.jp

1. Why the North Anatolian fault in Turkey ?

Along the North Anatolian fault a remarkable series of *Ms* 7+ earthquakes accompanied by conspicuous surface ruptures occurred between 1939 and 1967 (Fig.1). This series of earthquakes has attracted attention because of the westward migrating sequence of events. Learning whether a similar series of events has occurred repetitively in the past and whether it will be repeated in the future could play an important role to refine earthquake recurrence model; understanding earthquake interaction on long active faults and estimating maximum earthquakes occurred along the faults have great importance for seismic hazard assessment. In order to answer these questions, it is essential to clarify the earthquake recurrence records on individual fault rupture segments. To this end we have started trenching survey on the North Anatolian Fault at Ilgaz, near the boundary of the 1943 and 1944 earthquake ruptures since 1996 (*e.g.* Sugai *et al.*, 1997; 1998). Long recorded histories of earthquakes in Turkey give us invaluable opportunity to evaluate the surface rupture length and magnitude of individual paleoearthquakes.

2. Trenching survey

The trench site is located on marshy grassland in front of an alluvial fan toe formed by tributaries flowing on the south-facing slope of the Ilgaz Range (Fig.2). Three adjoining trenches were excavated across a single fault line running nearly east-west. Interviews with local villagers who remembered the earthquake revealed that

this latest surface rupture event occurred in 1943. The trench walls display a late Holocene record of sedimentation and earthquakes (Fig.3). The sediments are divided into over 100 beds of peat, humus, silt, sand, and gravel with thickness ranging between 1 to 20 cm. The sediments are also rich in radiocarbon-dating materials. Individual beds can be combined to 13 sedimentary units (Fig.4). Based on stratigraphic indicators appearing on the trench walls, such as angular unconformity, filled fissures, colluvial wedges, and liquefaction-induced features, four certain and one probable faulting events were recognized during the last 2000 years.

3. Timing of faulting events and their correlation with historical earthquakes

The radiocarbon dates of 46 samples from various horizons, indicate the timing of each faulting event: the preceding event (Event 2) occurred in between AD 1495 and 1850; Event 3 between 890 and 1190;. Event 4 between 640 and 810; Event 5 (probable event) between 0 and 150 (Fig. 5). It is highly probable that the event 2 and 3 produced the large historic earthquakes in 1668 and 1050, respectively. Approximate recurrence intervals between earthquakes varied from about 280 to 620 years.

4. Displacement-per-event and average slip rate

By combining the 3D-trenching and detailed topographic mapping (we made 1 to 100 scale topographic map with contour interval of 10 cm using total station), we can estimate the lateral slip per faulting event concerning the last three events; slip of the 1943, 1668 and 1050 earthquakes are estimated to be 2.5 to 3.0 m, 5.0 to 6.0 m, and 6.0 to 7.0 m, respectively (Sugai *et al.*, in preparation).

The time-slip diagram (Fig. 6) indicates that the average slip rate is 12.5±2.5 mm/y during the last millennium. This rate is almost the highest among the known rates which have been geologically evaluated along the North Anatolian fault. However, it is about the half of the rate given by GPS data (*e.g.* Oral *et al.*, 1995). This discord suggests that intraplate deformation should not be neglected at least in the central part of the North Anatolian fault.

5. Earthquake sequences along the NAF and its paleoseismoligical implications

The 1668 earthquake with the rupture length of over 400 km has been considered to be one of the maximum historical events along the North Anatolian fault (Ambraseys and Finkel, 1995). Slip of the 1668 and 1050 events is almost the same, 6±1m.

Considering the large slip of the 1050 earthquake and the eastward earthquake progression during 967-1050, we think that the 1050 rupture reached the east region with no-historical earthquake records (Fig. 7). On the other hand, the 1943 slip, 2.5m, which is less than a half of those of 1668 and 1050, implies that the 1943 event was triggered by the 1942 earthquakes. This may give us the reason why the recurrence interval between the 1943 and 1668 events (275 years) is shorter than that between the 1668 and 1050 events (618 years).

Reference

Ambraseys, N. N., 1970, Some characteristic features of the North Anatolian fault zone, *Tectonophysics, 9*, 143-165.

Ambraseys, N. N. and C. Finkel, 1995, *Seismicity of Turkey and adjacent areas, A historical review, 1500-1800*, Eren Yayincilik ve Kitapcilik Ltd., 224pp.

Barka, A. A., 1996, Slip distribution along the North Anatolian fault associated with the large earthquakes of the period 1939 to 1967, *Bull.Seism.Soc.Am., 86*, 1238-1254.

Oral, M. B., R. E. Reilinger, M. N. Toksoz, R. W. King, A. A. Barka, I. Kinik, and O. Lenk, 1995, Global positioning system offers evidence of plate motiond in Eastern Mediterranean. *EOS., 76*, 9-11.

Sugai, T., T. Yoshioka, O. Emre, T. Y. Duman, and I. Kuscu, 1997, Geologic evidence for four faulting events produced by the North Anatolian Fault at Ilgaz, during the past 2000 years, *Proceedings of the International Symposium in the Istanbul Technical Univ.,* 49-52.

Sugai,T, O. Emre, T. Y. Duman, T. Yoshioka and I. Kuscu, 1998, Geologic evidence for five large earthquakes on the North Anatolian Fault at Ilgaz, during the last two Millennia, *EOS., 79*, F615.

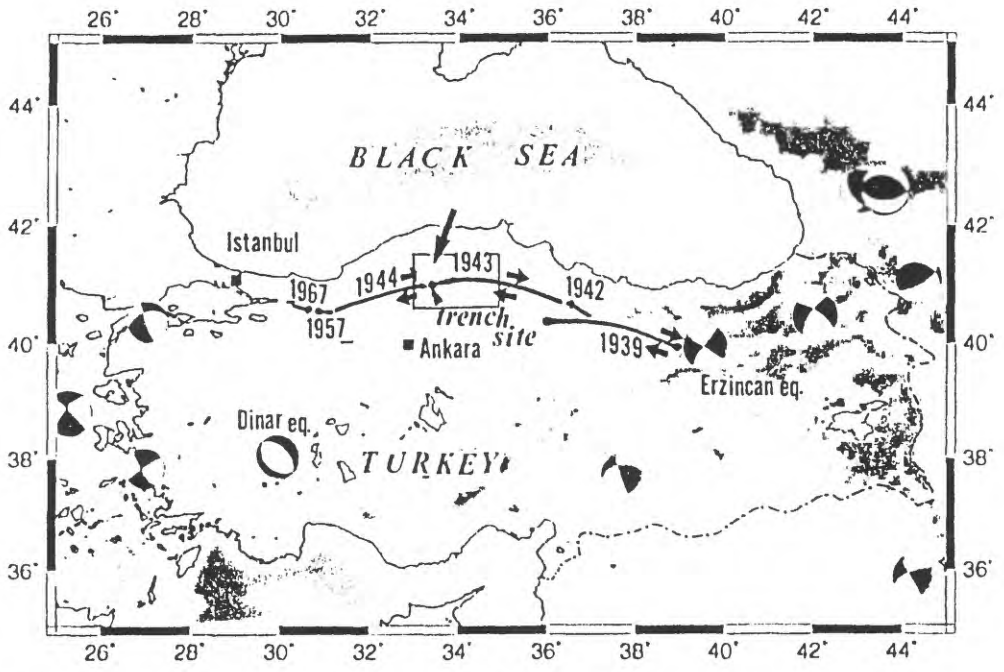

Figure 1. Surface ruptures between 1939 and 1967 along the North Anatolian fault and the trench sites. The fault plane solutions show the major earthquakes (M>5.9) in 1977-1996.

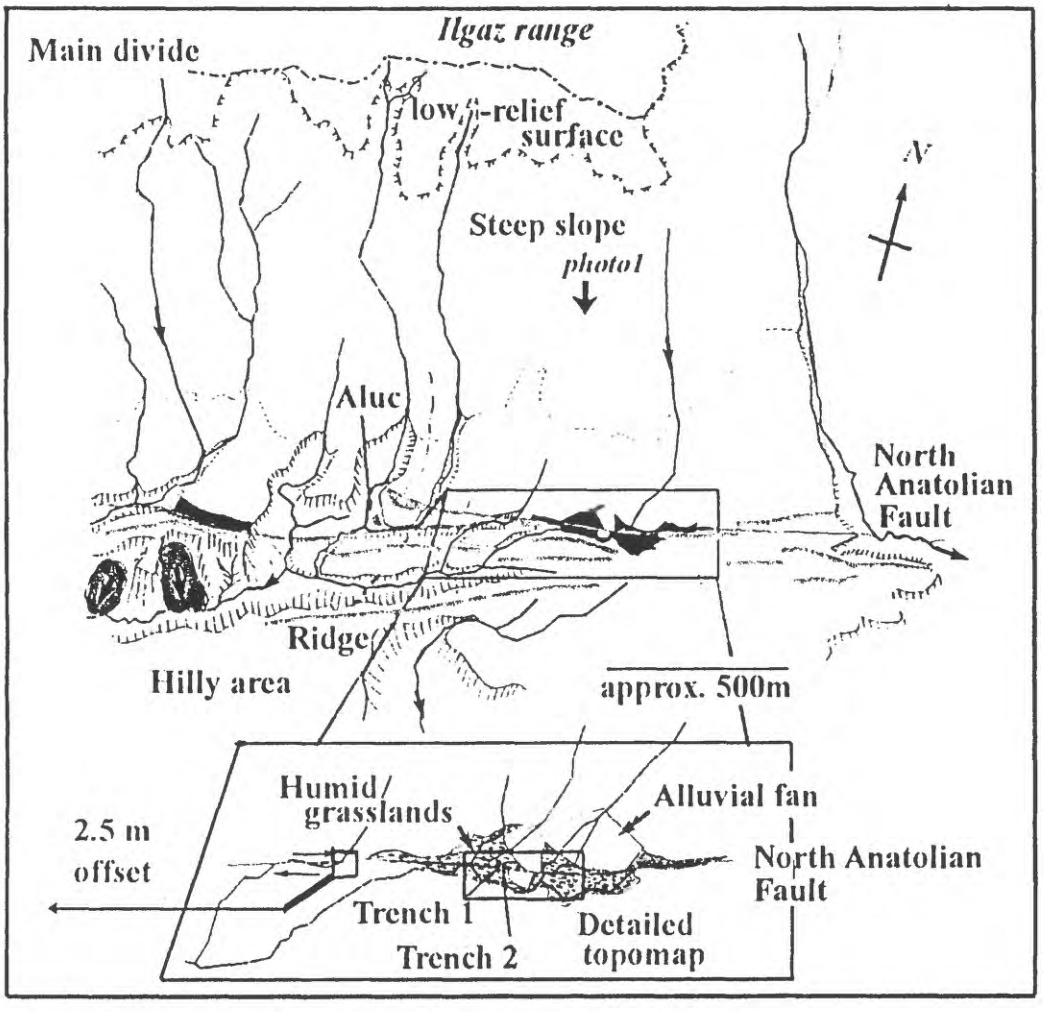

Figure 2. The Ilgaz-Aluc paleoseismic site on the1943 rupture segment .

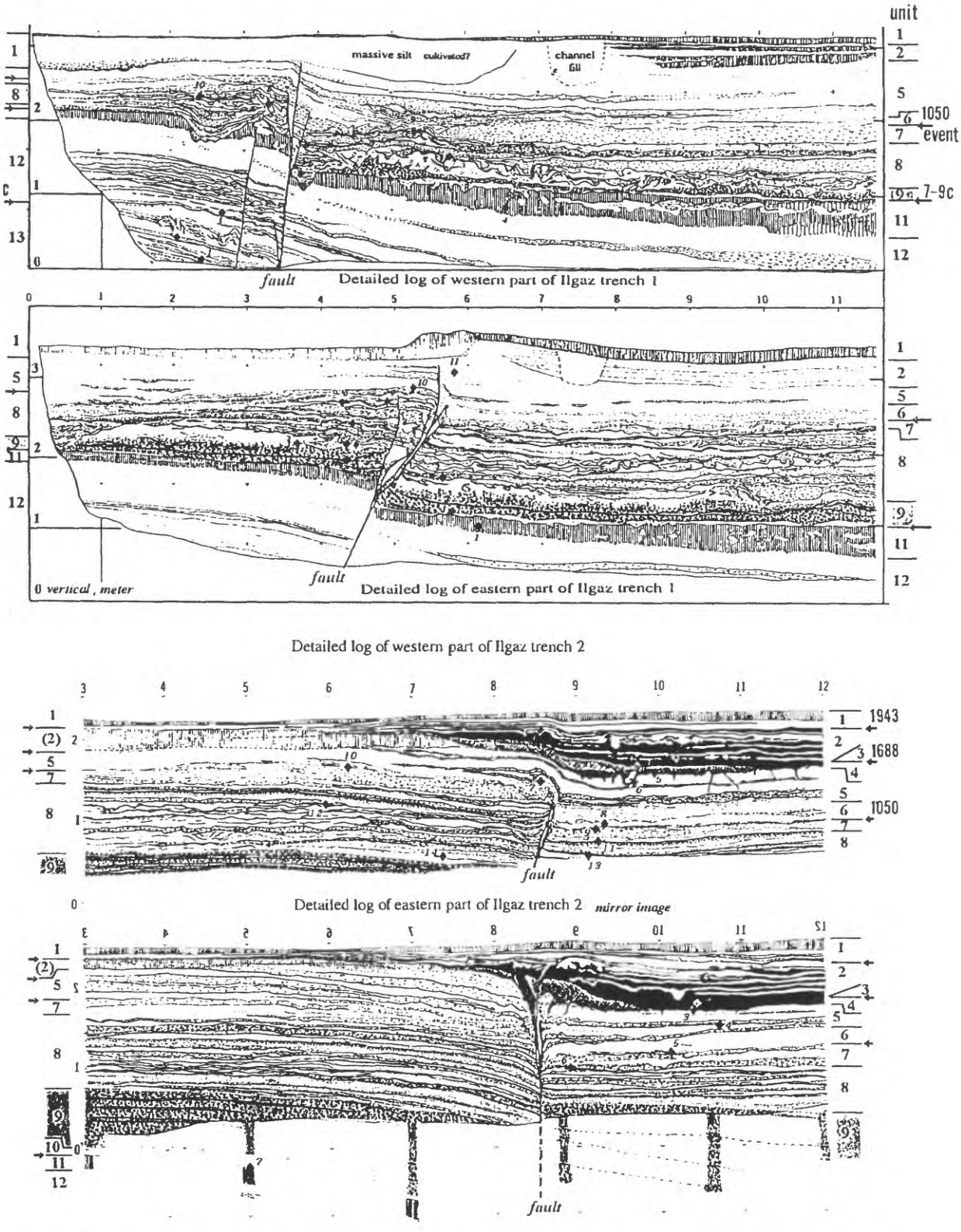

Figure 3. Logs of successive four walls of trench 1 and 2. View west along the North Anatolian fault; the eastern parts of the trenches are mirror images. Diamonds with numbers show locations of ^{14}C samples; their dates and approximate. age of each geologic unit are shown in Figure 5. Logs show evidence for five earthquakes during the past 2ka.

characteristics of geologic units	pollen analysis
unit 1: soil, silt deposited over the fault scarp (with 10 cm height).	±
unit 2: peat with thin silt, **deposited over the fault scarp**. (top) convolute bedding.	±
unit 3: **colluvial wedge** (with unsorted angular gravels).	
unit 4: peat and peaty silt	−
unit 5: (top):buried **fissures** filled with unit 4 (peat).	−
unit 6: silt and sand, deposited only downthrown side (dammed).	
unit 7: green gravels, basically control the present earth-surface slope	+
unit 8: clay, humic silt, sand, and gravels, alternated with lots of pine cone.	+
unit 9: angular gravels, lying with angular unconformity	+
unit 10: clay, severely eroded.	
unit 11: buried paleosol with **liquefaction**-induced features such as injected sand.	−
unit 12:(upper part): silt and clay, (lower part): silt and sand, lying with angular unconformity .	±
unit 13: sand and humic silt, convolute bedding, with the steepest average dip	+

* pollen analysis + (warm and/or humid) − (cool and/or dry) ± (same as the present conditions)

Figure 4. Characteristics of geologic units.

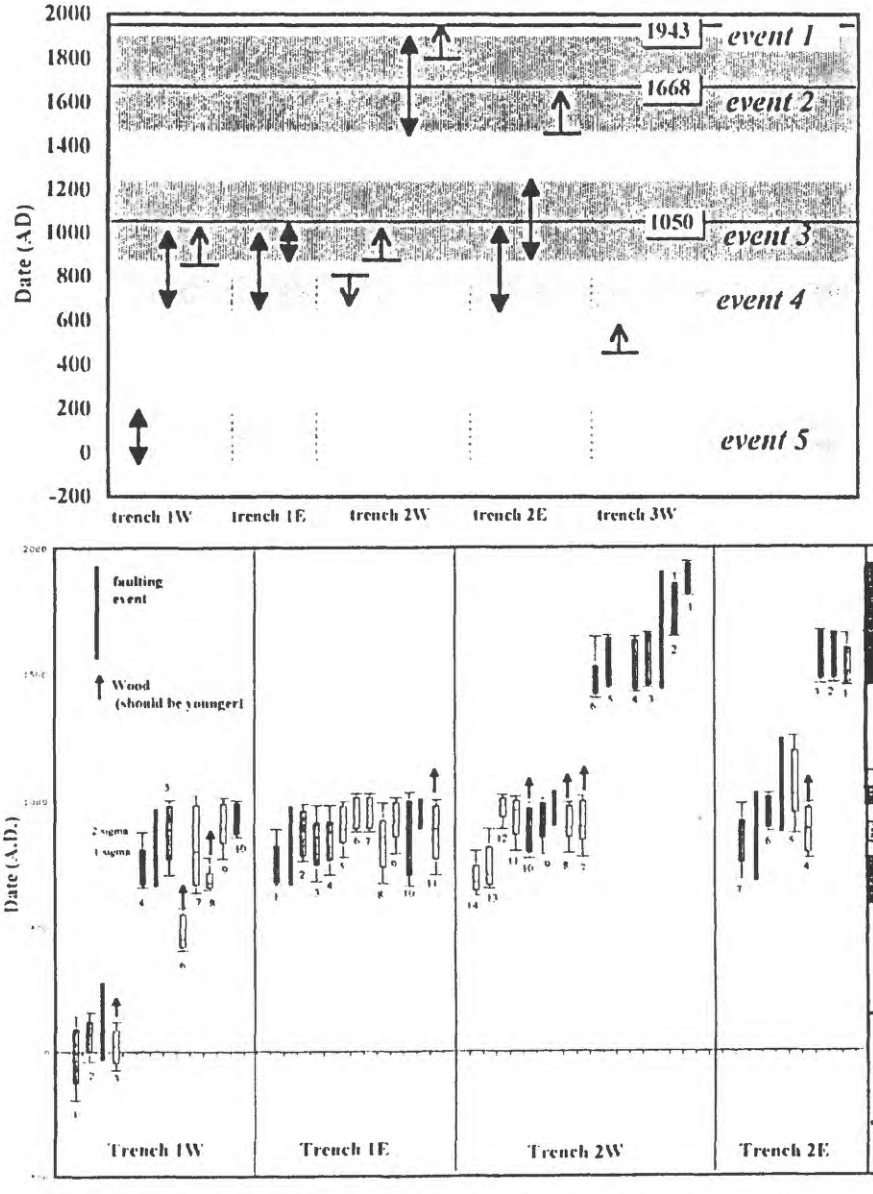

Figure 5. Timing of the five large earthquakes (top) in the past 2ka based on the ^{14}C dates (bottom:the number of samples from trench 1 and 2 is 42 in total, locations shown in Figure 3). The last three events of event 1, 2, and 3 can be correlated with the historical earthquakes of 1943, 1668, and 1050, respectively. Note that Turkey has long recorded histories of earthquakes (Figure 7)

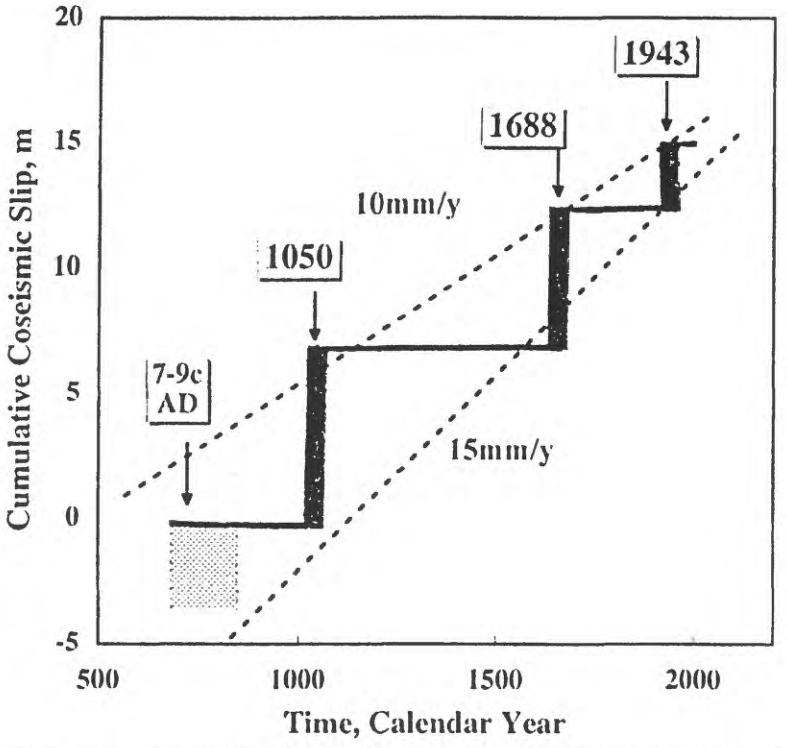

Figure 6. Slip history and average slip rate during the past 1 ka.

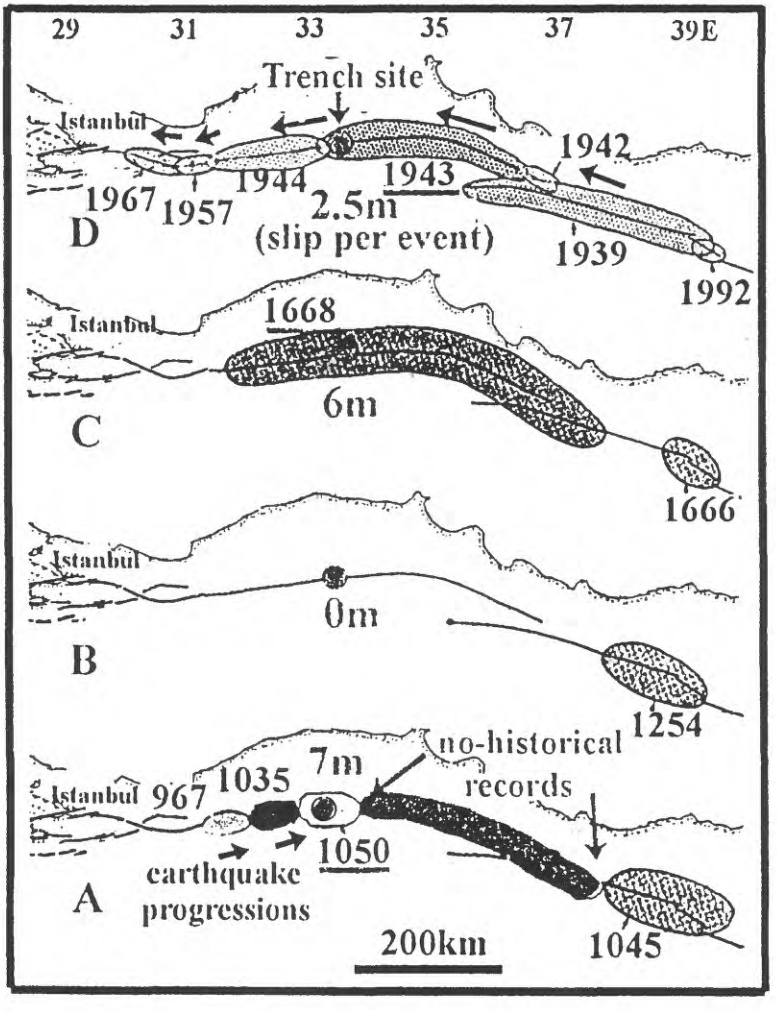

Figure 7. Earthquake sequences along the North Anatolian fault. Adding the trench data to Barka (1996), A, B and C sequences based on Ambraseys (1970) and Ambraseys and Finkel (1995).

Structure and paleoseismology of the Kongo fault system in Nara Prefecture

Kenji Satake [1], Toshihiko Sugai [1], Akira Sangawa [1], Makoto Yanagida [2], Hiroshi Yokota [3], Takaaki Iwasaki [4], Masashi Omata [4] and Akira Ishikawa [4]

[1] Geological Survey of Japan
[2] I.N.A. consultants Co. Ltd.
[3] Hanshin consultants, Co. Ltd.
[4] Geoscience, Co. Ltd.

satake@gsj.go.jp

New geophysical and geologic findings show, for the first time, subsurface branching and Holocene activity in the Kongo fault system. The system extends 18 km along the southwest side of the Nara basin, which contains the remains of Japan's capital city in the 8th century AD (Fig. 1). The Kongo fault system continues southward to the Median Tectonic Line, towards which it swings westward. In the north it contains three faults of parallel strike, called Yamaguchi, Kongo, and Yamada (Fig. 2). Seismic reflection surveys show that the Yamada and Kongo faults merge about 300 m below the surface (Fig. 3). They displace a prominent reflector, interpreted as the contact between granite and Pleistocene deposits, by 240 - 350 m. The displacement of Pleistocene beds and terraces implies vertical slip rates in the range 0.1-0.6 mm/year. The last major surface rupture produced faults seen in outcrop (Fig. 4) and in a trench (Fig. 5). It probably occurred in the first few centuries AD, as judged from a dozen radiocarbon ages (Fig. 6). The most closely limiting of these ages are 1900 $\pm$ 60 ^{14}C year BP (a piece of wood in the faulted strata) and 1780 $\pm$ 50 ^{14}C year BP (wood in overlying, unfaulted strata), or between 40 BC and AD 380. A minimum vertical displacement of 1.2 m, measured in the trench, implies an earthquake magnitude close to 7, comparable to the 1995 Kobe earthquake. The average recurrence interval is probably in the range of 2000 - 12,000 years. This range is broad because the slip rate is poorly known, and result the probability estimates for the next earthquake, on the basis of Probabilities, highly variable.

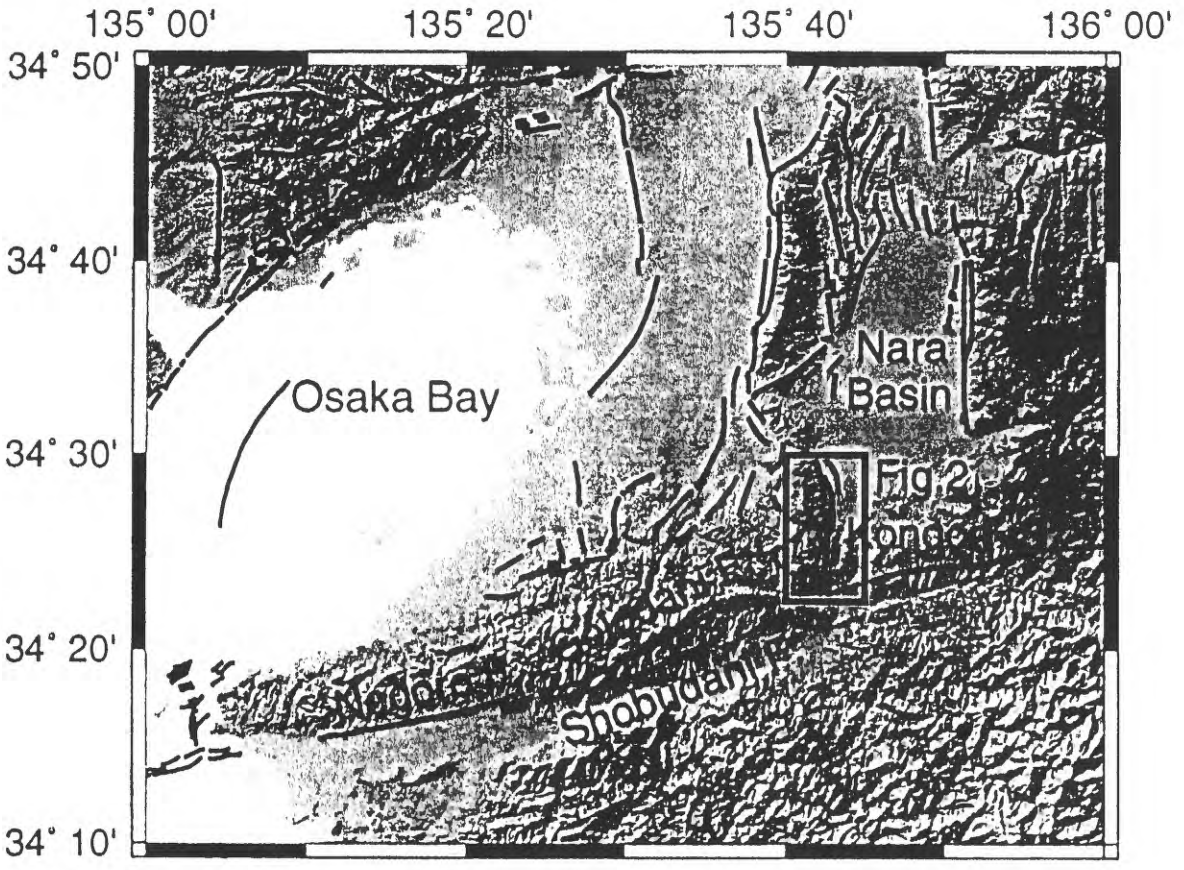

Figure 1. Active faults in the Kinki region. The Kongo fault system extends from the SW edge of the Nara basin toward E-W trending Median Tectonic Line. Topography from 50-m digital elevation model compiled by Geographical Survey Institute. Faults from map compiled by Research Group for Active Faults of Japan (1991).

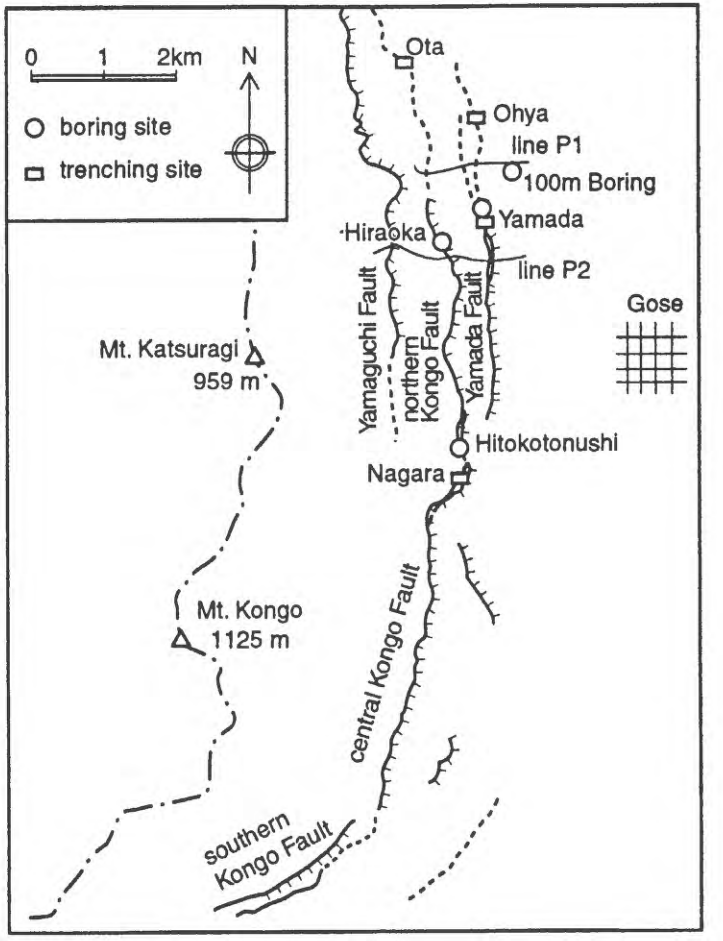

Figure 2. Survey sites in the Nara basin. The Kongo fault system is divided into three parts. In the north, three parallel fault strike southward. They merge at depth (Figure 3) and in a central area at the surface as well. The fault swings westward in the south. Seismic reflection surveys were made along two lines in the north. Outcrop and trenches were studied in the central area.

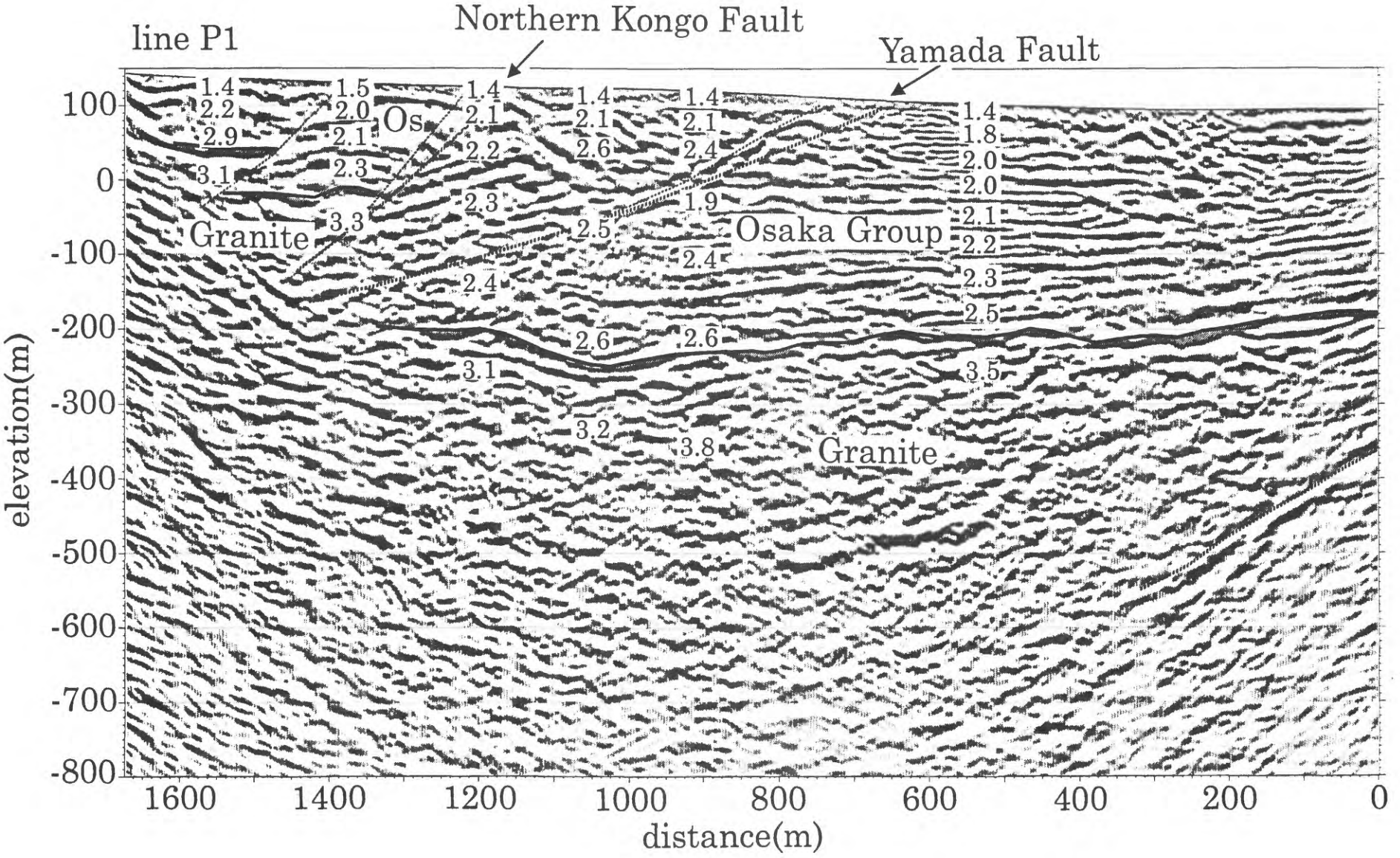

Figure 3. Migrated depth section of seismic reflection survey along northern line P1 (location, Figure 2), showing estimated velocity (in km/s), inferred faults and stratigraphy.

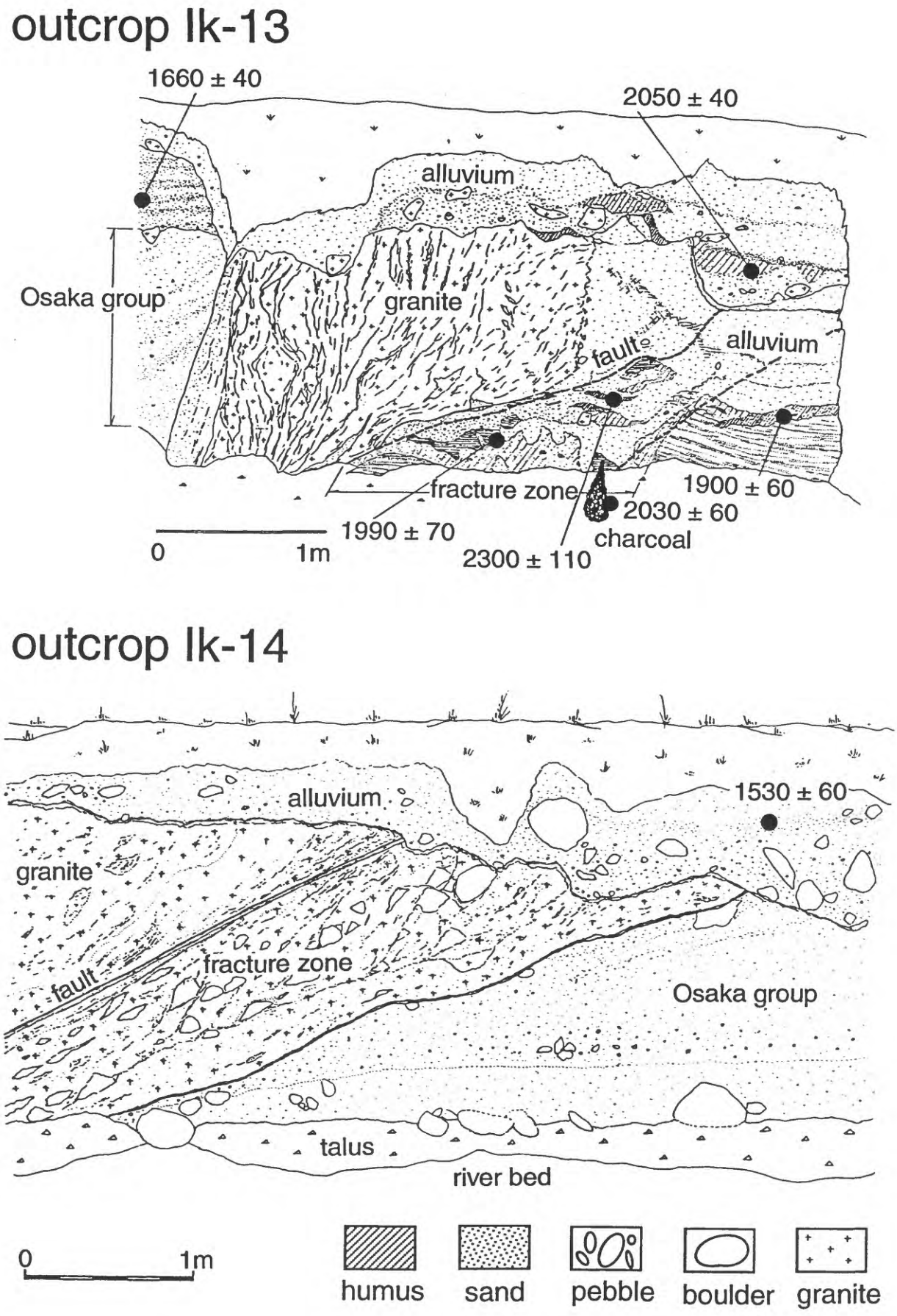

Figure 4. Sketches of two outcrop. At outcrop Ik13, fractured granite appears thrust over alluvium dated 1900 - 2300 ^{14}C year BP. At outcrop Ik14, two faults bounding a fracture zone about 1 m wide are covered by alluvium dated 1530 ± 60 ^{14}C year BP.

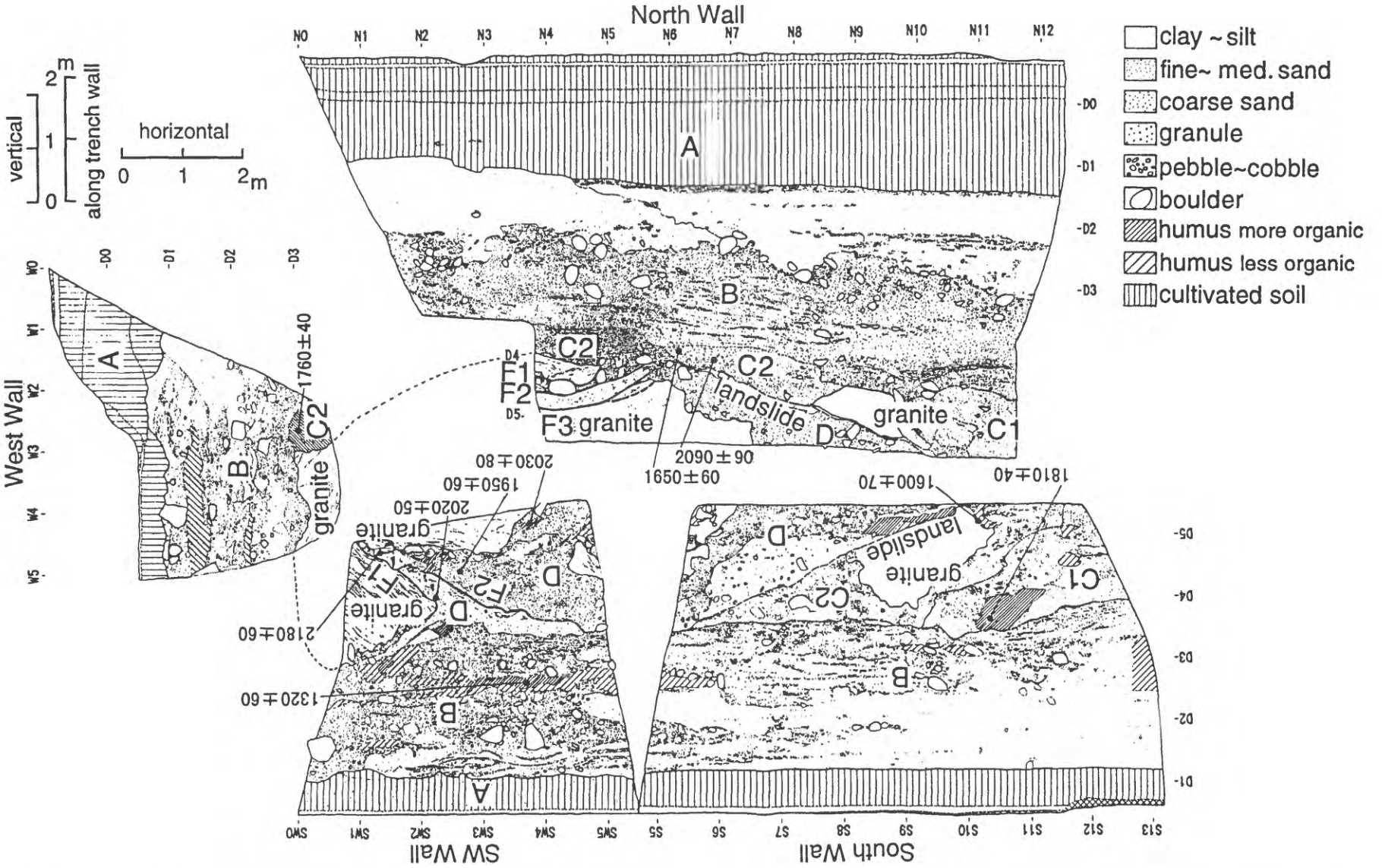

Figure 5. Sketches of trench NT2. The locations and estimated ages (^{14}C year BP) of samples are also shown. Unit A is artificial fill, units B, C1, C2 and D are debris flow deposits, and the basement is granite. At the bottom of unit C2 is a landslide plane. Organic sand from unit C2 gave an age of 1760 ± 40 ^{14}C year BP. The faults, labeled F1, F2 and F3, displace granite and debris flow deposit D (dated 1950 - 2180 ^{14}C year BP) by at least 1.2 m vertically. The faults are covered by unit B on the SW wall and by unit C2 on the west wall.

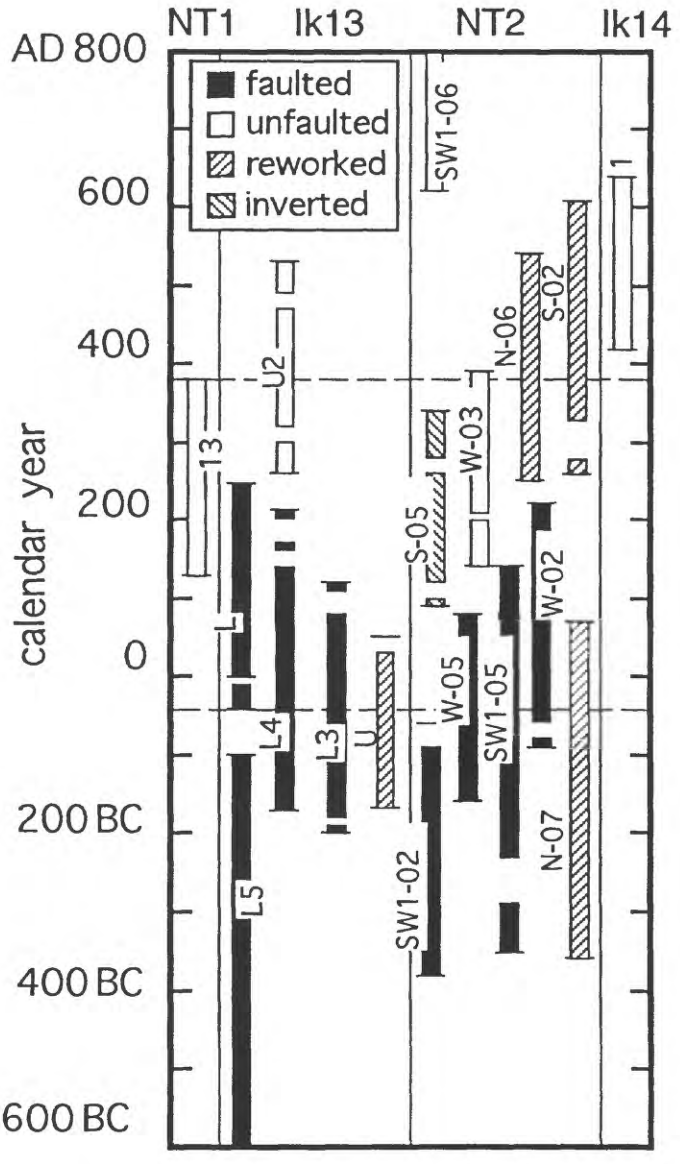

Figure 6. Calibrated ages of samples from outcrop (Ik13 and 14) and trenches (NT1 and 2). The youngest age of faulted strata is 40 BC-AD250 (IK13-L) or 1900±60 ^{14}C year BP. The oldest age of a layer over the fault is AD 130-380 (NT1-13) or 1780 ±50 year BP. Hence the most recent earthquake occurred between 40 BC and AD 380.

Sedimentary systems and earthquake events? confined by active faults : a case of the western Biwako fault system in the Hira-Adogawa region, Shiga prefecture, central Japan

Futoshi Nanayama [1], Kiyohide Mizuno [2] and Taku Komatsubara [1]

[1] Geological Survey of Japan
[2] Geological Survey of Japan, Osaka branch

nanayama@gsj.go.jp

1. Object

Many active faults are mapped west of Lake Biwa, and these have generated intra-plate earthquakes as documented in historical documents (e.g. Sangawa *et al.*, 1987 ; Taishi *et al.*, 1987,). For example, an earthquake in 1662 (2nd year of Kanbun period) on the western side of Lake Biwa caused significant ground subsidence and slope failure that caused great damage. Other earthquakes also caused ground subsidence and slope collapse. It is important to trace these evidence for long-term earthquake forecast and hazard reduction.

Geological Survey of Japan carried out systematic active faults analysis of the western coast and sub-bottom area of Lake Biwa in 1996. In this study, we try to identify earthquake traces in the sub-bottom acoustic profiles, piston cores from underwater slopes and boring cores from delta areas.

2. General topography of Lake Biwa

The Lake Biwa is the biggest lake in Japan, with 674 km^2 in area, total length of 235 km, situated at 85m above sea level, distributed Shiga prefecture in central Japan. This lake is divided into three divisions, North, Middle, South basins, from north to south. North basin is almost 80 m in depth, Middle basin is in 70 m in depth. These two basins are currently being subsided. On the other hand, South basin is only 5 m in depth and filling up to date (Uemura and Taishi, 1990).

In the bottom of the lake, the deepest parts of basins are situated along the western side, and gently inclined east to west. This inclined topography was created by cyclic subsidence by active fault system of the western Lake Biwa fault system. We think

this subsidence has occurred since 300-400 ka because of the age of the bottom clay of central part of Lake Biwa (Takemura and Yokoyama, 1989). Further, it was estimated that vertical movement is the rate of 0.5-0.7m/ka at present (Ikeda *et al.*, 1979).

3. Acoustic surveys off Hira area

We carried out acoustic surveys at underwater slope off Hira area by Sonoprove acoustic surveyor (Kaijyo Electonic: Type SP-3) and keeping the speed of research boat at 2-3 knots.

These acoustic profiles show many tectonic trends, like flexure, anticline, syncline in the SW- NE direction running parallel each other. Generally, these form a flexure zone inclined to NE direction, because of ductile deformation of thick loose sediments. We suggest that the flexure belt extends to main faults (Hira Fault?).

At the sub-bottom area, there are a few small faults dipping westward in the opposite direction of the slope. We suggest that these faults are subfaults occurred by main fault event under the ground. We estimated that these faults occurred at 2-3 ka and 1.1 ka by correspondence of acoustic reflections and piston cores data. Further, these reflections are compared with depth of regional tephra layers, furthermore, debris flow sediments and turbidites.

4. Analysis of piston cores off Hira area

We recovered total 54 m piston cores at six sites (Sites 1-6), 10 holes, total 54 m off the Hira delta. We identified many thin turbidites by description of sedimentary facies, X-ray photo analysis and magnetic susceptibility.

These cores are mainly consisted of biotubated offshore mud facies, occasionally interbedded the regional tephra (K-Ah: 6.3, U-Oki: 9.3, AT: 25, DNP: 60, Aso-4: 70, K-Tz: 80 ka etc.) and fine to coarse turbidites (T01-T10). We calculate the sedimentary rates of the sections without turbidite thickness by regional tephra and ^{14}Cdata, then estimate the event ages of turbidites. They are, T01: 1.2, T02: 1.5, T1: 3.1, T2: 3.8, T3: 4.7 , T4: 7.0, T5: 7.9, T6: 8.2, T7: 8.8, T8: 11.0, T9: 11.8, T10: 85 ka. Among these, T1 and T2 events corresponded to active fault events of sub-bottom off Hira area mentioned above.

5. Analysis of boring cores at the Hiragawa and Adogawa deltas

We recovered 50 m boring cores at Hiragawa delta (KH-50) and Adogawa delta (MN-50). These sediments are mainly Delta-plain and Alluvial fan facies consisting of loose coarse sand to conglomerate. However, we could identify some sedimentary facies and systems showing subsidence events by earthquake events (?).

In particular, in MN-50, we could identify two subsidence events at 3.5m (300 year. BP?) and 20m in depth (11 ka). In addition, in KH-50, we could identify large unconformity between 0.5 to 10 ka at 18 m depth. However, we could not understand in detail.

6. Conclusion

There are many active faults along the western side of Lake Biwa, and this lake is confined by activity of these faults. In particular, we know that causative faults of historical earthquakes, namely Kanbun 2 nen earthquake (1662 ; 300 year BP) and late Jomon earthquake (3 ka) were situated around this region (Sangawa *et al.*, 1987; Sangawa and Tsukuda, 1987; Taishi *et al.*, 1987). Taishi *et al.* (1987) already pointed out the debris flow sediments off Adogawa area were from these earthquake events. Finally, we could not say that all of these event sedimentations are caused by earthquakes. However, we emphasise that these are important indicators of earthquakes, and provide important information on cyclic activity of active faults.

Sedimentary characteristics of recent tsunami deposits from the 1993 Hokkaido nansei-oki tsunami, northern Japan

Futoshi Nanayama [1], Koichi Shimokawa [1], Kenji Satake [1] and Kiyoyuki Shigeno [2]

[1] Geological Survey of Japan
[2] Meiji consultant co., ltd., Japan;

nanayama@gsj.go.jp

Tsunami deposits can provide important evidence for the occurrence of prehistoric earthquakes. Prehistoric great earthquakes at the Cascadia subduction zone, for instance, have been inferred not only from geologic evidence for coseismic change in coastal land level, but also from sand sheets ascribed to associated tsunamis. For some such sand sheets, a storm origin can be convincingly discounted on the basis of stratigraphic position, architecture, and fossils. In other cases, however, the origin of a sand sheet can be ambiguous. In hopes of reducing such ambiguity, we studied modern tsunami and storm deposits on the Japan Sea coast of Hokkaido, in a trench 3 m wide, 9 m long, and 1.5 m deep.

The trench was located in Taisei, a village struck by a typhoon in 1959 and a tsunami in 1993. The typhoon generated a storm surge that lasted about an hour and reached a height about 6 m above ordinary high-tide levels. The tsunami, caused by a nearby earthquake of magnitude 7.8, comprised two main waves, the first having a maximum height of 6.8 m, the second 8.6 m. Effects included the transport of a house about 30 m inland.

The tsunami and storm deposits in the trench are similar in thickness, which in both cases decreases landward from a maximum of about 50 cm. The tsunami deposits can be divided into four layers. We correlate these layers with landward and seaward flow from the two main tsunami waves; the flow directions are shown by imbrication of gravel and the remains of knocked-down plants. The landward tsunami flow deposited marine sand and rounded gravel, whereas the return flow deposited a poorly sorted mixture of mud, sand, and gravel. Only the storm deposit shows foreset lamination. This deposit is mostly marine sand that is better sorted than any of the tsunami deposits.

Most recent paleoearthquake constraints and slip rates for a portion of the Hurricane fault, southwestern USA

Heidi D. Stenner [1], William R. Lund [2] and Philip A. Pearthree [3]

[1] US Geological Survey, Menlo Park, USA
[2] Utah Geological Survey, USA
[3] Arizona Geological Survey, USA

hstenner@usgs.gov

Slip rates over different Quaternary time intervals and the timing and size of the last ground-rupturing earthquakes are constrained along several portions of the Hurricane fault in northwestern Arizona and southwestern Utah, USA. The paleoseismic study involved total station mapping and profiling, soil age estimation, cosmogenic isotope dating, geomorphic modeling of fault scarps, and trenching of faulted landforms. The goal of these methods was to provide paleoseismic parameters for future seismic hazard analyses of this major fault whose earthquake chronology is previously unstudied. The 250-km-long normal fault exists on the eastern edge of the extensional Basin and Range physiographic province and traverses an area of growing population. Numerous fault scarps, developed in unconsolidated alluvial surfaces, increase in height with increased surface age, indicating recurrent dip-slip in the late Quaternary. No evidence for significant Quaternary horizontal offset was observed.

The most recent ground-rupturing event (MRE) along the northernmost Ash Creek section of the fault likely yielded a slip of ~2-3 m during the early Holocene or latest Pleistocene (Fig. 1). Slip rates along the Ash Creek section are the highest for the fault, at 0.36-0.41 mm/yr over the past 860 ka. Slip rate decreases to the south, along the southern Whitmore Canyon section slip is estimated at 0.05 –0.2 mm/yr for the past 90 ka and 0.07-0.13 mm/yr for the past 153 ka. The MRE produced ~2-4 m of slip during the early Holocene or latest Pleistocene and ruptured at least 15 km through the Whitmore Canyon section (Fig. 1).

The Anderson Junction section of the central Hurricane fault was studied in the most detail. Based on soil development in trench exposures, the MRE likely ruptured 5-10 ka. A 0.60 m displacement during the MRE, measured at the Cottonwood Canyon site in Arizona (Figs. 1 and 2), is probably representative of at least the 10 km

of fault to the north of the site, where fault scarps of similar size and age are preserved. Another 18 km of fault farther north may have also ruptured during the last event but evidence is lacking. The absence of evidence does not preclude rupture, however, as the effect on the landscape may be short-lived or obscured if faulting ruptured the bedrock base of the large Hurricane Cliffs (Fig. 3). Empirical relationships between surface displacement and the moment magnitude or rupture length for the Anderson Junction MRE yield a possible moment magnitude of 6.1-7.0 and a minimum rupture length of 19 km.

At the Cottonwood Canyon site, a large fault scarp developed in a 70-125 ka alluvial fan records 18.5-20 m of displacement, yielding a slip rate of 0.1-0.3 mm/yr. The large scarp gives evidence that the last 0.60 m-displacement event is not likely to be typical of previous late Quaternary faulting events recorded at Cottonwood Canyon. Over 30 events occurring about every 2-4 ka are required to have produced the large scarp if the MRE is the typical earthquake. For a recurrence interval of 2-4 ka at least two events would likely have taken place during the Holocene. Evidence only exists for one Holocene event, possibly implying a longer average recurrence interval. The atypical nature of the MRE at Cottonwood Canyon may be due to that site's proximity to a potential rupture boundary zone.

The 0.1-0.3 mm/yr slip rate at Cottonwood Canyon, since the latest Pleistocene, is roughly similar to the 0.23-0.42 mm/yr rate obtained for the past 300 ka by Hamblin *et al.* (1981) along the same section of fault, indicating that the slip rate may be constant over the late Quaternary. During the Holocene, however, only one 0.60 m-slip event has occurred at Cottonwood Canyon, a slip rate of 0.04 to 0.12 mm/yr. Either the recurrence interval of large events is larger than the duration of the Holocene, with the Holocene time window being too short for the slip rate to average to the long-term rate; or the recurrence interval is less than 10 ka but there is a slip deficit, with rupture overdue.

References

Hamblin, W. K., P. E. Damon, and W. B. Bull, 1981, Estimates of vertical crustal strain rates along the western margins of the Colorado Plateau, *Geology 9*, 293-298.

Stewart, M. E. and W. J. Taylor, 1996, Structural analysis and fault segment boundary identification along the Hurricane fault in southwestern Utah, *J. Structural Geology, 18*, 1017-1029.

Stewart, M. E., W. J. Taylor, P. A. Pearthree, B. J. Solomon, and H. A. Hurlow, 1997, Neotectonics, fault segmentation, and seismic hazards along the Hurricane fault in Utah and Arizona: an overview of environmental factors in an actively extending region, *Brigham Young University Geology Studies, 42 II*, 235-277.

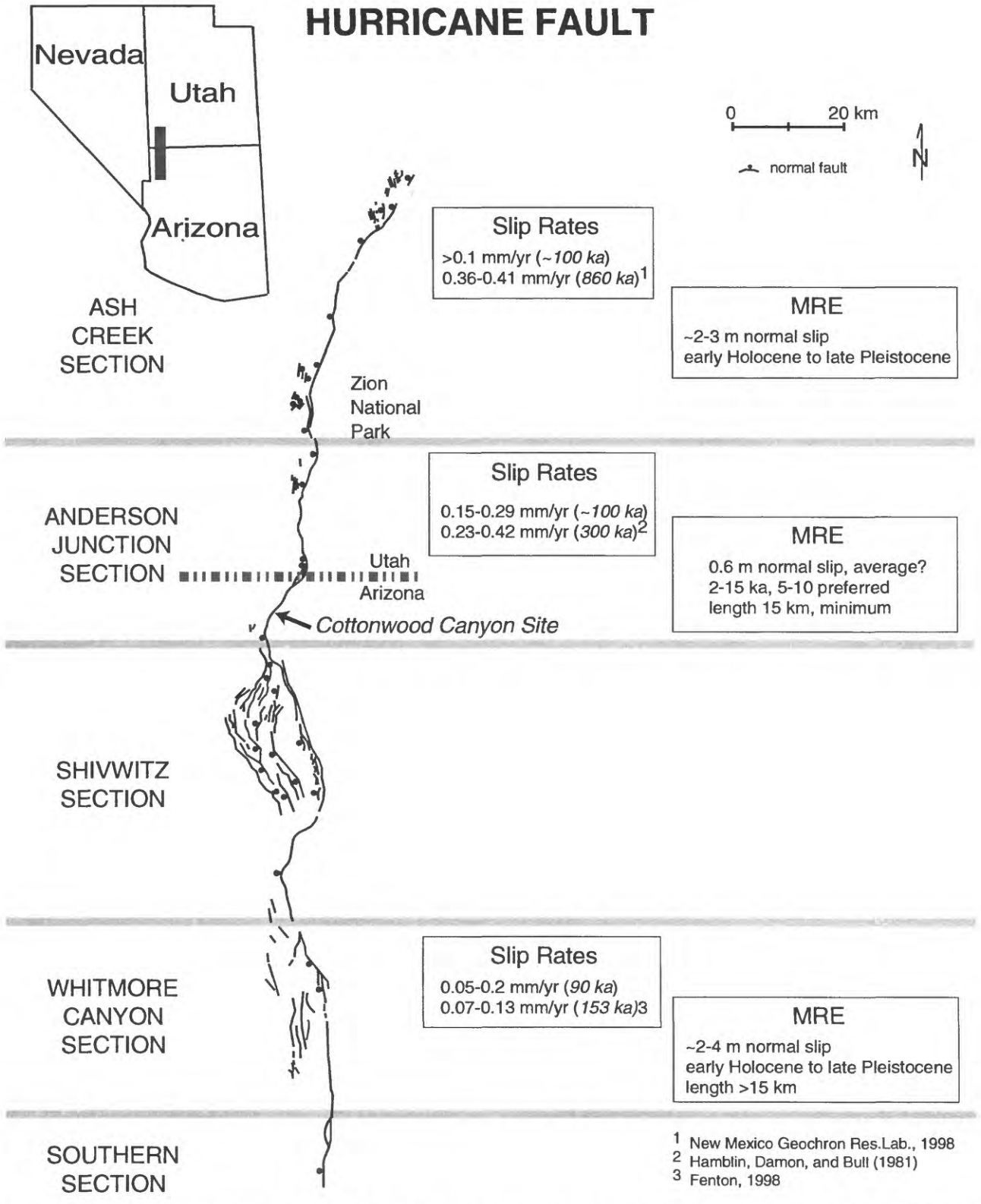

Figure 1. Map of the Hurricane fault, in the southwestern United States, showing the divisions of the 5 sections. The sections are identified by major fault step-overs, convex bends, changes in number of fault strands, and cumulative displacement changes (Stewart and Taylor, 1996; Stewart and others, 1997). Shown also are the characteristics of the most recent event (MRE), determined from this study, and the slip rates over different periods of time for different sections along the fault.

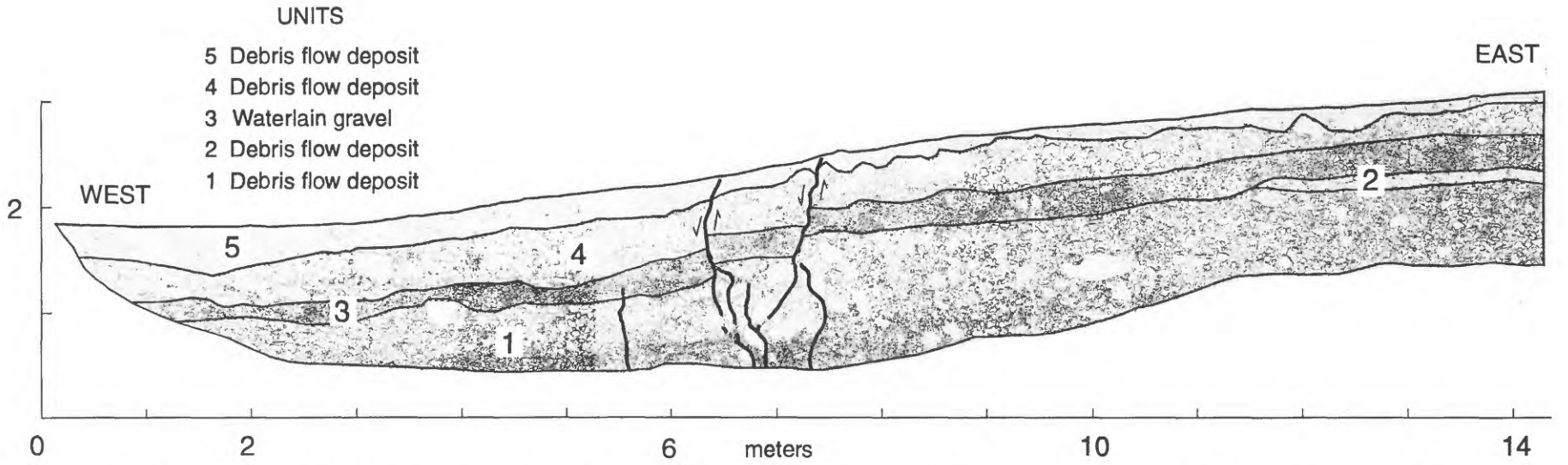

Figure 2. Log of trench across the Hurricane fault at Cottonwood Canyon. Stratigraphy shows 60 cm of down-to-the-west displacement across the fault zone. The faulted alluvial surface is ~8-15 ka, based on soil development. An unfaulted 2-6 k.y. surface nearby constrains the timing of the ground rupturing event, and a preferred event timing is 5-10 ka.

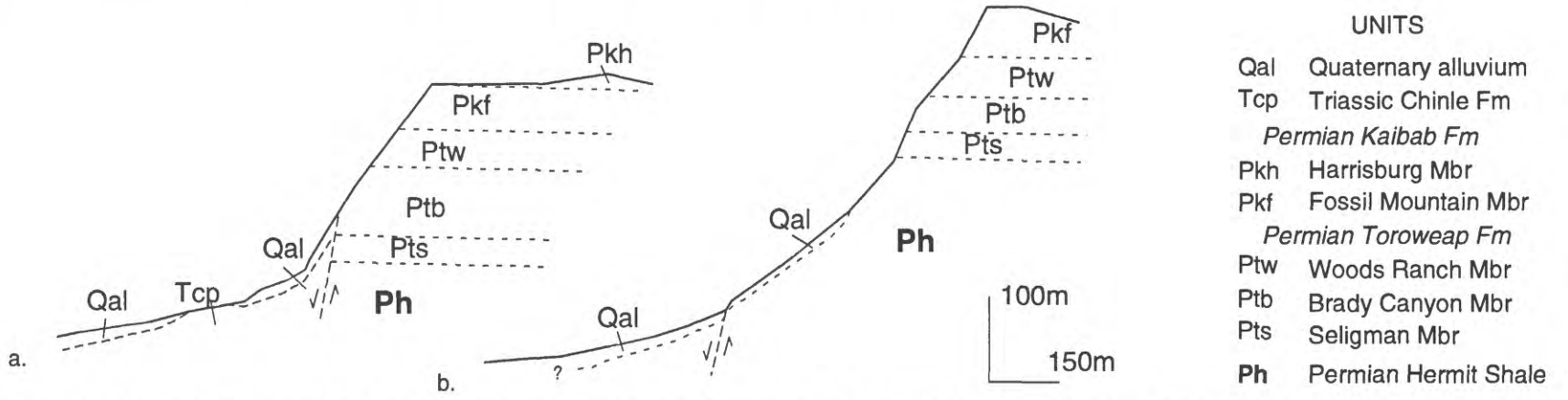

Figure 3. Schematic geologic cross-sections across the Hurricane fault. The Hermit Shale (**Ph**) is less resistant to erosion than the Toroweap and Kaibab Formations. In (a) the Hermit Shale does not crop out and the cliff slope is steeper than in (b) where the Hermit Shale does crop out. The cliff has eroded farther away from the fault trace in situation (b) and preserves evidence of late Quaternary rupture that may not be preserved in the steeper and bedrock conditions of (a).

Deformation of Quaternary deposits and ground surface caused by bedrock fault movements -Trenching studies and model experiments-

Keiichi Ueta [1], Kazuo Tani [1], Nobuhiro Onizuka [2],
Takahiro Kato [3] and Katsuyuki Maruyama [3]

[1] Central Research Institute of Electric Power Industry, Japan
[2] Toyo Univ.
[3] Chiba Univ.

ueta@criepi.denken.or.jp

Field and literature surveys of earthquake faults as well as model tests were made to investigate the deformation of the unconsolidated sediments overlying bedrock faults. The summary of the results is shown below.

(1) The development pattern of shear bands strongly depends on the fault type and the fault dip of the basement. En echelon shear bands (dip-slip fault), three-dimensional shape and kinematic evolution of Riedel shears (Fig. 1), principle displacement shear zone (strike-slip fault), tilting and rotation blocks, and en echelon grabens (oblique-slip fault) were observed in the model tests.

(2) The location of the surface fault rupture strongly depends on the fault type, the fault dip and the thickness and density of the sand mass. In the case of the normal fault, the location of the surface fault rupture is just above the bedrock faults, which have no relationship with the fault dip (Fig. 2). On the other hand, the location of the surface rupture of the reverse fault has closely relationship with the fault dip. The horizontal distance of surface rupture from the bedrock fault (W) normalized by the height of sand mass (W/H) does not depend on the height of sand mass. The values of W/H from the test agree well with those of earthquake faults.

(3) When the fault rupture propagate to the surface through the overburden, the fault displacement of the reverse and strike-slip fault in the bedrock is larger than that of the normal fault (Fig. 3). The normalized base displacements required to propagate the shear rupture zone to the ground surface from the tests agree well with that of earthquake faults.

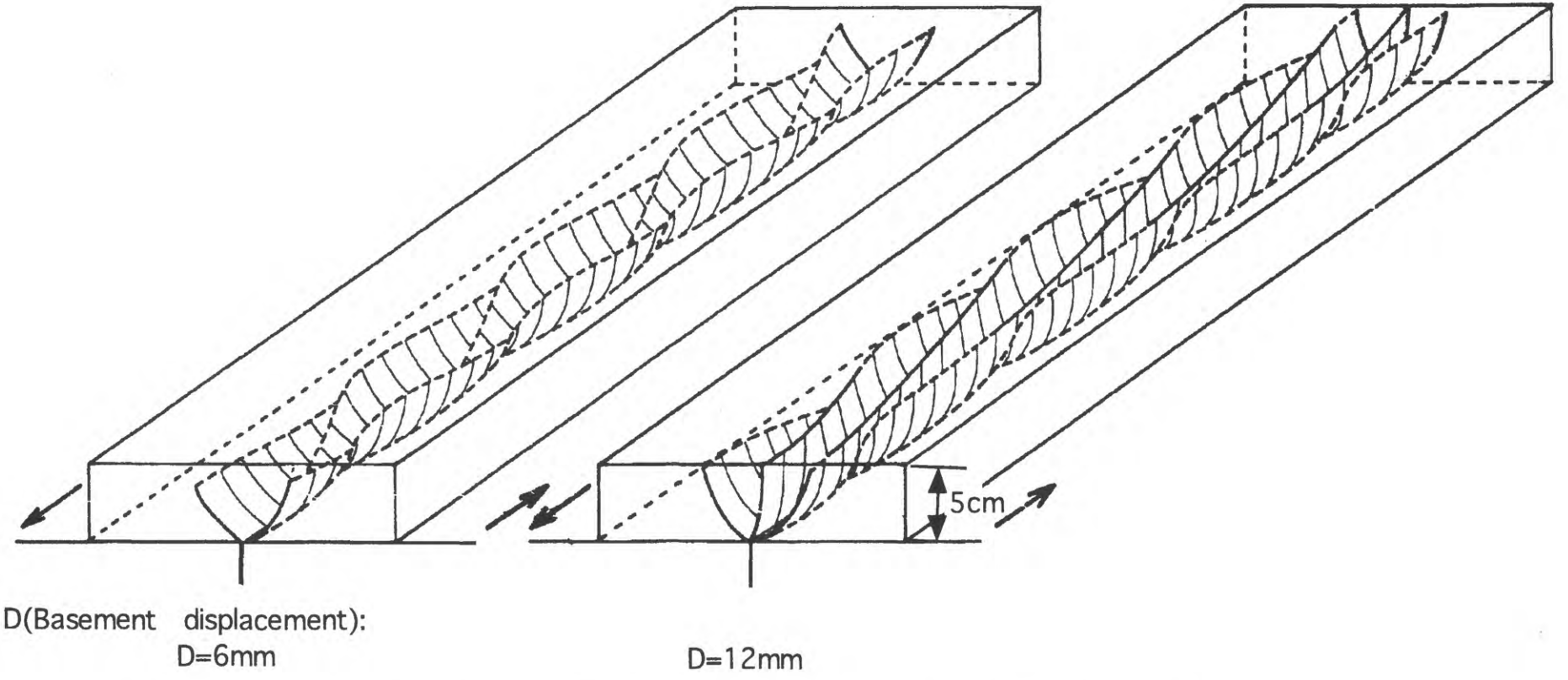

Fig. 1. Schematic diagram of 3D kinematic evolution of Riedel shears in sandpack visualized by CT scans.

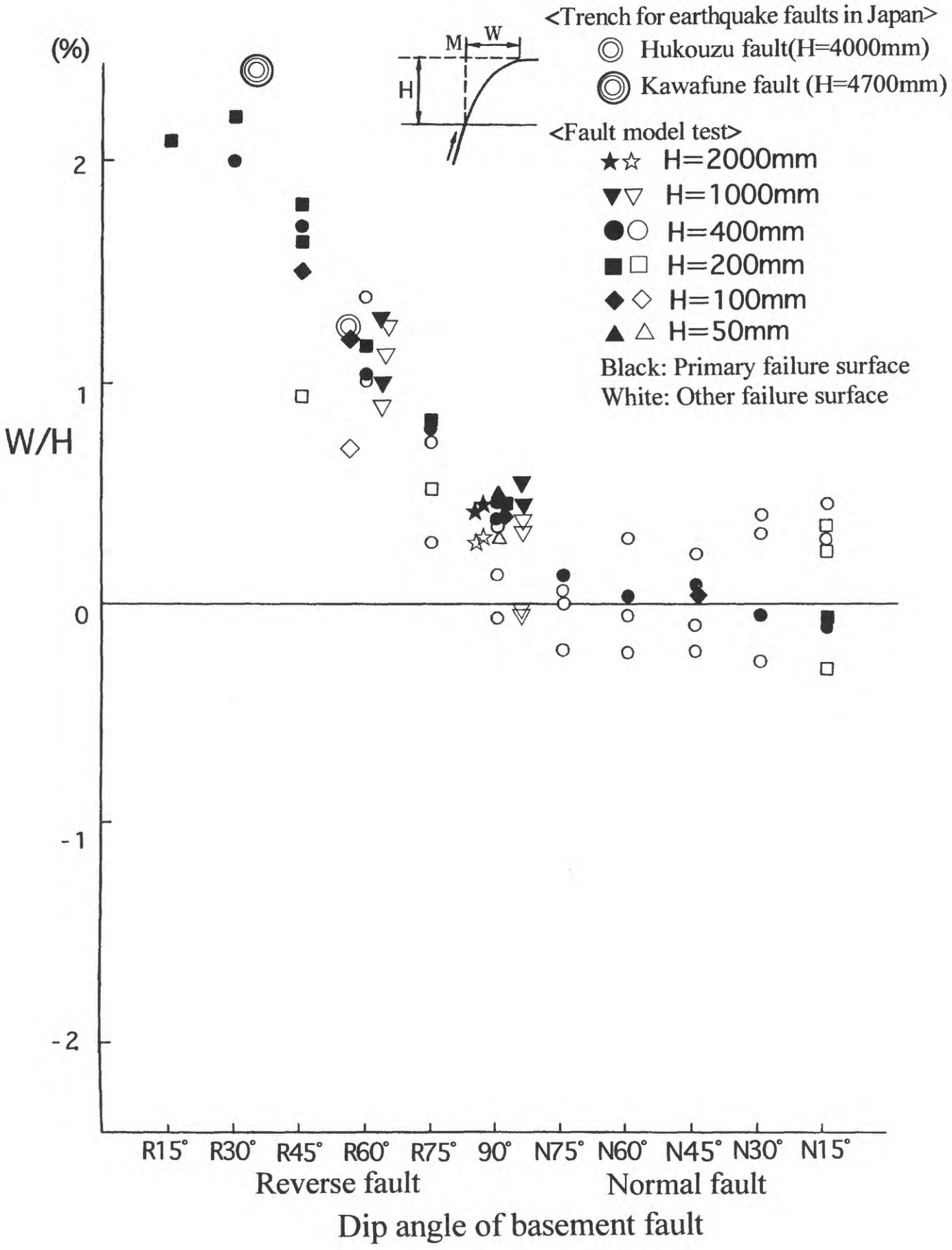

Fig. 2. Variation of W/H (see key sketch) for location of surface rupture in sand pack (fault model test) and unconsolidated sediments (earthquake fault) over dip-slip fault as function of dip angle and thickness of sand pack and unconsolidated sediments.

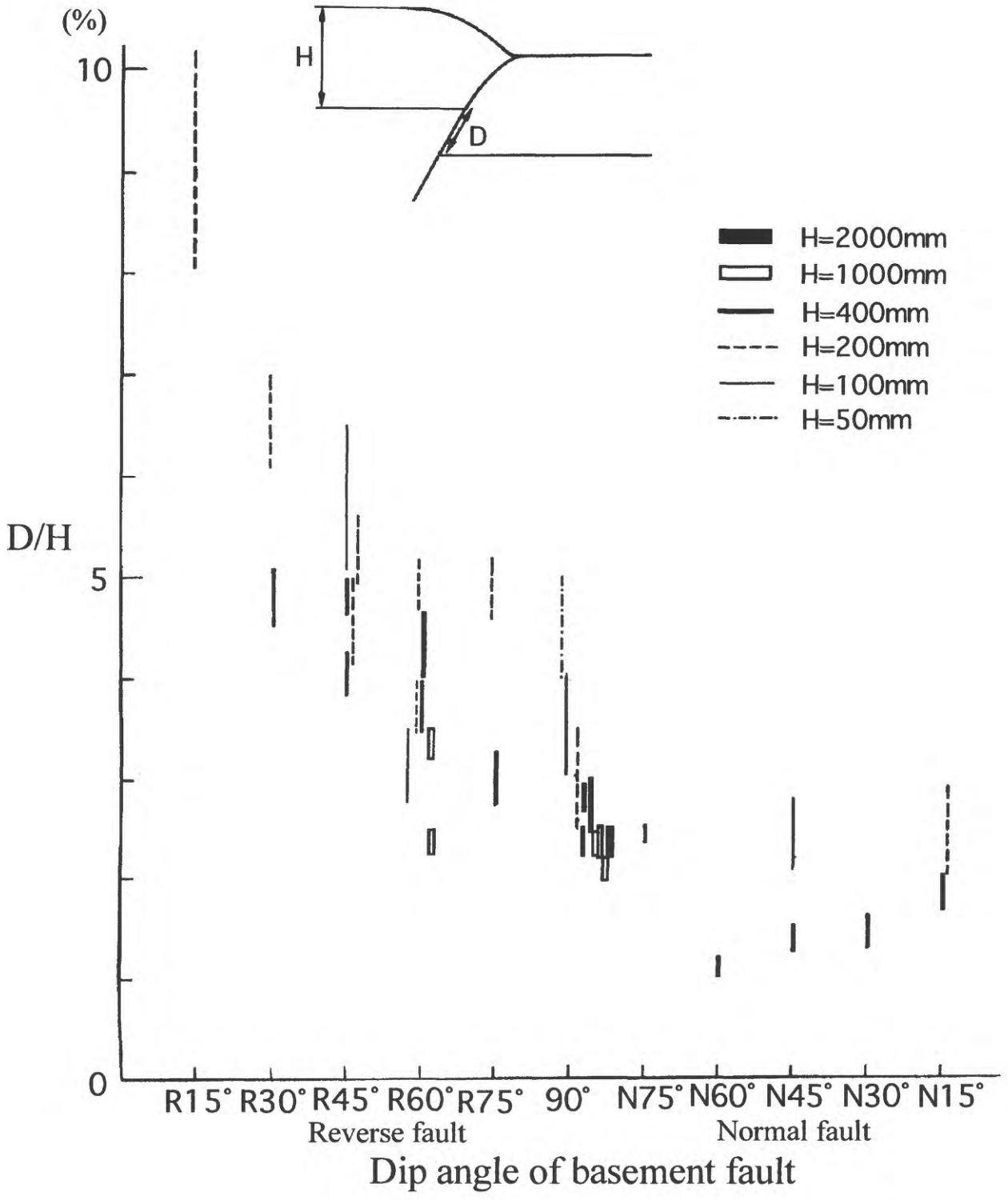

Fig. 3. Normalized base displacement required to propagate rupture zone to ground surface (D/H: see key sketch) as function of dip angle and thickness of dense sand pack.

Recent surface-faulting events along the southern part of the Itoigawa-Shizuoka Tectonic Line, central Japan

Shinji Toda, Daisuke Miura, Shintaro Abe, Katsuyoshi Miyakoshi and Daiei Inoue

Central Research Institute of Electric Power Industry, Japan

toda@criepi.denken.or.jp

The Itoigawa-Shizuoka Tectonic Line (ISTL) is a large complex fault system of north trending east-dipping reverse, northwest trending left-lateral strike-slip, north trending west-dipping reverse faults that extends for approximately 150 km in central Japan (Fig. 1). The ISTL is not only one of the most active and largest faults but the crucial fault system for the seismic hazard assessment because of large population in the urban areas along it. Recent trenching studies at the north-central ISTL exhibit the possibility that a huge earthquake, as large as M = 8.0, involving multiple segments, has occurred at AD 762 or AD 841 (ca. 1200 year BP). They also suggest that the next earthquake reaching M 8.5 will occur at the ISTL as a whole, despite no paleoseismological information in the southern ISTL is available. To examine the possibility of such a huge shock involving the entire ISTL, we conducted several trench excavations across the Hakushu, Shimotsuburai, and Ichinose faults in the southern ISTL (Fig. 1), in which none of previous studies exposed the faults directly. We consequently found evidence for one or two surface-rupturing earthquakes in the trenches.

The Hakushu fault, 10 km in length, is located at the north region of the southern ISTL, and shows north trending piecemeal linear scarps. A profile of the seismic reflection revealed the westward low-dipping structure reaching the scarp. Daibo trench (Loc.2 in Fig. 1) exposed evidence for the most recent event of the Hakushu fault. Radiocarbon ages recovered from the sediments associated with the event indicate that the surface-rupturing earthquake occurred sometime between 6600 and 7100 year BP.

The Shimotsuburai fault, which extends for 12 km and sandwiched by the Hakushu and Ichinose faults, represents continuous sharp linear scarps. At Tozawa (Loc.3 in Fig. 1) and Asahimachi-Yamadera (Loc.4 in Fig. 1), the trenches exposed evidence for the multiple events produced by activity of the westward dipping low-

angle thrust fault. The most recent event at both sites has a common range of the dates constrained into 1400 – 2400 year BP. An estimated coseismic slip along the fault is about 1.2 m but vertical separation (throw) is about 2.5 m at Tozawa. As much as 3 m of the net slip is also inferred in the Asahimachi-Yamadera trench. The penultimate event which evidence exposed in Tozawa trench occurred sometime between 4900 and 8400 year BP. A recurrence interval between the recent two events thus ranges 2500 to 7000 so that about 5000-year interval is estimated as an average. It allows us to estimate a slip rate of the Shimotsuburai fault is less than 1mm/yr, which is coincide with the rate inferred from previous geomorphic studies.

The Ichinose fault, which shows discontinuous linear scarps totally extending 9 km, is located at the most southern region of the entire ISTL. Two parallel-running fault scarps separated as wide as 5 km intercalate widely-developed terraces, the oldest of which gently tilts to the west. A profile of the seismic reflection and such topographical features suggest that thin-skinned structure has been developing around the fault. Kamimiyaji trenches (Loc.5 in Fig. 1) were sited on the most frontal (basin-side) scarp of 1.5 – 2.5 m high, and exposed evidence for the recent two thrust-faulting events. Despite some artificial disturbance near the surface, we estimate that the most recent event on the Ichinose fault occurred at from 4100 to 6100 year BP. Offset of the strata in the trench indicated that coseismic displacement is about 2 m. The timing of the penultimate event identified as a colluvial wedge is constrained into between 9600 and 11000 year BP. A coseismic slip at that time is almost the same as the recent one. A recurrence interval between the recent two events ranges 3500 to 6900 years, so that about 5000-year interval is estimated as an average. Thus, the slip rate of the Ichinose fault is about 0.5 mm/yr if we ignore some amounts of the plastic deformation and slip on the other lineaments.

We now put these results into the time-space diagram of rupture history of the ISTL (Fig. 2). It allows us to examine the possibility of the seismic coupling among the three parts (several geometric segments) of the ISTL. Regarding the timing of the most recent event, there is no evidence for the historically-documented AD 762 and 841 earthquakes in trenches of the southern part, although simultaneous ruptures involving multiple segments are still suggested in central to northern parts of the ISTL. The average recurrence intervals of about 5000 years in the southern ISTL are obviously longer than those of about 700 – 3000 years in the central and northern ones. Also, slip rates of the faults in the south are slower than those in the central and northern parts. In addition to these paleoseismological data, seismic reflection profiles revealed that the

faults in the southern part are thrust faults dip 20° - 30° to the west, in contrast to the left-lateral strike-slip faults in the central part. These facts fundamentally suggest that the thrust faults in the southern ISTL have never ruptured with the strike-slip faults in the central one during the past 10,000 years. Such a weak coupling between both parts implies that probability of the huge earthquake by entire rupture of the ISTL is extremely low even there is a possibility of the multiple ruptures of the central and northern parts. As long as the space-time diagram in Fig. 2 is concerned in detail, however, the possibility of the simultaneous dynamic ruptures of the central and southern parts still remains around 7000 years ago. We thus might need to seek the possibility of the synchronisation and stress triggering related to it.

From the viewpoint of the tectonic deformation in central Japan, the strain partitioning might occur if the east-west crustal shortening has been continuing during the Quaternary time. In other words, the ISTL is no longer responsible for the entire deformation around the area. Instead, some thrust faults extending parallel to the northern and southern ISTL accommodate the east-west compressional strain (see an inset map in Fig. 1) so that slip rate of the southern part of the ISTL is much slower than the central part, around which there is a few minor strike-slip faults to accommodate the strain.

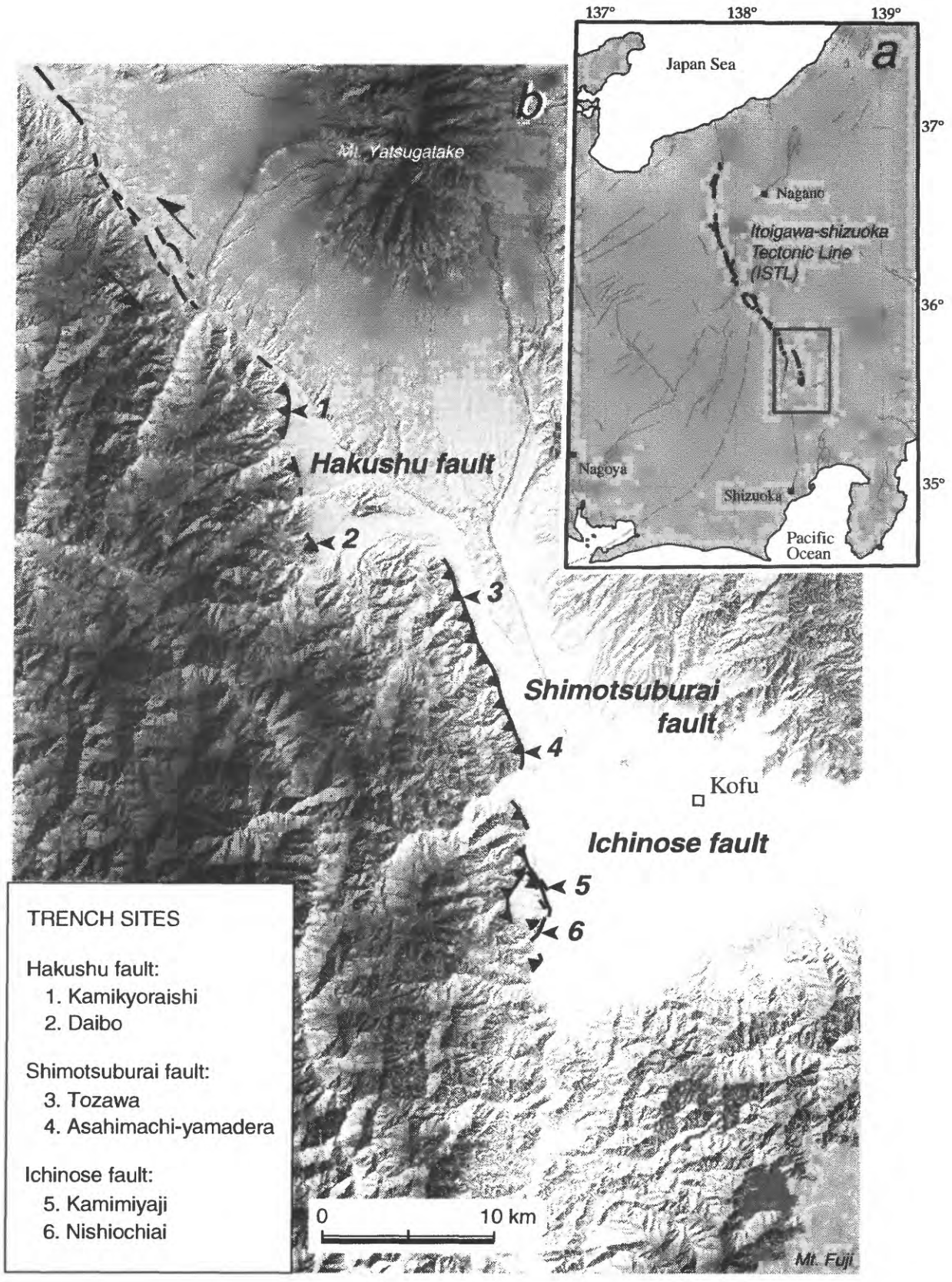

Figure 1. (a) Distribution of the Itoigawa-Shizuoka Tectonic Line (ISTL) active fault system in central Japan. (b) Study faults and trench excavation sites in the southern part of the ISTL.

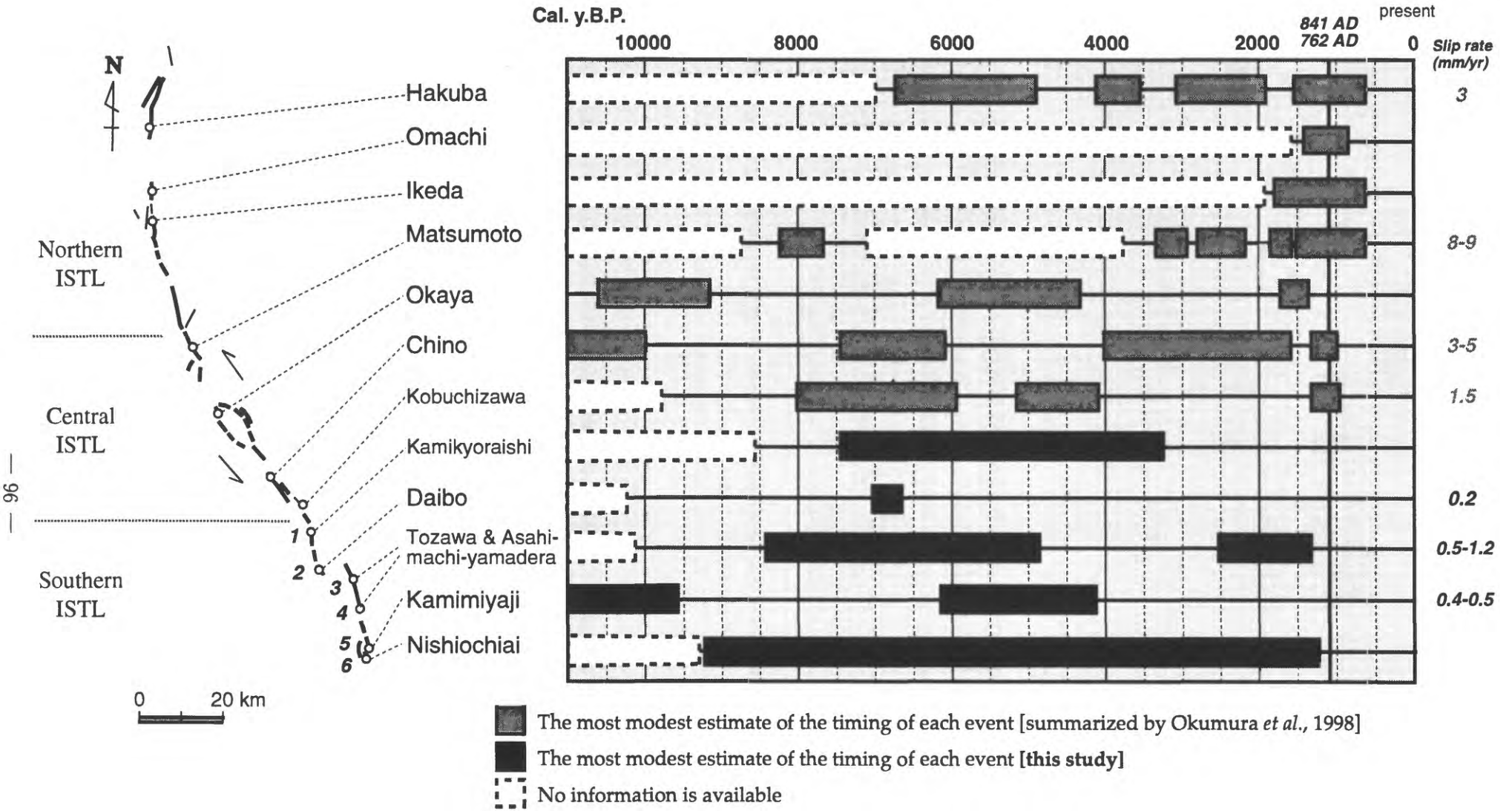

Figure 2. Space-time diagram of surface-rupturing earthquakes on the ISTL during the past 11000 years. The distribution of the faults and times of the events on the northern-central ISTL are based on Shimikawa *et al.* (1995) and Okumura *et al.* (1998), respectively. Fault activity, such as slip rate and recurrence interval of fault segments composing the fault system is various. In addition, there is no evidence that entire fault system has ruptured simultaneously on their surface traces.

Faulting processes of the 1955 Futatsui Earthquake (M=5.9), Akita Prefecture, inferred from pre- and coseismic elevation changes

Taku Komatsubara and Yasuo Awata

Geological Survey of Japan

komatsub@gsj.go.jp

The Futatsui earthquake of October 19, 1955 occurred in the north Dewa Hills, in the Inner Arc of the Northeastern Honshu Arc (Fig. 1). This earthquake was not so large (M=5.9); however, pre- and coseismic elevation changes were observed by precise leveling (Miyamura and Okada, 1956). We try to restore the faulting processes based on these leveling data.

1. Leveling data

First-order leveling surveys were done in 1902, 1938, 1942, 1949, 1955 (after the earthquake), 1959 and after that, crossing the epicenter of the 1955 earthquake. They indicate the following crustal movements.

- 1902 to 1942: Gentle warping consistent with the folding of Neogene had occurred, but no distinct tilting occurred near the epicenter.
- 1942 to 1949: 6×10^{-6} eastward tilting had occurred in a several-km-wide zone west of the 1955 epicenter.
- 1949 to 1955 (just after the earthquake), 1959 : 8×10^{-6} westward tilting had occurred in the same zone where the eastward tilting had occurred during the last leveling interval. Height change between 1938 and 1955 indicates that about 14 cm uplifting at the epicenter toward the eastern side of Nanakura Anticline occurred with asymmetrical folding.
- After 1959: No distinct crustal movement has been observed.

2. Analysis by elastic dislocation model

Simple static, elastic dislocation theory is applied for restoring processes of fault movements (Fig. 3). In this study it is assumed that the geometry of the fault plane is approximated with a combination of several rectangular fault segments; slip is uniform

over each segment. The formulation was derived by Mansinha and Smylie (1971), on the assumption that the upper crust is a homogenous elastic body whose Poisson's ratio is 0.25. We determined fault parameters (Table 1) by a trial and error method. Four models were tried.

- Model 1 (High angle reverse fault and flat detachment in the middle part of the seismogenic layer) : This model makes a good fit between the observed and calculated values, and the reverse dipping between 1942 and 49 is interpreted as a preslip on the detachment. But there is no evidence of detachment in the middle part of the seismogenic layer (Fig. 4). Note that in this model the width and slip should be larger on the deep detachment than on the shallow reverse fault.
- Model 2 (Listric reverse fault; the deeper end lying at the bottom of the seismogenic layer (about 20km in depth)): This model is in conformity with the observed values on the hanging wall side, but is not able to explain the narrow depression at the footwall side (Fig. 5).
- Model 3 (Listric reverse fault with flat detachment at the base of the seismogenic layer): This model is the most possible fault geometry among these four models from the geological point of view (Fig. 6). But this model fault makes a similar displacement to Model 2.
- Model 4 (Step-like reverse fault with terrace at the middle part of the seismogenic layer): This model makes a good fit between the observed and calculated. Nearly constant slip makes surface displacement same as the observed values in this model (Fig. 7). The flat terrace should lie in the middle part of the seismogenic layer.

3. Discussion

These calculations suggest that a flat detachment or terrace on the fault may lie in the middle part of the seismogenic layer, or the observed height changes might be anomalous in the footwall side.

If the former is true, our Model 1 and 4 mean that depth of the detachment in the middle part of seismogenic layer may correspond to the base of Neogene.

If the later is true, our Model 2 and 3 suggest preseismic slip at the base or in the lower part of the seismogenic layer is larger than that on the reverse fault in the shallower part. Two benchmarks in the footwall side of the fault are just on the fault and large scale landslide area, thus the elevation change at these points might be influenced by these surface disturbance.

In any case, these leveling data show that even such moderate sized earthquake accompanied preseismic crustal movement. They suggest that preseismic slips on the detachment started 6 to 13 years before earthquake, then the slip propagated to shallower part, and that the preslip on the deeper fault segments may be larger than the coseismic slip on the shallower segments.

Reference

Miyamura, M. and A. Okada, 1956, Geodetic measurements of first order leveling along the Yoneshiro River. (Third Report), *Bull. Earthq. Res. Inst. Univ. Tokyo*, 34, 373-380 (in Japanese with Germany Abstract).

Mansinha, L. and D. E. Smylie, 1971, The displacement field of inclined faults, *Bull. Seismol. Bull. Am.*, *61*,1433-1440.

Table 1 Parameters of model faults

Fault Model Depth (km)	Dip Angle	Length (km)	Offset (mm)	Term of Faulting
Model 1				
0~7	75°	2	160	1955-49
7~8	5°	8	200	1955-49
8~15	5°	8	300	1949-42
Model 2				
0~1	60°	4	170	1955-49
1~7.5	45°	4	170	1955-49
7.5~15	45°	4	400	1949-42
Model 3				
0~1	60°	4	170	1955-49
1~7.5	45°	4	170	1955-49
7.5~15	45°	4	400	1949-42
15~20	5°	4	800	1949-42
Model 4				
0~5	75°	4	160	1955-49
5~6.5	15°	4	200	1955-49
6.5~15	60°	6	250	1949-42

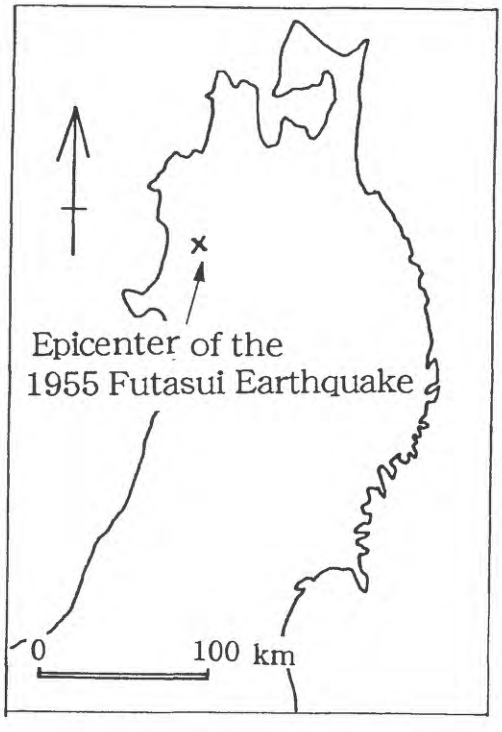

Figure 1. Epicenter of the 19 December 1955 Futatsui earthquake (140.18°E, 40.27°N).

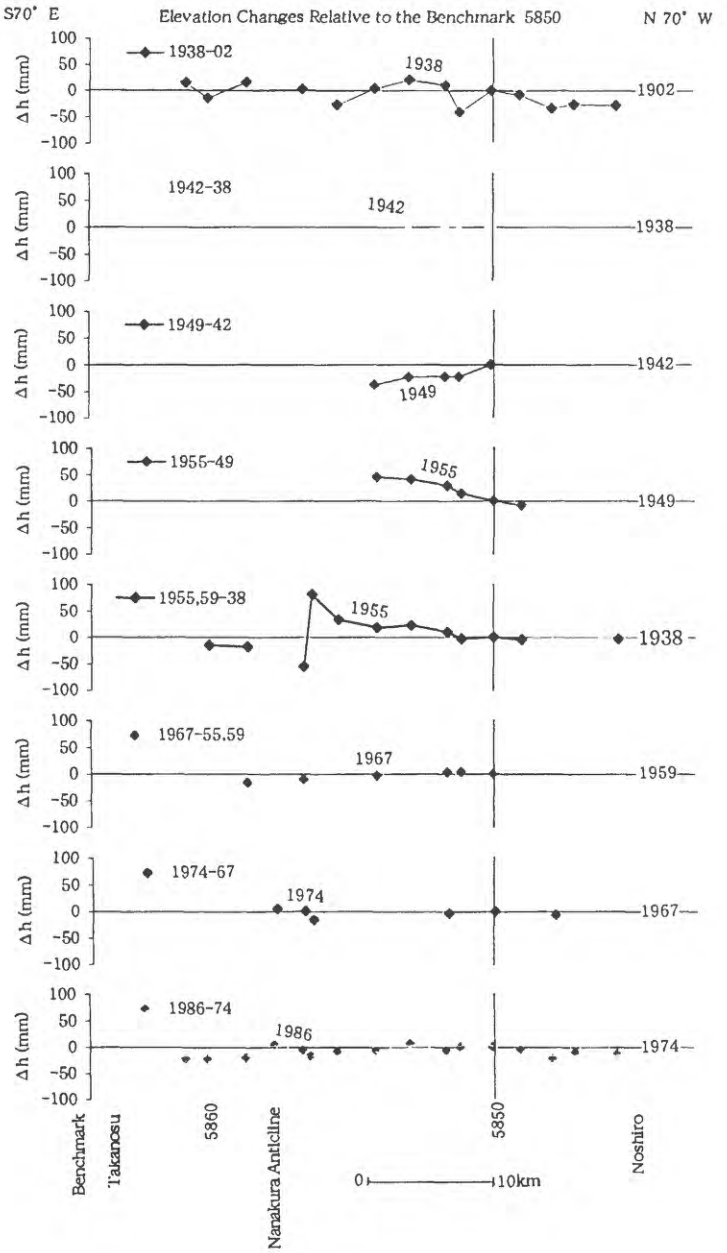

Figure 2. Elevation changes along the Yoneshiro River (based on the first order benchmark levelings by the Geographycal Survey Institute and Miyamura and Okada, 1956).

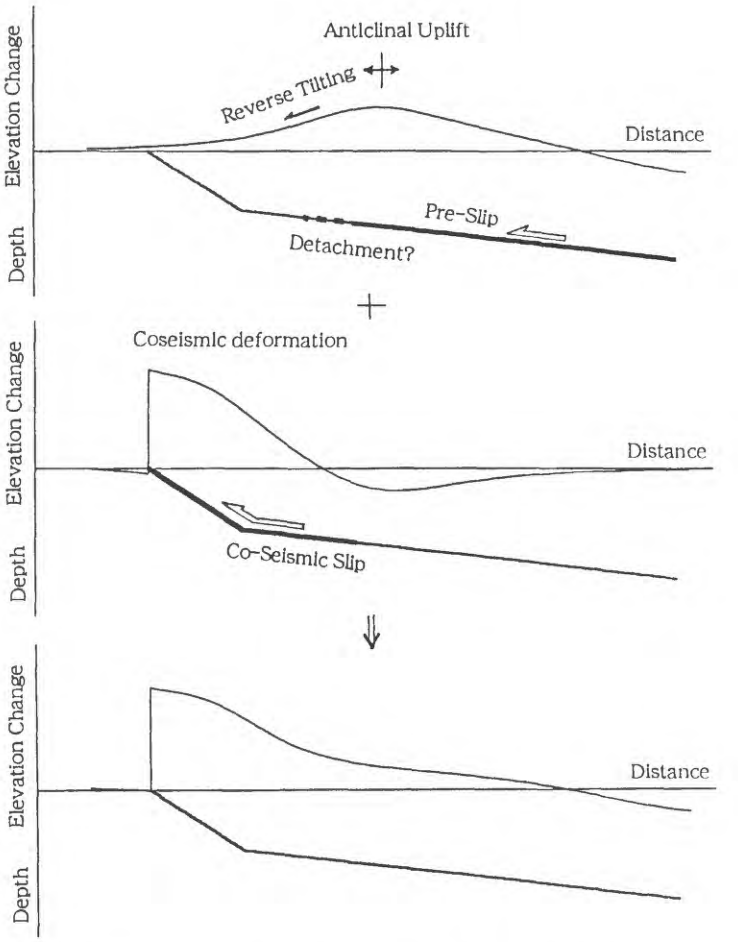

Figure 3. Hypothetical model on the pre-and coseismic slips and elevation changes.

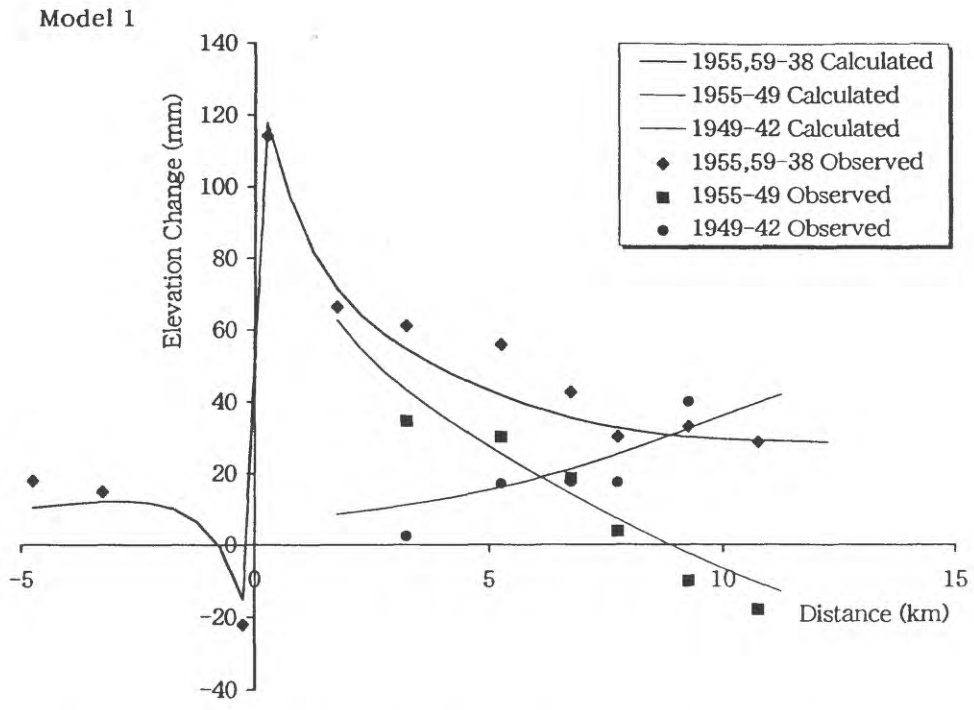

Figure 4. Observed elevation changes and calculated deformation by Fault model 1.

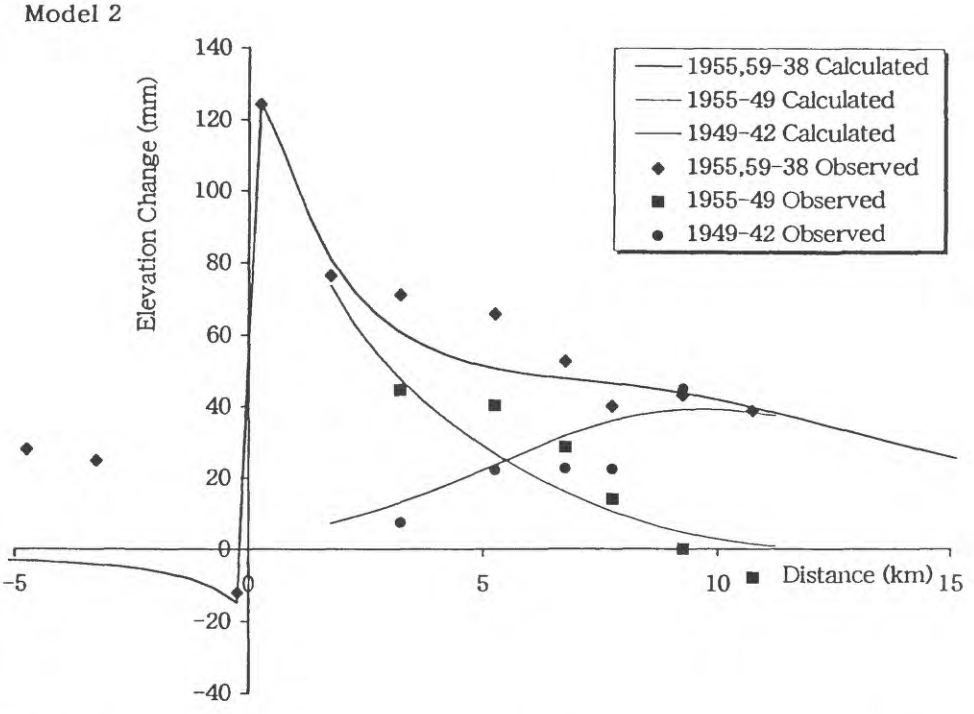

Figure 5. Observed elevation changes and calculated deformation by Fault model 2.

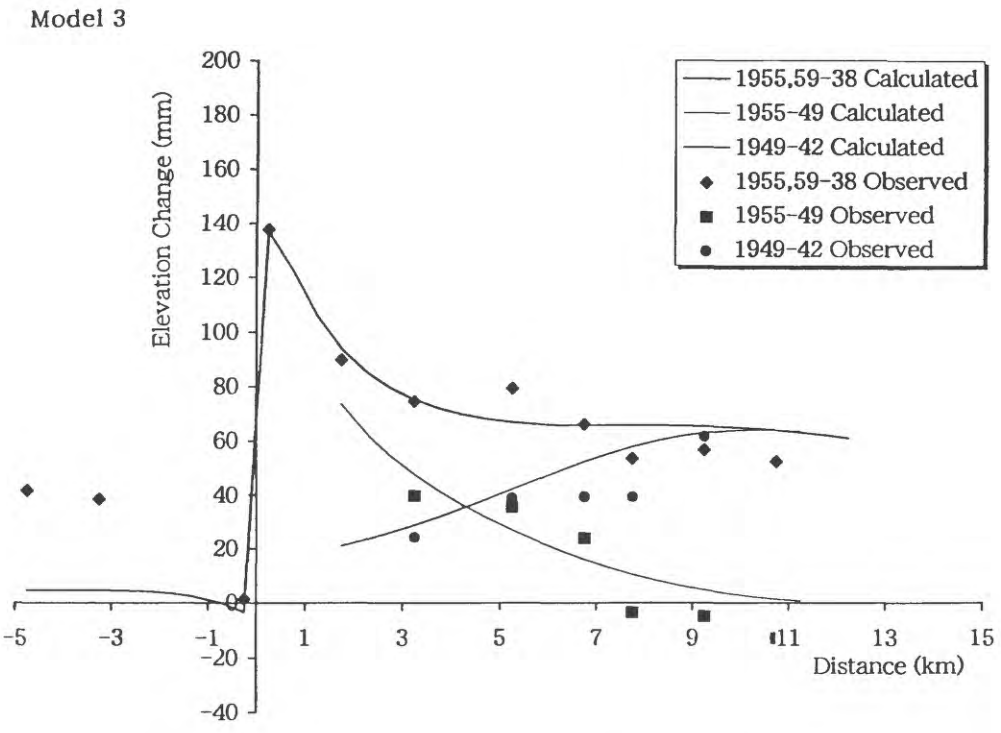

Figure 6. Observed elevation changes and calculated deformation by Fault model 3.

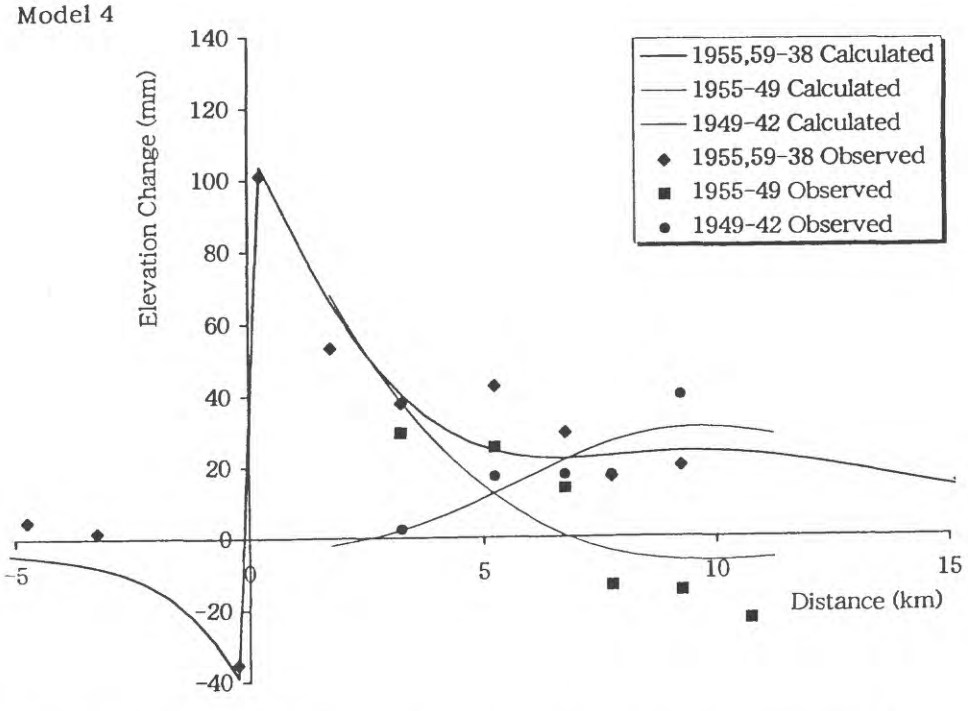

Figure 7. Observed elevation changes and calculated deformation by Fault model 4.

Subaqueous sand blow deposits induced by the 1995 Southern Hyogo Prefecture (Kobe) earthquake, Japan

Akihisa Kitamura [1], Eiji Tominaga [1] and Hideo Sakai [2]

[1] Shizuoka Univ.
[2] Toyama Univ.

seakita@ipc.shizuoka.ac.jp

The 1995 Southern Hyogo Prefecture (Kobe) earthquake (*M*7.2) occurred in the region around Kobe City and Awaji Island in Southwest Japan. Coseismic liquefaction caused subsidence of the land and damage to sea wall caissons on the man-made Port Island at Kobe City. A 2- to 3-m-wide zone behind the caissons of the northern wharf on the island subsided into the intertidal zone. Subaqueous sand blow deposits were observed within the subsided area. These deposits consist of upward-fining sequences and are subdivided into three parts, in ascending order: graded coarse- to medium-grained sand, parallel-laminated fine- to very-fine-grained sand, and massive mud. Grain fabric analysis of this sequence shows that the main depositional processes changed from a combination of flow and allied processes to the force of gravity. Still water is essential for gravity to be the dominant influence in deposition. Because subaerial sand blow deposits and sills were not formed by sedimentation in still water, the grain fabric produced by gravity alone is a useful criterion for distinguishing between subaqueous sand blow deposits and other liquefaction-induced deposits.